HEPATIC STELLATE CELL TRANSDIFFERENTIATION: PRO-FIBROGENIC EFFECTORS

by

Ashley Marie Lakner

A dissertation submitted to the faculty of
The University of North Carolina at Charlotte
in partial fulfillment of the requirements for the
degree of Doctor of Philosophy in
Biology

Charlotte

2011

Approved by:

_____
Dr. Laura W. Schrum

_____
Dr. Iain H. McKillop

_____
Dr. Mark G. Clemens

_____
Dr. Daniel A. Nelson

_____
Dr. Daniel Rabinovich

ABSTRACT

ASHLEY MARIE LAKNER. Hepatic stellate cell transdifferentiation: profibrogenic effectors. (Under direction of DR. LAURA W. SCHRUM)

Hepatic fibrosis is a significant cause of morbidity and mortality worldwide and can be described as exacerbated wound-healing marked by excessive deposition of extracellular matrix components, predominantly type I collagen. Chronic injury stimulates accumulation of scar matrix synthesized by hepatic stellate cells (HSCs) resulting in distortion of normal liver architecture, disruption of blood flow and organ dysfunction. In a normal healthy liver, HSCs are found in the quiescent state functioning to store vitamin A in the form of retinyl esters, regulate sinusoidal microcirculation, and maintain normal basement membrane conditions. Following exposure to fibrogenic stimuli, HSCs transdifferentiate to activated myofibroblast-like cells marked by increased proliferative and hypercontractile properties.

Currently there are no FDA-approved treatments for hepatic fibrosis. Outside of surgical resection, orthotopic transplantation is an option for certain disease states; however, the current list of patients in need of transplant far exceeds the annual donor rate. As HSCs are considered the primary effector cells of fibrosis, targeting various points of transdifferentiation and resolution to impede disease development/progression is of therapeutic interest. The process of HSC transdifferentiation is classically divided into initiation and perpetuation phases, each characterized by unique cellular events.

Examination of genetic programming in early HSC transdifferentiation revealed coordinate changes in gene expression by components of JAK/STAT signaling. Chemical inhibition of this signaling pathway blocked HSC activation morphologically and through interruption of genetic reprogramming denoted by significantly decreased pro-fibrotic

gene expression. Post-transcriptional regulation of HSC transdifferentiation (initiation and perpetuation phases) is controlled, in part, by changes in global microRNA (miR) expression patterns. Specifically, miR 19b was significantly decreased in activated compared to quiescent HSCs. Overexpression of miR 19b in culture-activated HSCs significantly decreased pro-fibrotic transforming growth factor beta (TGFβ) signaling by direct inhibition of TGFβRII and subsequent decreases in collagen expression and markers of HSC activation. miR 19b expression was also significantly decreased in rodent models of fibrosis and in liver tissue from fibrotic patients, indicating miR 19b as a novel biomarker and possible therapeutic. Finally, examination of transdifferentiation resolution has indicated involvement of HSC apoptosis. However, newly transdifferentiated stellate cells display increased resistance to apoptotic stimuli. Aquaporins (AQP) are known regulators of programmed cell death in mediation of the apoptotic volume decrease necessary for downstream caspase and nuclease activation. Analyses showed AQP expression was significantly decreased in activated compared to quiescent HSCs. Quiescent HSCs expressing multiple AQP homologs responded to osmotic challenge, an effect abrogated by functional inhibition of AQPs. Similarly, quiescent HSCs were significantly more responsive to apoptotic stimulation, which was also abrogated by AQP inhibition. In vitro studies were confirmed in vivo utilizing liver tissue from a mild-fibrotic animal model. Dual fluorescent immunohistochemistry showed strong colocalization of aquaporins with quiescent, but not activated stellate cells.

HSC transdifferentiation is highly complex with multiple pro-fibrotic signaling networks conferring phenotype-specific genetic reprogramming observed in hepatic

fibrosis. These studies provide insight into novel factors controlling initiation, perpetuation and resolution stages of HSC transdifferentiation as well as new avenues to be explored for therapeutic intervention.

ACKNOWLEDGEMENTS

During the past four years in the doctoral program I have made both professional and personal advancements that have readied me for the next stage of my life. I am appreciative of the faculty and staff at both UNCC and Carolinas Medical Center for their dedication to student development. I show immense gratitude to the members of my advising committee for their time, encouragement and invaluable mentorship throughout this process. Conducting my dissertation research under the direction of Dr. Laura Schrum has been a privilege. I would most certainly not be at this stage in my scientific career without her unwavering guidance and support. She has taken great care to go above and beyond duties as a PhD advisor by giving me opportunities and challenges to shape me into the independent researcher I am today. I will forever be thankful to her for this priceless experience. I would also like to thank former and present members of the Schrum Lab that I have had the opportunity to interact with. Dr. Cathy Moore and Stephani Day were instrumental in my early days in the laboratory and I am grateful for their mentoring as well as the mentoring and conversations I have shared with Dr. Kyle Thompson. I am also thankful to my colleague Whitney Ellefson, M.S. for her continual professional and emotional support. I must acknowledge my family for their love, guidance and encouragement which has enabled me to stay the course. Specifically, I would like to emphasize my deep gratitude for my mother who has always pushed me to succeed academically; if it were not for her many sacrifices I would not have been able to achieve this accomplishment. Finally, words can not begin to express my appreciation for the love and support I have received from my fiancé Frank, who has undoubtedly been my biggest champion along this journey.

TABLE OF CONTENTS

LIST OF TABLES x

LIST OF FIGURES xi

LIST OF ABBREVIATIONS xiii

CHAPTER 1: INTRODUCTION 1

HEPATIC FIBROSIS 1

HEPATIC STELLATE CELLS 4

HEPATIC STELLATE CELL TRANSDIFFERENTIATION 5

PROMINENT SIGNALING COMPONENTS AND PATHWAYS IN HSC TRANSDIFFERENTIATION 10

HORMONE AND NEUROTROPHIC SIGNALING 10

WNT SIGNALING 11

GROWTH FACTOR SIGNALING 12

CYTOKINE AND CHEMOKINE SIGNALING 14

TRASCRIPTIONAL REGULATION OF HSC TRANSDIFFERENTIATION 17

POST-TRANSCRIPTIONAL REGULATION OF HSC TRANSDIFFERENTIATION 23

FIBROSIS RESOLUTION 29

DISEASE DETECTION AND THERAPEUTIC STRATEGIES 32

DISSERTATION AIMS 36

CHAPTER 2: MATERIALS AND METHODS 42

CHAPTER 3 MATERIALS AND METHODS 42

HSC ISOLATION AND CULTURE 42

TREATMENT OF HSCS 43

ISOLATION OF RNA AND QUANTITATIVE PCR 43

MICROSCOPY 44

DATA ANALYSIS 44

CHAPTER 4 MATERIALS AND METHODS 44

MIRNA ISOLATION, PURIFICATION AND MICROSCOPY 44

PRIMARY HEPATIC STELLATE CELL ISOLATION AND IMAGING 45

QUANTITATIVE REAL-TIME POLYMERASE CHAIN REACTION AND IMMUNOBLOTTING 46

TRANSIENT TRANSFECTION 47

IMMUNOCYTOCHEMISTRY AND IN SITU HYBRIDIZATION 47

HUMAN TISSUE SAMPLES 48

STATISTICAL ANALYSIS 48

CHAPTER 5 MATERIALS AND METHODS 49

ANIMALS 49

MATERIALS 49

HSC ISOLATION AND CULTURE 49

TREATMENT OF HSCS AND MORPHOLOGICAL ASSESSMENT 50

REVERSE TRANSCRIPTION PCR (RT-PCR) AND REALTIME PCR 50

CELL LYSATE PREPARATION AND IMMUNOBLOTTING 51

OSMOTIC CHALLENGE AND CELL SWELLING 51

CASPASE ACTIVITY 52

DUAL FLUORESCENT IMMUNOHISTOCHEMISTRY 52

STATISTICAL ANALYSIS 53

CHAPTER 3: DAILY GENETIC PROFILING INDICATES JAK/STAT SIGNALING PROMOTES EARLY HEPATIC STELLATE CELL TRANSDIFFERENTIATION 54

INTRODUCTION 54

RESULTS 56

DISCUSSION 60

CHAPTER 4: MIR 19B: NOVEL BIOMARKER AND INHIBITOR OF HEPATIC STELLATE CELL-MEDIATED FIBROGENESIS 74

INTRODUCTION 74

RESULTS 76

DISCUSSION 81

CHAPTER 5: ALTERED AQUAPORIN EXPRESSION AND ROLE IN APOPTOSIS DURING HEPATIC STELLATE CELL ACTIVATION 110

INTRODUCTION 110

RESULTS 111

DISCUSSION 115

CHAPTER 6: SUMMARY AND FUTURE DIRECTIONS 128

REFERENCES 137

APPENDIX: ABSTRACTS AND MANUSCRIPTS PUBLISHED 162

LIST OF TABLES

TABLE 3.1: Primers used in this study 65

TABLE 4.S1: Primers used in this study 102

TABLE 4.S2: List of differentially expressed miRs detected in activated vs. quiescent HSCs 103

TABLE 5.S1: Primers used in this study 127

LIST OF FIGURES

FIGURE 1.1: Intrahepatic effects of liver injury 37

FIGURE 1.2: Representative light micrographs of HSCs 38

FIGURE 1.3: Transdifferentiation of HSCs 39

FIGURE 1.4: TGFβ signaling stimulates and perpetuates HSC transdifferentiation 40

FIGURE 1.5: miRs involved in HSC transdifferentiation 41

FIGURE 3.1: Gene expression profile time course 66

FIGURE 3.2: Clustered genetic and day analyses 67

FIGURE 3.3: Gene expression markers during different stages of HSC activation 68

FIGURE 3.4: Inhibition of JAK/STAT signaling pathway: morphological alterations 71

FIGURE 3.5: Inhibition of JAK/STAT signaling pathway: cluster analyses 72

FIGURE 3.6: Inhibition of JAK/STAT signaling pathway: genetic alterations of fibrotic markers 73

FIGURE 4.1: Differential miRNA expression in quiescent vs activated HSCs 87

FIGURE 4.2: miR 19b negatively regulates TGFβRII expression 90

FIGURE 4.3: miR 19b exerts inhibitory effects on TGFβ target gene collagen 93

FIGURE 4.4: miR 19b inhibits paracrine TGFβ signals 95

FIGURE 4.5: HSC activation is inhibited by miR 19b 96

FIGURE 4.6: Down-regulation of miR 19b in rodent models of hepatic fibrosis 100

FIGURE 4.7: miR 19b is a putative biomarker for human hepatic fibrosis 101

FIGURE 4.S1: Efficient transfection of miR 19b in activated HSCs 105

FIGURE 4.S2: miR 19b does not regulate SMAD4 expression in activated HSCs 106

FIGURE 4.S3: Collagen secretion is inhibited by miR 19b in activated HSCs 107

FIGURE 4.S4: In situ hybridization of miR 19b in normal and fibrotic rat liver 108

FIGURE 4.S5: Immunohistochemistry of quiescent and activated markers of HSCs 109

FIGURE 5.1: Aquaporin expression in quiescent and activated HSCs 120

FIGURE 5.2: HSC plasma membrane water permeability 121

FIGURE 5.3: Morphological response to an apoptotic stimulus 122

FIGURE 5.4: Effect of aquaporin channel inhibition on caspase-3 activity 125

FIGURE 5.5: HSC aquaporin expression in a model of liver injury 126

LIST OF ABBREVIATIONS

AP-1	activator protein-1
Apaf-1	apoptotic protease activating factor 1
APC	adenomatous polyposis coli
AQP	aquaporin
αSMA	smooth muscle-alpha actin
ATRA	all-trans-retinoic acid
Bcl-2	B-cell lymphoma 2
BDL	bile duct-ligation
BMP	bone morphogenic protein
C/EBP	CCAAT-enhancer-binding protein
CB	cannabinoid
CBR	cannabinoid receptor
CCl_4	carbon tetrachloride
CCR	chemokine receptors
CD-14	cluster of differentiation-14
CpG	cytosinephosphoguanine
CTGF	connective tissue growth factor
CYP	cytochrome P450
DISC	death-inducing signaling complex
DMN	dimethylnitrosamine
ECM	extracellular matrix
EGF	epidermal growth factor

EMT	epithelial-mesenchymal transition
ERK	extracellular regulated kinase
EZH2	enhancer of zeste homolog 2
GFAP	glial fibrillary acidic protein
gp130	glycoprotein 130
GSK-3	glycogen synthase complex-3
GTx	gliotoxin
H	histone
HCC	hepatocellular carcinoma
HGF	hepatocyte growth factor
HSC	hepatic stellate cell
ICAM-1	inter-cellular adhesion molecule-1
IFN	interferon
IKK	IκB kinase
IL	interleukin
JAK	janus kinase
JNK	c-jun n-terminal kinase
K	lysine
KLF	kruppel-like transcription factors
LAP	latency-associated peptide
LPS	lipopolysaccharide
LRP	low density lipoprotein receptor-related protein
LXRα	liver x receptor alpha

M6PHSA	mannose-6-phosphate-albumin
MAPK	mitogen activated protein kinase
MCP-1	monocyte chemotactic protein-1
MeCP2	methyl-CpG-binding protein 2
MEK	MAPKK/MAP kinase kinase
MeSP1	mesoderm posterior-1
miR	microRNA
MMP	matrix matalloproteinase
NAFLD	non-alcoholic fatty liver disease
NASH	non-alcoholic steatohepatitis
NF-κB	nuclear factor-kappaB
PARP	poly (ADP-ribose) polymerase
PDGF	platelet derived growth factor
PI3K	phosphatidylinositol 3-kinase
PPAR	peroxisome proliferator-activated receptor
PTX	pentoxifylline
PXR	pregnane X receptor
Rac-1	Ras-related C3 botulinum toxin substrate-1
RANTES	regulated upon activated, normal t cell expressed and secreted
RAR	retinoic acid receptor
RISC	RNA-induced silencing complex
ROS	reactive oxygen species
RXR	retinoid x receptor

SAMe	S-adenosyl-L-methionine
SNP	single nucleotide polymorphism
Sp1	specificity protein 1
SREBP-1C	sterol regulatory element binding protein-1C
STAT	signal transduction and activator of transcription
TGF	transforming growth factor
TGFβR	transforming growth factor beta receptor
TIMP	tissue inhibitor of metalloproteinase
TLR	toll-like receptor
TNF-α	tumor necrosis factor-alpha
TRAIL	TNF-related apoptosis-inducing ligand
UTR	untranslated region
VEGF	vascular endothelial growth factor

CHAPTER 1: INTRODUCTION

Hepatic fibrosis

Hepatic fibrosis is a significant cause of morbidity and mortality and can be described as an exacerbated wound-healing response marked by excessive deposition of extracellular matrix (ECM) components, predominantly type I collagen. Accumulation of ECM in the subendothelial space of Disse initiates a deleterious chain of events beginning with damage to the hepatocytes. Alterations in liver architecture are deemed transient and reversible during acute injury, whereas accumulation of scar tissue in chronic injury diminishes possibility of reversion [1-2]. Sustained hepatic insult can stem from a wide array of sources, including, but not limited to, viral hepatitis B/C infection, chronic alcohol consumption, and inborn errors in drug/xenobiotic metabolism. Geographic distribution of fibrosis is expansive; viral and parasitic infections stimulate disease development in the Eastern hemisphere, whereas chronic alcohol consumption is the major underlying cause in the US and Western Europe [3]. Left untreated, chronic injury can progress from early stages of mild inflammation and steatosis to a fibrotic and ultimately cirrhotic liver (end-stage liver disease), categorized by distortion of liver parenchyma and blood flow accompanied by organ failure. Additional health complications arising from the fibrotic disease state correlate with increased morbidity and mortality, and include portal hypertension, general metabolic impairments, ascites and encephalopathy [4].

Interestingly, while previous leading causes of death in the US have decreased in past decades (lung cancer, heart disease; American Cancer Society Statistics 2011), there is an increased burden of chronic liver disease reflecting the nation's struggle with obesity, an emerging risk factor, and increased prevalence of hepatitis C-mediated fibrosis/cirrhosis [3]. This health burden confers additional disease risk, with a high percentage of chronic liver disease patients developing hepatocellular carcinoma (HCC), which is the fastest rising neoplasm incidence in the US and Western Europe [5].

In progression from chronic injury to a fibrotic state (Figure 1.1), there are numerous changes in liver architecture. Hepatocytes lose microvilli and cellular polarity and undergo apoptosis/necrosis. The sinusoidal endothelial cell population lose their fenestrae causing capillarization of the sinusoids. Resident macrophages become activated and begin to secrete cytokines and chemokines. Lymphocytes will also infiltrate the injured tissue and evoke a heightened inflammatory response. Lastly, but of highest importance, is activation of the non-parenchymal hepatic stellate cell population [6-8]. Hepatic fibrosis is initiated by increased secretion and deposition of ECM proteins, primarily type I collagen, by the hepatic stellate cell (HSC) and hepatic myofibroblast pools. Comparable to normal ECM conditions, type I and III collagens are abundant, but injurious conditions contribute to the rise in type I over type III collagen [9-10]. Accompanying increased collagen deposition is decreased fiber degradation resulting from suppression of matrix metalloproteinase (MMP) activity and increased expression of tissue inhibitor of metalloproteinases (TIMPs). MMPs are subdivided into five categories: interstitial collagenases, gelatinases, stromelysins, membrane-type collagenases, and a metalloelastase (MMP-12). MMP1 is the predominant interstitial

collagenase in humans, while MMP8 and 13 serve identical function in rodents [11-12]. A variety of inflammatory cytokines and growth factors stimulate expression of MMP13, which is synthesized by both parenchymal and non-parenchymal liver cells. The imbalance in fibrinolysis and fibrinogenesis is also regulated by TIMP expression. TIMPs 1, 2, 3 and 4 inhibit target MMPs by directly binding to catalytic domains. In addition to regulation of MMP expression, TIMP 1 indirectly inhibits HSC apoptosis [13]. Attempts to tilt the delicate balance of MMPs and TIMPs has been examined as a therapeutic approach. Overexpression of MMP8 via adenovirus abrogated carbon tetrachloride (CCl_4) and bile duct-ligation (BDL) models of hepatic fibrosis in rats [13-14].

Fibrotic scarring is inevitable in the presence of high ECM turnover, with a close topographical relationship between inflamed areas of the liver and those that develop fibrosis. A wide range of cytokines and soluble signals are implicated as fibrogenic mediators, including transforming growth factor beta (TGFβ) through its regulation of collagen, TIMPs and MMPs. Histological patterning of scar matrix are consistent in patients with cirrhosis regardless of etiology; however, initial location of inflammation and scarring in earlier disease states are stimulus specific.

Despite recent advances in uncovering cellular and molecular events governing fibrotic wound-healing, no drug has been FDA-approved as an effective anti-fibrotic agent, underscoring the need for novel therapeutic approaches. In the lack of clear clinical progress, the organ itself aids in sustaining life and function of the fibrotic patient, as immense regenerative capacity of the liver, specifically hepatocytes, lends to slow disease progression. Although etiologies of chronic liver disease are variable, fibrosis remains the underlying commonality and thus of high interest in treatment of

chronic liver disease. While recent studies have turned focus to additional sources of circulating fibrocytes within the liver as fibrogenic mediators, the majority of research to date has been placed on understanding contributions made by stellate cells, which have long been considered the main effector cells of hepatic fibrosis [2, 13-15].

Hepatic stellate cells

HSCs once referred to as Ito cells, are lipid-rich cells found within the perisinusoidal space of Disse along the basolateral surface of hepatocytes with long dendritic-like processes encapsulating neighboring sinusoidal endothelial cells (Figure 1.1). Vitamin A is sequestered within the liver (50-80% of the body's stores), and resident HSCs store approximately 90% of total hepatic vitamin A. While principal cellular functions include storage of retinyl esters and subsequent secretion of retinol into portal blood flow when required, these cells also regulate hepatic microcirculation. HSCs are responsive to both vasoconstrictors and vasodilators, including endothelin-1 and nitric oxide, emphasizing the role of the cell as a liver-specific pericyte [16].

Traditionally considered of mesenchymal origin, numerous studies have also demonstrated expression of both neural and neuroendocrine markers in HSCs, and more recently an epithelial-mesenchymal transition (EMT) process has been proposed as a possible source of stellate cells, further complicating the true origin [17-18]. As HSCs expresses both neuronal (nestin, glial fibrillary acidic protein (GFAP) and p75 neurotrophin receptor) and mesenchymal markers (vimentin), the neural crest has been suggested as the point of origin [16, 19] . However, studies analyzing genetic lineage of these cells in drosophila failed to support this hypothesis, instead pointing to a mesoderm origin. It is well-established that mesoderm-derived progenitor cells give rise to both

adipocytes and neural cells, both of which express HSC markers. Of recent note, the septum transversum mesenchyme is a plausible origin, as mesenchymal cells in the septum transversum are locked into place by hepatoblasts and endothelial cells during development [20]. This hypothesis has been validated in a mouse model in which cell lineage analysis was performed using ROSA26 reporter mice with cre-recombinase driven by mesoderm specific gene (mesoderm posterior-1, MesP1) promoter [21-22].

Stellate cells, named for their star-like morphology, comprise a mere 1.4% of total liver volume with approximately 4-6 HSCs : 100 hepatocytes. Under normal physiological conditions the HSC resides in a quiescent lipid-rich state (Figure 1.2), serving functions described previously. However, following hepatic injury, microenvironment-derived signals (primarily increased cytokine levels) stimulate activation of HSCs, wherein they transdifferentiate from a quiescent vitamin A storing cell to a myofibroblast-like cell (Figure 1.2). Myofibroblasts mediate the process of wound-healing in several solid organs. Not normally found in healthy tissues, sources of trauma, inflammation and infection stimulate the generation of myofibroblasts through transdifferentiation of resident cells [15, 23].

Hepatic stellate cell transdifferentiation

The HSC transdifferentiation process is highly complex with a multitude of changes occurring in cellular morphology and patterns of gene expression (Figure 1.3). The quiescent phenotype possesses various adipogenic features tightly regulated by expression of peroxisome proliferator activated receptor gamma (PPARγ), the master regulator of adipogenesis [16]. The phenotypic shift from an adipogenic genetic profile to the myofibroblast is mirrored in the process of adipocyte differentiation. Like adipocytes,

HSCs store high concentrations of triglycerides in addition to retinyl esters. Additionally, both quiescent HSCs and adipocytes express type IV collagen as opposed to activated HSCs and pre-adipocyte fibroblasts, respectively. Interestingly, cytokines which suppress adipocyte differentiation stimulate activation of the HSC [epidermal growth factor (EGF), transforming growth factor alpha (TGFα), and interleukin-1β (IL-1β)] [24-26].

Once recognized by autofluorescence, retinyl esters, and expression of GFAP, newly activated HSCs are characterized by expression of cytoskeletal protein smooth muscle-alpha actin (αSMA) [27]. Parallel activation of resident macrophages (Kupffer cells), infiltration of monocytes and damage to parenchymal cells spur initiation of HSC activation through release of soluble factors [19, 28]. Platelet-derived growth factor (PDGF) and TGFβ are secreted into the hepatic microenvironment and bind to HSC surface receptors promoting the activated genetic program of the cell, stimulating pro-fibrotic intracellular signaling cascades. Concomitant with activation, increased proliferative and contractile properties are obtained promoting sustained HSC activation (Figure 1.3). Classically the process of HSC transdifferentiation has been subdivided into initiation and perpetuation phases, each categorized by unique cellular and molecular events [16].

During initiation of transdifferentiation (termed pre-inflammatory stage), changes in gene expression and cell phenotype prime the HSC to respond to paracrine signaling, predominantly from damaged hepatocytes and increased surrounding reactive oxygen species (ROS) [29-30]. Perpetuation of HSC activation involves both autocrine and paracrine signaling pathways which regulate retinoid loss, contractility, proliferation and general fibrogenic features of the activated phenotype. Classic initiation factors include

hepatocyte growth factor (HGF), vascular endothelial growth factor (VEGF), interleukin-6 (IL-6) and, most notably, TGFβ [16].

Increased circulation of these and other proinflammatory factors from injured hepatocytes triggers HSC activation. Importantly, apoptotic fragments released by hepatocytes are received as fibrogenic signals by both HSCs and Kupffer cells. During this process cytochrome (CYP) P450 enzymes are synthesized which generate ROS and stimulate increased collagen expression. The parallel process of Kupffer cell activation contributes to stellate cell transdifferentiation through cytokine signaling, predominantly TGFβ [31-32]. Additionally, as a consequence of hepatic fibrogenesis, gut permeability facilitates increased circulating levels of lipopolysaccharide (LPS), which can trigger an immense inflammatory response simultaneously activating macrophages and HSCs [33]. It is well-established that cirrhotic patients exhibit increased LPS in systemic and portal blood tracts. In addition to predominant cytokines initiating HSC and Kupffer cell activation [34], direct interaction of LPS and fibrotic signaling components (e.g. toll-like receptors, TLRs) further stimulates fibrotic gene expression and sustained HSC activation [35]. Like resident liver macrophages, human HSCs express TLR4 and are able to respond to LPS stimulation. TLR4 and co-receptors MD-2 and cluster of differentiation-14 (CD-14) transmit immunogenic signals to induce activation of Nuclear Factor-kappaB (NF-κB) and c-jun n-terminal kinase/activator protein-1 (JNK/AP-1) signaling pathways in activated HSCs [36-37]. Following LPS treatment, TLR4 activation up-regulates various chemokines including monocyte chemotactic protein-1 (MCP-1) and RANTES (regulated upon activated, normal T cell expressed and secreted) and down-regulates expression of bone morphogenic protein (BMP) [37]. TGFβ signaling is also increased as

a consequence of active TLR4 [38]. Studies utilizing HSCs isolated from collagen promoter-driven GFP transgenic mice exhibited increased collagen promoter activity when stimulated with LPS, with synergistic effects observed when cells were pretreated with LPS followed by TGFβ [38]. HSCs also express TLR2, a receptor for gram positive bacterial cell wall components, and TLR9, which recognizes bacterial unmethylated cytosinephosphoguanine (CpG)-containing DNA and induces transdifferentiation of HSCs in the presence of denatured DNA from apoptotic hepatocytes [33]. Functional genomic scans of chronic HCV patients identified seven single nucleotide polymorphisms (SNPs) that may predict risk of developing cirrhosis, with TLR4 T3991 SNP serving as the second most predictive [39]. Taken together, TLR signaling appears critical in activation of HSCs in the context of fibrosis.

Following initial robust paracrine signaling, the perpetuation phase describes distinctive changes in cellular behavior dictated by a wide array of soluble factors that cause a net effect of full myofibroblast genetic reprogramming. Post-liver injury, HSCs and other myofibroblasts migrate to sites of tissue injury to participate in active wound repair through secretion of ECM components [40]. Connective tissue growth factor (CTGF) serves as a fibrogenic signal for HSCs, observed to stimulate progression of non-alcoholic steatohepatitis (NASH) to fibrosis by increasing proliferation and chemotaxis [41]. HSCs are known to migrate towards several cytokine chemoattractants, among which PDGF is most prominent [42]. PDGF-stimulated HSC chemotaxis involves movement of the cell body towards the stimulus, concurrent spreading at the leading edge of the cell and retraction of the lagging edge. These processes are highly linked to myosin phosphorylation events and non-muscle myosin isoforms are reported to be involved in

stellate cell migration [43-44]. Expression of αSMA is increased with HSC transdifferentiation which confers increased migratory and contractile properties. Portal hypertension is a major complication of fibrosis/cirrhosis characterized by increased vascular resistance resulting in dangerous elevations in portal pressure and tissue-specific hypoxia [45]. As noted previously, HSCs are responsive to vasomodulatory signals and in hepatic injury HSCs are capable of constricting single sinusoids, thereby impeding blow flow. Following acute injury, contractile properties of the HSC prevents toxic blood flow to the liver; however, chronic disease states are associated with a permanent contractile HSC phenotype, disadvantageous to organ function [46].

Factors contributing to the perpetuation phase of activation all serve a common purpose to increase the myofibroblast-like nature of the cell (i.e. increasing proliferation, contractility, chemotaxis and fibrotic gene expression). Following adequate tissue repair, decreased inflammatory signals and withdrawal of the injurious stimulus, the next proposed stage in transdifferentiation is resolution [2, 47-48]. However, fate of a single HSC is unclear; some have speculated a reversion to quiescence while others indicate programmed cell death will clear cells from the newly repaired area [48-51]. Conversely, studies have also indicated activated cells become highly resistant to apoptotic signals, which in turn only perpetuates the fibrotic response through sustained HSC activation [52].

Prominent signaling components and pathways in HSC transdifferentiation

Hormone and neurotrophic signaling

Past decades of research have illustrated key pathways regulating the process of HSC activation, including initiation and perpetuation phases. The intrinsic lipocyte nature of the HSC in coordination with the known role of adipokines in mediating non-alcoholic fatty liver disease (NAFLD) has drawn investigators to examine adipokine signaling pathways that may regulate HSC activation. Adipokines are classically derived from adipose tissue, but are produced by resident hepatic cells including the HSC. Leptin is known to promote HSC-mediated fibrogenesis and increase levels of TIMP1 through stimulation of the janus kinase (JAK) and signal transduction and activator of transcription (STAT) signaling pathway [53-55]. Leptin also induces HSC transdifferentiation through repression of PPARγ, which regulates and maintains the quiescent program of the cell. In a positive feedback loop, increases in leptin hormone and leptin-mediated signaling are further increased following transdifferentiation as expression of leptin receptor (OB-R) is significantly up-regulated in activated HSCs [56-57].

Additional hormonal mediators contribute to hepatic fibrosis, including thyroid-enhanced HSC activation and disruptions to the hypothalamic pituitary gonadal axis resulting in altered levels of androgens and estrogens [58-59] . Recent studies from our laboratory have shown that adrogenization increases susceptibility to alcohol-induced liver damage and that estrogen replacement in adulthood appears protective. In addition to pituitary-derived signals, neurotrophic factor signaling, specifically opioids, promote HSC transdifferentiation (increased proliferation and collagen production) and have

recently been investigated for anti-fibrotic therapy through use of receptor-antagonists [60-61]. Our lab recently reported that Nalmefene, a derivative of the opioid receptor antagonist Naltrexone, exerts immunomodulatory activity and decreases HSC activation in vitro. Another morphinan derivative, JKB-119, lacking receptor antagonism, also decreased HSC activation and significantly decreased hepatic injury in an in vivo model of acute inflammation [62]. Following liver injury, neuroendocrine factors are up-regulated, and activated HSCs transduce these signals via specific receptor expression, of which highly fibrotic cannabinoid (CB) signaling is of current research interest [63-65]. Endogenous HSC cannabinoid 2-AG increases CB1 receptor (CB1R) and subsequent pro-fibrotic target gene expression. Efforts to develop CB1R antagonists have been successful in pre-clinical animal models with treatments leading to decreased steatosis and inflammation [63]. Conversely, studies have shown CB2 receptor to possess anti-fibrotic hepatoprotective properties [66]. In cirrhotic rats CB2 agonist treatment attenuated fibrosis and CB2 knockout mice exhibited delayed liver regeneration in a CCl_4 model of liver injury [65].

Wnt signaling

Canonical Wnt signaling is also prominent in regulation of HSC transdifferentiation. The Wnt signaling network is comprised of secreted glycoproteins, Wnt family ligands, and both frizzled and low density lipoprotein receptor-related protein (LRP) families of receptors. The classical pathway involves β-catenin stabilization and subsequent gene expression, notably those involved in cell cycle progression [67-68]. Specifically, Wnt ligands bind to frizzled receptors to induce and increase β-catenin and up-regulate transcription of target genes. In the absence of ligand binding, the

axin/glycogen synthase complex-3/adenomatous polyposis coli (axin/GSK-3/APC) complex promotes proteolytic degradation of β-catenin and interrupts intracellular signaling [69]. Wnt proteins Wnt10b and Wnt3a are expressed in activated HSCs and are known to suppress adipocyte differentiation via PPARγ and CCAAT-enhancer-binding protein (C/EBPβ) inhibition. Forced expression of co-receptor antagonist Dikkopf-1 initiates reduction in nuclear β-catenin thereby restoring expression of PPARγ and converting myofibroblasts to quiescent cells capable of lipid retention [69]. Already reported to promote differentiation of both skeletal and smooth muscle cells and inhibit differentiation of adipocytes, Necdin is a new contributor to this classical pathway. Necdin directly interacts with the Wnt10b promoter in activated HSCs inducing Wnt expression [70]. Site-directed mutagenesis of the promoter binding site abrogated necdin-mediated Wnt expression. Interestingly, silencing of this protein not only inhibited Wnt10b expression, but also reduced methyl-CpG-binding protein 2 (MeCP2) and histone 3 lysine 2 (H3K2) methylation which prohibits reversion of the HSC phenotype [70].

Growth factor signaling

PDGF signaling is perhaps one of the most well-described cascades regulating HSC activation [15-16, 71]. The principal mitgogen for mesenchymal cells consists of a family of A, B, C and D polypeptides which promote cell migration, proliferation and survival by binding to cognate receptors, PDGFRα and PDGFRβ. Following ligand-receptor binding, dimerization of receptor subunits is observed and tyrosine residues within the intracellular domain are phosphorylated. This single event leads to activation of phosphatidylinositol 3-kinase-Akt (PI3K-Akt) and Ras-mitogen activated protein

kinase (Ras-MAPK) pathways which regulate pro-fibrotic gene expression. Activation of Ras in turn activates serine threonine kinases of the Raf-family, which subsequently phosphorylate MAPKK/MAP kinase kinase (MEK 1/2) activating extracellular regulated kinases (ERK 1/2). Once activated ERK 1/2 translocates to the nucleus to act as a regulator of gene expression, including those genes involved in cell cycle progression, apoptosis resistance and ECM remodeling [43, 71-72]. Previously, PDGF has been viewed as a promising target for pharmacological inhibition. Tyrosine kinase inhibitory compounds, such as Sorafenib, have proved moderately effective in treatment of HCC, a disease with underlying fibrosis, and may elicit similar effects in rodent models of strict hepatic fibrosis [73]. During perpetuation, canonical Akt signaling is stimulated by PDGF, leptin and other soluble factors. Parallel to Akt, JNK is activated by PDGF and additional factors upstream of MAPK affecting growth and cell survival signals. Inhibition of JNK in mice resulted in diminished fibrogenesis indicating that it too may serve as a potential target [40, 42].

Signals propagated by EGF and TGFα also stimulate the proliferative phenotype of the HSC, and again, via autocrine signaling, those same HSC-secreted growth factors are necessary to facilitate paracrine hepatocyte proliferation required during liver regeneration [55, 74-75]. Responsiveness to growth factors, of which only a select few have been described, initiates remodeling of the inflammatory milieu predominated by fibrillar collagens. A positive feedback loop is also established at this stage of disease wherein additional matrix-bound growth factors, notably TGFβ, are released as a byproduct of increased matrix stiffness and protease activity [32]. HSCs are not only an

important source of growth factors, but also of hepatic cytokines, underscoring the importance of autocrine control of HSC activation.

Cytokine and chemokine signaling

HSCs secrete and respond to pro-fibrotic cytokine signals, complicating our understanding of regulatory networks in a classical sense. Specifically, continual wound-healing perpetuated by HSC activation is associated with increased IL-6 expression/signaling as a byproduct of hepatocyte injury. Circulating IL-6 through binding of specific IL-6 receptors subsequently recruits two molecules of glycoprotein 130 (gp130) to initiate the signaling cascade in the HSC [23, 76]. Classically, signal transduction is carried out by JAK2/STAT3; however, IL-6 may also propagate signals through parallel growth factor cascades. IL-6-ligand binding results in up-regulation of the acute phase response during immunogenic reaction to hepatic injury and perpetuation of HSC activation [76]. Inflammatory responses within the liver are also modulated by chemokine signaling pathways. Several chemokines and chemokine receptors are secreted and expressed by the HSC [77]. Recent work has identified specific chemokine receptors (CCR), CCR1 and CCR5, as fibrogenic factors as they generally promote migration of the HSC and subsequently enhance fibrosis by increasing inflammation [78]. Induced by NF-κB signaling, CCR5 stimulates HSC migration and proliferation, and CCR5 deficient mice are associated with markedly reduced hepatic fibrogenesis in both CCl_4 and BDL models of hepatic fibrosis. Conversely, chemokines can be anti-fibrotic. CXCR3 knockout animals were shown to have a prominent pro-fibrotic phenotype, further substantiating the need for a deeper understanding of the chemokine impact on fibrotic disease progression and possible reversion [79].

Persistent inflammatory signaling is a critical component preceding and corresponding to levels of hepatic fibrogenesis. Activated HSCs secrete and respond to inflammatory cytokines and through expression of specific adhesion molecules (e.g. inter-cellular adhesion molecule-1, ICAM-1), interact directly with populations of immune cells [80]. Amplification of fibrotic signals is produced by an intact positive feedback loop wherein activated HSCs stimulate inflammatory responses from immunogenic cells, which in turn secrete cytokine signals that are recognized and interpreted by the HSC [81]. However, certain classes of immune cells, specifically natural killer cells, act independent of the positive feedback loop and maintain anti-fibrotic properties as they kill activated HSCs through production of interferon gamma (IFN-γ) [82]. Several ongoing studies are examining the key interplay between HSCs and resident and infiltrating immune cells in fibrosis development and progression [83].

In the hepatic microenvironment, TGFβ signaling regulates cellular wound-healing responses including ECM production, growth and apoptosis. TGFβ is widely acknowledged as the most potent fibrogenic cytokine regulating HSC-mediated fibrosis (Figure 1.4) [84-85]. TGFβ along with 35 structurally related proteins comprise the TGFβ superfamily, which includes three isotypes of the cytokine (β1, β2, β3). Intracellular cleavage of pro-TGFβ produces latency-associated peptide (LAP) and mature TGFβ (C-terminal fraction) together forming a biologically inactive small latent complex. The secreted large latent complex is then formed when the small complex is paired with a latent TGFβ binding protein [85-86]. While not directly synthesized by intact hepatocytes, necrotic hepatocytes along with activated Kupffer cells and infiltrating immune cells, are sources of secreted large latent complex TGFβ [32, 85]. Matrix

fixation of the large latent complex is a pre-requisite for activation of the cytokine by proteases. Upon activation, TGFβ binds to the heteromeric receptor complex containing TGFβ type I (TGFβRI) and II (TGFβRII) receptors. Both autocrine and paracrine signaling propagates through the SMAD family of transcriptional activators. In the presence of TGFβ ligand, receptor-activated SMADs (R-SMADs), SMAD 2 and 3, are phosphorylated directly by TGFβRI kinase. Following phosphorylation, R-SMADs bind to common mediator SMAD4 and translocate to the nucleus to induce pro-fibrotic gene expression [32]. TGFβ plays a central role in mediating cellular crosstalk between inflammatory and collagen producing cells. Following liver injury, blood and tissue TGFβ levels are elevated stimulating the fibrotic response as both Kupffer and hepatocytes release the cytokine into the inflammatory milieu, inducing differentiation of neighboring cells. TGFβ signal transduction plays a critical role in establishment of the myofibroblast phenotype, as it directly up-regulates hallmarks of activation (αSMA and collagen), propelling the disease state forward. Sustained TGFβ signaling increases matrix synthesis and HSC proliferation, marking the perpetuation phase of transdifferentiation (Figure 1.4) [15, 87].

Multiple points of intervention within TGFβ signaling have been targeted to ameliorate and/or reverse fibrosis. Previous studies have shown that antioxidant S-adenosyl-L-methionine (SAMe) exerts hepatoprotective effects. In a two-hit model of fibrosis, animals treated with SAMe displayed decreased TGFβ and SMAD3 mRNA corresponding to significantly decreased fibrosis [88]. Recently, in vitro studies have shown that SAMe significantly decreases type I collagen in activated HSCs, a mechanism mediated by increased polyubiquitination [89]. Overexpression of negative regulator

SMAD7 or inhibition of TGFβ receptors (soluble receptor and knock-out models) decreased hallmarks of HSC activation, particularly type I collagen and αSMA, dramatically blunting chronic wound-healing [84, 90]. Anti-fibrotic potential of adenoviral vectors expressing truncated TGFβRII significantly reduced as well as reversed dimethylnitrosamine (DMN)-induced fibrosis in several studies [85]. In vitro and in vivo (BDL) experiments demonstrated antisense mRNA and monoclonal antibodies against TGFβRII abrogated TGFβ signaling and HSC activation accompanied by additional tumor suppressive effects, [91-93] emphasizing the importance of this signaling cascade in the foundation of and perpetuation of HSC-mediated hepatic fibrosis.

While the aforementioned classical pro-fibrotic signaling pathways are more elucidated than newly emerging pathways (Wnt, leptin, cannabinoid), further experimentation is still required to fully understand the exact mechanisms by which these pathways are governed and potential mechanisms of crosstalk in transdifferentiation of the HSC.

Transcriptional regulation of HSC transdifferentiation

Changes in gene expression are required for HSC transdifferentiation to occur, as several signaling cascades become suppressed or activated during this critical transition period [94]. Mechanisms of gene regulation are complex and include a wide array of factors extending beyond traditional transcription factors (activators and repressors). In recent years epigenetic regulation of HSC activation has been uncovered providing new areas of translational research. Transition from a quiescent to activated stellate cell is accompanied by modulation of hundreds of genes. The shear plasticity of the HSC

facilitates this change and promotes cellular responsiveness to a variety of external cues, including inflammatory mediators and circulating fibrotic molecules. Several types of transcription factors have been described in detail for their roles in regulating transdifferentiation.

HSCs express several basic helix-loop-helix transcriptional regulators, including MyoD, sterol regulatory element binding protein-1C (SREBP-1C), c-myb and c-Myc. Specifically, expression of c-myb is induced with HSC activation both in vitro and in vivo [95]. Studies have demonstrated interaction of c-myb with the αSMA promoter leading to heightened protein expression. Additional studies in rat HSCs transduced with a c-myb antisense gene displayed diminished expression of not only αSMA, but also type I collagen and TGFβ accompanied by decreased cell proliferation [96].

The family CCAAT-enhancer-binding protein C/EBP family of transcription factors are also well noted in HSC literature as determinants of collagen expression [95, 97-98]. While actions of the beta isoform appear to involve regulation of collagen expression by binding to a TGFβ responsive element in the presence of hydrogen peroxide (ethanol metabolite), opposite effects are seen with isoform α. Expression of C/EBPα is decreased in HSC transdifferentiation with forced expression in activated HSCs proving inhibitory to proliferative and fibrogenic signals, with additional in vivo studies pointing towards a role as a negative regulator of ECM production [97].

Well known Kruppel-like transcription factors (KLFs) bind to GC-rich and related CACCC boxes found in regulatory regions of pro-fibrotic genes, notably collagens. Stellate cells express several KLFs, including KLF6 and KLF10 [95, 99]. Like KLFs, highly related zinc-finger specificity protein 1 (Sp1) enhances procollagen gene

transcription via promoter binding. Additional crosstalk with SMAD3, transducer of classical TGFβ signaling, facilitates enhanced collagen promoter activity by Sp1 [100-102]. KLF6 is dramatically induced during the early phase of HSC activation which coincides with increased suppression of the quiescent program. KLF6 stimulates transcription of collagen and TGFβ along with cognate receptors TGFβRI and TGFβRII [103-104].

TGFβ achieves pro-fibrotic signaling action via HSC activation. After the signaling cascade has been triggered, phosphorylation of SMAD2/3 on specific serine residues occurs inducing R-SMADs to complex with Co-SMAD4. SMAD dimers then translocate to the nucleus to drive downstream target gene expression. SMAD7 serves as an inhibitory SMAD via interactions with cell surface receptors (via ubiquitination, or inactivation by deposhophorylation) [86]. HSCs express several SMAD transcriptional regulators, with in vitro data indicating expression of SMAD2 during initiation phases of activation, whereas SMAD3 is only detected in fully transdifferentiated cells [105]. In the setting of fibrosis, expression of the negative regulator SMAD7 is silenced which alleviates suppression of fibrotic signaling derived from the SMAD2/3/4 complex. In a rodent model of CCl_4-induced liver fibrosis utilizing SMAD3 knockouts, suppression of procollagen gene expression and HSC proliferation were observed [106]. Additional studies by Dooley et al. have shown attenuation of fibrosis in vivo via forced overexpression of SMAD7 (adenoviral delivery) results in inhibition of R-SMADs and marked down-regulation of type I collagen and αSMA expression [107]. Crosstalk between TGFβ and additional transduction pathways, including ERK1/2 and BMP,

occurs via SMADs further affirming the powerful properties of these transcriptional regulators [42].

Human HSCs also express high levels of pregnane X receptor (PXR), which functions as a strict liver and intestine xenobiotic receptor activated by steroids and antibiotics [108]. Activation of PXR, through a series of molecular events, leads to up-regulation of CYP3A, facilitating metabolism of ~60% of prescription drugs. PXR maintains a regulatory role in lipid homeostasis through inhibitory actions to bile and metabolic signaling pathways [109]. Rifampicin antibiotic treatment targets PXR and results in inhibition of TGFβ and Wnt signaling pathways, attenuating fibrosis with long-term treatment reducing proliferative capacity and activation of the HSC [108]. In contrast to the human condition, rodent HSCs do not express this particular receptor, as knockout mice were unresponsive to PXR activator pregnenolone-16alpha-carbonitrile [110].

To compliment the retinoid storage capacity of quiescent HSCs, expression of both retinoid x receptor (RXR) and retinoic acid receptor (RAR) transcriptional regulators is observed. Following ligand binding and nuclear translocation, both factors bind to respective response elements to stimulate target gene transcription [111]. However, studies examining the role of these receptors in HSCs have been conflicting. While Milliano and Luxon demonstrated RAR subtypes were down-regulated upon culture-activation , others have shown RARα expression to be increased in the activated phenotype indicative of retinoid responsiveness [112]. All-trans-retinoic acid (ATRA) and 9-cis retinoic acid are ligands for RAR and RXR, respectively. Interestingly, while ATRA suppresses collagen expression without affecting proliferation, binding of 9-cis-

RA suppressed both type I collagen synthesis and HSC proliferation [113]. Studies employing agonists to further elucidate protective effects of these transcription factors have been successful in vivo [114], with RXRα transfection along with vitamin A administration attenuating the fibrotic response in mice.

As briefly mentioned previously, quiescent HSCs do express transcription factors such as C/EBP and SREBP-1C, which along with liver X-receptor alpha (LXR-α) and PPARγ, regulate transdifferentiation of adipocytes [115]. All aforementioned factors are silenced during HSC activation and forced expression of both PPARγ and SREBP-1C has been shown to reverse cells to the quiescent phenotype denoted by restored vitamin A and lipid storage capacity. PPARs are key regulators of fat metabolism and lipid retention, and all isoforms (α, β, γ, δ) are expressed in the HSC [116-117]. PPARγ has received the most attention in the past two decades for its multifunctional role in adipocyte differentiation and transcriptional co-factor role in the dimerization of RXR [118]. Forced expression of the down-regulated nuclear receptor in activated HSCs stimulates partial reversion of the fibrogenic phenotype, marked by decreased type I collagen, inhibition of TGFβ signaling and subsequent re-expression of additional adipogenic transcription factors [116, 119]. Recent studies on the role of natural antioxidant curcumin as a fibrotic treatment attributed its protective effects to re-expression of PPARγ and abrogation of inhibitory SMAD-PPARγ promoter site binding [120-122]. The intricate role of PPARγ in reversal of HSC activation has been studied in depth, demonstrating both natural and synthetic ligands for PPARγ are able to suppress activation. Additionally, elegant studies by Mann et al. revealed a novel epigenetic mechanism by which PPARγ expression is lost during HSC activation, and through both

in vitro and in vivo manipulation studies, restoration of PPARγ and reversion of fibrogeneis was achieved [123]. The interplay between this master regulator of HSC transdifferentiation and other nuclear receptors, notably RXR and RAR, hold clinical promise as combination ligand treatment in culture-activated HSCs demonstrated a synergistic anti-fibrotic effect [95].

NF-κB is as a master regulator of immune/inflammatory signaling pathways. Hepatic functions of NF-κB also include regulation of wound-healing in fibrosis. NF-κB is composed of 5 subunits, which hetero or homo-dimerize to form NF-κB and exert transcriptional influence by binding to distinct consensus sequences. Studies utilizing p50 subunit knockout mice showed increased susceptibility to inflammation and fibrosis [124]. Following stimulation from various factors, including tumor necrosis factor-alpha (TNF-α) and LPS, IκBα is phosphorylated by IκB kinase (IKK) on specific serine residues resulting in proteosome-mediated degradation of IκBα. Removal of the inhibitor enables NF-κB to translocate to the nucleus and regulate transcription of target genes. NF-κB proteins are not restricted to one phenotype of the HSC; however, levels of transcriptionally active NF-κB are markedly increased post-activation. Proinflammatory genes IL-6, IL-8 and ICAM-1, require NF-κB for adequate expression in the activated HSC. NF-κB activation also produces anti-apoptotic signals; however stimulation of activated human HSCs with NF-κB inhibitors results in apoptosis [125-126]. Mann and colleagues have examined the mechanism by which NF-κB activation is essentially reprogrammed in the activated HSC [123]. Constant suppression of IκBα expression is observed post-HSC activation, which creates a paradox as NF-κB is transcriptionally active. The suppression has been attributed to a transcriptional repressor, CBF1, which is

induced during culture-activation prohibiting binding site access [123]. Additional properties of the DNA itself lend to repression, as methylation patterns recruit additional repressor molecules including methyl-CpG binding proteins and other epigenetic factors.

Post-transcriptional regulation of HSC transdifferentiation

Coordinate changes in gene transcription and simultaneous transcriptional repression occur during transition of quiescent to activated HSCs. For transdifferentiation to occur, it appears the quiescent genetic program must be suppressed, namely through silencing of PPARγ, for activation of the myofibroblast program to begin [127-129]. Recently, studies have provided evidence for epigenetic regulation of HSC transdifferentiation [127, 129]. Alterations in HSC phenotype/gene expression arise during development, transdifferentiation and disease; however, these variations are not associated with changes to the underlying DNA sequence and are thus termed epigenetic [130]. Epigenetic regulation through methylation of DNA has been well described. This process occurs through addition of a methyl group to the 5' position of cytosine residues in the CpG dinucleotide. Site-specific DNA methylation induces repression of gene expression, whereas unmethylated CpG sites correspond to genes that are constitutively expressed [130-131].

In recent years focus of epigenetic research has shifted to include a broader range of epigenetic mechanisms, with a concentration on modifications to chromatin structure. The unit of chromatin structure consists of 146 base pairs of DNA wrapped around an octamer of histones (H) containing two copies of H2A, H2B, H3, and H4. Higher-order chromatin is essential for functional organization of chromosomes as well as epigenetic gene regulation. Histone modifications have been identified as important epigenetic

mechanisms that influence chromatin structure. Modifications include, but are not limited to, methylation, acetylation and phosphorylation. Distinct modifications of histone tails regulate transcriptional "on" or "off" states and influence condensation state of chromatin and thus accessibility of transcription factors [132-133]. Post-translational modification of the histone N-termini, especially in the case of H3 and H4, have been well described in drosophila and more recently in higher-order vertebrates. Several groups have identified key lysine (K) residues on histone tails that once "marked" with modifications can then be interpreted by transcriptional complexes to give rise to specific phenotypes. Histone H3 when methylated at K9 or K27 conventionally leads to transcriptional repression, whereas methylation at K14 or K36 leads to transcriptional activation [130-131, 133-135]. Histone marks that initiate repression are applied by different enzymes and complexes, including polycomb group proteins.

A recent publication by Mann et al. examined the role of epigenetics during HSC transdifferentiation [123, 128]. Treatment of HSCs with a global DNA methylation inhibitor (5-aza-2-deoxycytidine) prevented quiescent HSCs from transdifferentiating into myofibroblast-like cells [123]. Further examination of transdifferentiation markers revealed a significant increase in both IκBα and PPARγ expression. Additionally, MeCP2 was directly implicated in this process. MeCP2 has been shown to promote repressed chromatin structure and was only detected in the activated/myofibroblast-like form of the HSC. However, MeCP2 knockdown by RNA interference does not alleviate gene repression completely, indicating involvement of other mechanisms [136]. For MeCP2 and several other methyl-CpG-binding proteins to contribute to repression, they must first

be recruited to the target gene and studies have shown this process is mediated by polycomb group proteins [137-139].

CBF1 and MeCP2 contribute to methylation of CpG islands during stellate cell transdifferentiation [95, 123]. Levels of both factors are low in quiescent HSCs, contributing to heightened expression of IκBα and inhibition of pro-fibrotic NF-κB activity. When expression of CBF1 and MeCP2 are increased, NF-κB is disinhibited promoting sustained HSC activation. Additional studies by this group have expanded our knowledge of this regulatory network, wherein PPARγ is the target of epigenetic silencing by MeCP2. The transcriptional silencing is a product of a series of molecular events in which a specific microRNA (miR 132) is markedly reduced as a result of HSC activation resulting in overexpression of MeCP2, which binds to the PPARγ promoter region to displace RNA polymerase-II. H3K9 methylation as a marker of transcriptional repression is observed at the 5'end of the target transcript [128]. In concert with MeCP2 is enhancer of zeste homolog 2 (EZH2), a constituent of the polycomb repressive complex, which induces chromatin modifications necessary for sustained repression [128]. Treatment of quiescent HSCs with an EZH2 inhibitor prevented activation in vitro. These seminal studies provide the first clear link between microRNAs, epigenetic machinery and vital transcripts in HSC transdifferentiation.

Post-transcriptional regulation of gene expression involves numerous modifications to the mRNA, including alterations at both 5' and 3' ends in addition to splicing of transcripts. The 3' untranslated regions (UTR) of mRNAs contain key stability elements subject to various regulatory proteins as well as miR binding sites. miRs are small non-coding RNAs which regulate gene expression through perfect

complementarity of the miR to the target sequence, inducing mRNA instability and subsequent endonucleolytic cleavage or alternate 5' modifications [140]. Imperfect base pairing with the 3' UTR of target mRNAs results in gene translation inhibition [141]. Research focusing on miR modes of action has primarily examined interactions with the 3' UTR of target genes; however, recent studies have expanded our knowledge, demonstrating miRs can interact with the 5' UTR as well as with DNA methylation machinery and affect chromatin status [142]. Since their discovery in 1993, miRs have been described in all multicellular organisms and are associated with a breadth of biological functions including proliferation, cellular differentiation, immunity as well as tissue remodeling and various human disease states, notably cancer [143]. Although much remains to be learned, miRs have already been shown to influence expression of many mRNAs and proteins important in liver homeostasis, health and disease.

Commonalities of miR expression can be seen among fibrotic disorders of different organ systems, including both cardiac and renal fibrosis, with an overarching effect of the miR 29 family in regulation of cellular differentiation and in translation of ECM [144]. Additionally, miRs involved with translation of pro-fibrotic TGFβ/SMAD signaling are shared amongst pathologies. Roderburg et al. examined miR expression profiles in a CCl_4 rodent model of hepatic fibrosis [145] and microarray analyses revealed 31 differentially expressed miRs, 10 of which were overexpressed in fibrotic tissue, including miRs 125-p, 199b, 221, and 302c. Marked down-regulation was observed in a pool of 21 miRs; specifically, miR 29 family members were significantly reduced. Additional experiments in an alternate model of fibrosis (BDL) confirmed miRs 29b/c were significantly reduced compared to sham controls. Down-regulation of miRs

29a/b/c was also observed in explanted liver samples with patients denoted by a Desmet fibrosis score of 2-4. Interestingly, low plasma levels of miR 29a correlated with advanced stage liver fibrosis in human patients. The hypothesis that low miR levels in tissue correlate with low miR in the circulating plasma is in opposition to recent hypotheses that an inverse correlation between tissue and plasma miR concentrations exists as a byproduct of vesicle-mediated miR release [146]. Hepatic fibrosis is influenced by several epigenetic factors controlling the wound-healing response. Recent studies by Mann et al. showed that miR 132 is significantly decreased in fibrotic livers as demonstrated in two different models (BDL, CCl_4), and this down-regulation affected HSC activation [128]. Collectively, these studies emphasize that during development of fibrosis there are important changes in miR expression which regulate wound-healing transcripts; however, effects exerted by miRs appear to act in concert with other epigenetic factors to direct disease progression.

Recently, studies examined miR expression in the HSC (Figure 1.5) as a possible avenue to affect fibrogenesis development and progression. Specifically, miRs 150, 187, 194 and 207 were shown to be significantly down-regulated in HSCs isolated from BDL animals compared to sham controls, while let 7 family members were significantly up-regulated [147]. Overexpression of miRs 150 and 194 in human HSCs (LX-2) resulted in proliferation inhibition as well as decreases in type I collagen and (αSMA), hallmarks of HSC activation. Specific action of these two miRs includes inhibition of c-myb and Ras-related C3 botulinum toxin substrate-1 (Rac-1), which both contribute to development and progression of fibrosis. Additional studies examined differential expression in quiescent (day 2) and activated (day 14) rat HSCs showing 12 up-regulated and 9 down-

regulated miRs, of which 15b, 16, 122, 138, 140 and 143 were validated [148-149]. Gene ontology revealed specific linkages between the miR 15/16 family and anti-apoptotic pathways important in HSC activation. Administration of miR mimics induced B-cell lymphoma-2 (bcl-2) inhibition and subsequent apoptosis in activated stellate cells, an important aspect of potential therapeutic targeting. Additional studies by Guo et al. further demonstrated that lentiviral delivery of miR 16 greatly reduced cyclin D1 levels in addition to inhibiting proliferation and increasing apoptosis in activated HSCs [149]. More recent studies by Ogawa et al. showed that TGFβ1 or IFN-α stimulation validated in silico analyses of miR-pro-collagen [col α1(I)] mRNA binding sites [150]. miRs 29b, 143 and 218 demonstrated the highest degree of homology to the col α1(I) 3'UTR and were further analyzed. miR 29b directly bound to the 3'UTR was effective at suppressing type I collagen at both mRNA and protein levels. Potential anti-fibrotic benefit to miR 29b was also validated in vivo using a murine CCl_4 model of injury. In vitro studies conducted by Roderburg et al. also showed overexpression of miR 29b in murine HSCs resulted in decreased collagen expression and that both LPS and NF-κB are involved in the down-regulation of this miR [145]. Improved understanding of the regulation of HSC activation by miRs will undoubtedly advance our knowledge of many liver etiologies.

miRs are processed from precursor molecules into pre-miRs within the nucleus. Once exported to the cytoplasm, the hairpin is cleaved by Dicer and strand selection occurs producing a mature miR available to associate with the RNA-induced silencing complex (RISC) [151]. Seminal studies have demonstrated miR biogenesis and processing are directly controlled by constituents in the TGFβ pathway. Several miRs are post-transcriptionally induced by TGFβ and nuclear accumulation of R-SMAD proteins

promotes Drosha-mediated miR processing [152-153]. In addition to HSC-mediated actions, increased levels of TGFβ observed in fibrosis may affect disease pathology by affecting global miR biogenesis/expression.

Fibrosis resolution

Death of hepatocytes and non-parenchymal cells is a central feature of chronic liver disease despite variation in etiology. The liver performs numerous critical processes, ranging from metabolism to detoxification, which requires profuse amounts of energy reliant on aerobic strategies [3, 154]. Increased cell death and impaired tissue regeneration are commonalities in most hepatic diseases, but unlike other organs the liver is capable of regenerating from extreme cell loss through stimulation of cell cycle machinery and increased hepatocyte proliferation. For example, post-70% hepatectomy (rat), a time frame of one week or less is sufficient for the liver to regenerate to original mass [155]. However, regenerative capabilities can be stunted if cellular loss exceeds an unknown threshold. Unfortunately, in hepatic fibrosis derived from chronic ethanol abuse, rate of hepatocyte cell death exceeds regeneration time frames, allowing a window for HSCs to displace functional hepatocytes with synthesized scar matrix, compromising hepatic function culminating in organ failure [10, 156-157].

While cell death is undesirable in the parenchyma, resolution of hepatic fibrosis has been achieved through induction of apoptosis in collagen producing stellate cells. HSC-associated apoptotic mechanisms of cell death are set apart from the highly prominent necrotic death of hepatocytes, wherein cellular components are essentially spilled into the extracellular space [49, 158]. Necrosis is commonly the result of metabolic perturbations including drug-induced liver injury and hepatotoxicity, whereas

apoptotic, or programmed cell death, is a highly ordered cascade of intracellular events, initiated by the apoptotic volume decrease (AVD), designed to minimize inflammatory responses commonly provoked during necrosis.

During the AVD intracellular K+ levels decrease from 140mM to < 35mM, a pre-requisite for downstream caspase and nuclease activation [159-160]. These, and other, changes in intracellular solute concentrations result in the creation of a sustained osmotic gradient and net water loss from the cell resulting in the cell "shrinkage" characteristic of all apoptotic cells [159, 161]. Previous studies demonstrate water movement during the AVD occurs via aquaporins (AQPs) [159-160, 162]; a family of transmembrane proteins ubiquitously expressed in plant and animal cells [163]. Additionally, inhibition of AQP-dependent water movement during the AVD significantly slows the progression of apoptosis [160-161, 164]. Of the known 13 mammalian homologs [165-166], seven have been identified in the liver and play important roles in hepatobiliary physiology and patho-physiology, including cell death in hepatic tumor cells [162, 167].

Classically, following an apoptotic stimulus, the intrinsic (mitochondrial-mediated) pathway of apoptosis is activated. External cues induce proapoptotic proteins of the bcl2 family (bax, bad, bim) and subsequently activate release of cytochrome C from mitochondria. Cytosolic cytochrome C couples with Apaf-1 (Apoptotic protease activating factor-1) to form the apoptosome, where the first initiator caspase (caspase-9) is cleaved. In contrast to intrinsic pathways, extrinsic apoptosis is mediated by binding of an extracellular ligand to a specific transmembrane receptor, forming the death-inducing signaling complex (DISC). Upon activation, initiator caspase-8 is also capable of cleaving caspases 3 and 7. Once execution by either caspase-8 or caspase-9 has been

achieved, apoptotic signaling culminates in cleavage of poly (ADP-ribose) polymerase (PARP) and highly distinctive nuclear events including chromatin condensation and DNA degradation with characteristic cytoplasmic blebbing. Apoptotic cells eventually fragment into apoptotic bodies and are phagocytized by neighboring cells (primarily by macrophages). Various stimuli initiate cellular apoptosis, including death receptor ligands (Fas and TNF-α), growth factor deprivation and DNA damage [168]. Studies by Iredale and colleagues showed that in coordination with resolution of biliary fibrosis there was a significant decrease in activated HSCs denoted by decreased αSMA immunohistochemical staining which coincided with an increased rate of apoptosis [9-10].

Recovery from chronic liver injury is characterized by increased apoptosis of HSCs, subsequent reductions in TIMP levels and increased degradation of fibrous scar matrix [16]. Regression of hepatic fibrosis has been reported in various rodent models of the disease. Specific induction of apoptosis in HSCs by TNF-related apoptosis-inducing ligand (TRAIL) was achieved in studies by Tamir et al., proposing a unique therapeutic target for hepatic fibrosis, as hepatocytes do not express the necessary TRAIL-R2/DR5 receptor to progress through TRAIL-mediated apoptosis [169].

While additional factors (including doxorubicin and etoposide) typically induce apoptosis in parenchymal cells, previous studies have shown that as a byproduct of activation, newly transdifferentiated stellate cells display increased resistance to apoptotic stimuli [52]. While activated HSCs do have the capacity to undergo apoptosis via specific targeting by pro-apoptotic agents or spontaneously, increased resistance to proapoptotic signals is observed. Studies have utilized several pharmacological agents to induced

apoptosis in the HSC. Gliotoxin (GTx), perhaps best characterized of these agents, is a fungal metabolite inhibitory to NF-κB-mediated cell survival. GTx treatment induces apoptosis in both human (LX-2) and primary rat HSCs, and reduced fibrotic injury in a CCl_4 model [170-173]. Interestingly, culture-activated cells compared to freshly isolated HSCs display heighted bcl-2 expression, which could contribute to increased resistance to apoptosis [52].

Disease detection and therapeutic strategies

Chronic alcohol consumption, hemeochromatosis, NASH and severe viral infection can all lead to development of hepatic fibrosis. Of particular importance is the relationship between fibrosis and obesity. With obesity on the rise in the Western world, there is a parallel rise in NASH , which can progress to fibrosis and in some cases HCC with underlying cirrhosis [174]. Only in recent history has hepatic fibrosis been considered reversible. Removal of the etiological agent has induced reversion of the fibrotic condition in patients with hepatitis C, biliary fibrosis and autoimmune hepatitis. Experimental rodent models of hepatic fibrosis have corroborated these results and highlighted the withdrawal of proinflammatory and fibrogenic cytokines, namely TGFβ, for decreased ECM production and reduced numbers of activated HSCs [3].

Critical progress has been made in elucidating signaling pathways, transcriptional regulators and epigenetic factors governing HSC-mediated fibrogenesis. Obstacles are still present prohibiting translation of basic science advances to the clinical setting; however, with the constant influx of new technologies and collaborative efforts, several challenges of progress should be met in the near future.

One such challenge to advancement is the need for accurate disease detection/biomarkers of fibrosis disease progression. Liver biopsy, while standard care of practice, only provides a small window (~1/50,000th of the organ) into the status of liver tissue and underlying cellular microenvironment [3]. Additionally, due to the invasive nature of the procedure, a limited number of biopsies are permitted for any one individual patient. To this end, miR expression signatures have been implicated as novel potential indicators of stage and activity of disease in human patients, with recent studies showing strong correlations and predictive success between miR expression and disease outcome [175-178].

Currently there are no FDA-approved treatments for hepatic fibrosis. Outside of surgical resection, full organ transplantation is an option for certain disease states; however, the current list of patients in need of transplant far exceeds the annual donor rate [174]. While there are no drug regimes targeting transcription factors specifically in the HSC, targeting of PPARγ as well as NF-κB has been successful in other disease states [179]. A class of drugs known as glitazones, currently in use for the treatment of type 2 diabetes mellitus, stimulate insulin production via activation of quiescence regulator PPARγ; however, side-effects of this particular class of drug treatment remain substantial as liver enzymes are elevated in fibrotic patients which may counter-act benefits of glitazone therapy. Additionally, drugs targeting human PXR activation may also prove therapeutically beneficial. Rifampicin is currently prescribed for biliary cirrhosis to limit pruritus, but has also been shown in clinical trials to reduce serum levels of alkaline phosphatase (marker of liver damage) [15].

Drug targeting has been limited with regards to dominant pro-fibrotic TGFβ signaling; however, studies in rodents have demonstrated manipulation of this pathway holds therapeutic potential. Specifically, attenuation of fibrogenesis was achieved through TGFβ surface receptor and SMAD inhibition [84]. However, drug/therapy development targeting TGFβ signaling must also consider the paradoxical role of the cytokine in fibrosis, as TGFβ possesses anti-inflammatory properties and is also an important regulator of hepatocyte proliferation necessary for organ regeneration.

As is always the case, clinical applications of new discoveries, such as existence and manifold roles of miRs in liver physiology and pathophysiology, lag behind laboratory-based discoveries summarized above. Thus, currently, profiles of miRs in various liver diseases and corresponding alterations in expression patterns as prognostic indicators or for categorization of liver diseases have not been introduced to routine clinical practice. A likely application will be the profiling of miR expression in hepatic tumors as an aid to prognosis and, perhaps, to help guide therapeutic decisions and choices of therapies.

It seems that therapy directed at influencing the hepatic levels of selected miRs such as miR 122, already shown to play an important role in affecting levels of serum cholesterol and levels of the HCV, both in cell culture [180-181] and chimpanzee models [182], will find a place in clinical therapeutics. Indeed, phase II clinical studies of locked nucleic acids that down-regulate miR 122 expression are already in progress, and results of these are awaited with high interest. Similarly, therapeutic alteration of miR 196 [183] and, in future, other miRs seem likely also to be pursued. However, there are high costs

and lengthy duration usually needed for approvals of all new drugs. Then, too, the unwanted side-effects of such treatments may limit their clinical application. [184]

Therapies are desperately needed to bridge the time lapse between patients awaiting and receiving donor organs, as current options are limited to liver cell transplantation which has only shown mild clinical success due to donor hepatocyte insufficiency and high cell death following transplantation [3]. It is clear after review of the current literature that in HSC-mediated fibrogenesis there is not a common cure-all for the disease. Certain treatments designed to inhibit signals that promote deleterious HSC activation adversely effect signaling networks critical to neighboring cells (e.g., hepatocyte growth factor inhibition). Therefore, in efforts to identify putative therapeutic targets to ameliorate HSC activation and hepatic fibrosis, one must diversify experimental models, incorporating physiological relevant components of the hepatic microenvironment. Additionally, new advances will likely be derived from systems of combination therapy. The field of carcinogenesis and cancer therapy has validated benefits of combination therapies as synergistic effects are observed giving rise to increased disease suppression and increased recovery rates [185-187]. When examining inhibitory actions against HSC activation to attenuate fibrosis ,the value of combination therapies and possible synergistic effects on cellular and molecular components must also be examined. While promise of gene therapy has been lacking in past years, recent studies are providing new vector systems that may improve safety and efficacy of anti-fibrotic drug delivery directly to the HSC. Previous studies have shown antibody-targeted delivery (αSMA) of GTx to be an effective antifibrogenic therapy [188]. Studies have also observed that neo-glycoprotein mannose-6-phosphate-albumin (M6PHSA)

accumulates efficiently in HSCs during liver fibrosis and when coupled to anti-fibrotic pentoxifylline (PTX) reduced collagen expression significantly in activated HSCs [189]. Studies are still needed to uncover unique gene expression profiles and cellular qualities during varying stages of activation for cell-specific targeting to be successful in the absence of parenchymal or systemic effects.

The process of HSC transdifferention is highly complex with breadth and depth existing in pro-fibrotic signaling networks conferring genetic reprogramming. Therefore, this dissertation examined multiple points of HSC transdifferentiation to uncover novel targets for therapeutic intervention and/or combination therapy. Specifically this dissertation examined the following:

1. Transcriptional regulation of the initiation phase of transdifferentiation through JAK2/STAT3. The central **aim** of this study was to investigate an array of 21 genes over 10 consecutive days in culture to identify candidate signaling pathways and genes which peak early in expression to initiate and commit the HSC to activation/transdifferentiation.
2. Post-transcriptional regulation of TGFβ-mediated HSC transdifferentiation by miR 19b. We **hypothesized** that decreased miR 19b in activated HSCs directly promotes fibrogenesis through regulation of TGFβRII.
3. AQP-mediated apoptotic mechanisms regulating resolution stages of transdifferentiation. We **hypothesized** that decreased AQP expression in the activated HSC confers increased resistance to apoptosis.

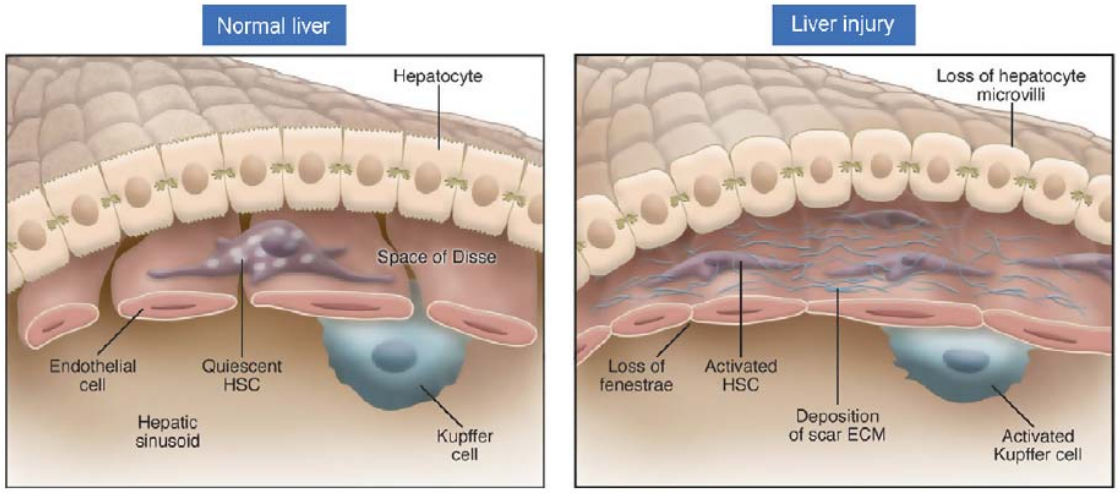

Figure 1.1 Intrahepatic effects of liver injury. The liver is comprised of four major cell types, hepatocytes, sinusoidal endothelial cells, Kupffer cells and HSCs. In a setting devoid of injury, plates of hepatocytes and non-parenchymal cells in hexagonal arrangement radiate from the central vein forming functional subunits of the liver. Injury to the parenchyma results in activation and recruitment of inflammatory cells. Release of soluble factors including TGFβ activate HSCs and stimulate wound-healing. Deposition of fibrillar scar matrix and other sinusoidal events observed in liver injury are depicted above. (Figure from Iredale, *Pharmacological Research*, 2008) [190]

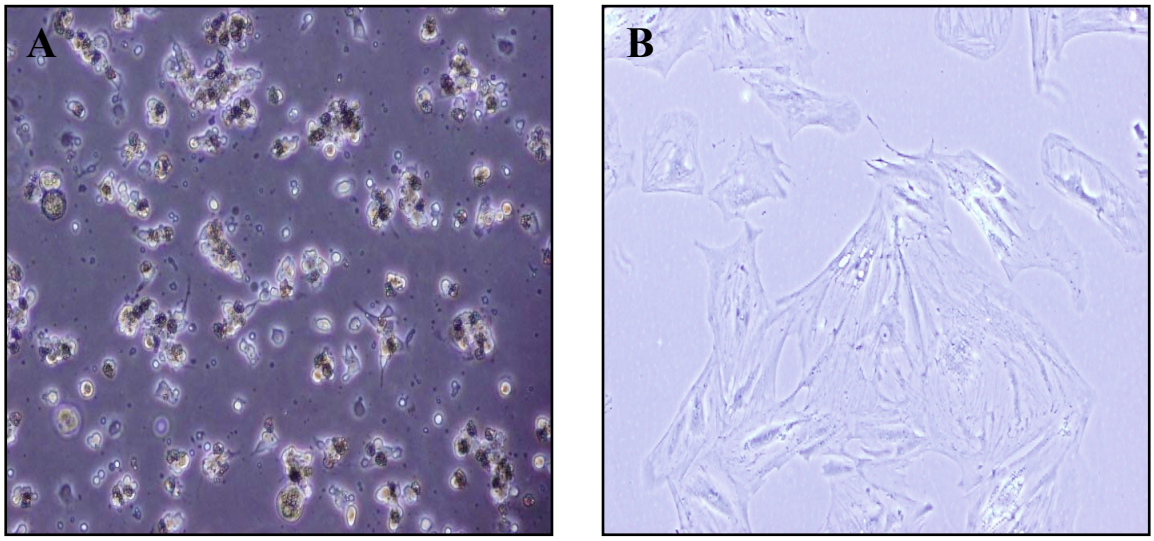

Figure 1.2 Representative light micrographs of HSCs. The quiescent phenotype is depicted in panel A, while fully activated myofibroblast-like cells appear in panel B. In the normal liver HSCs reside in the quiescent state, spindle-like in shape with cytoplasmic projections, but exposure to hepatic insult stimulates transdifferentiation of the cell producing an activated HSC denoted by stretched polygon morphology and loss of autofluorescent properties.

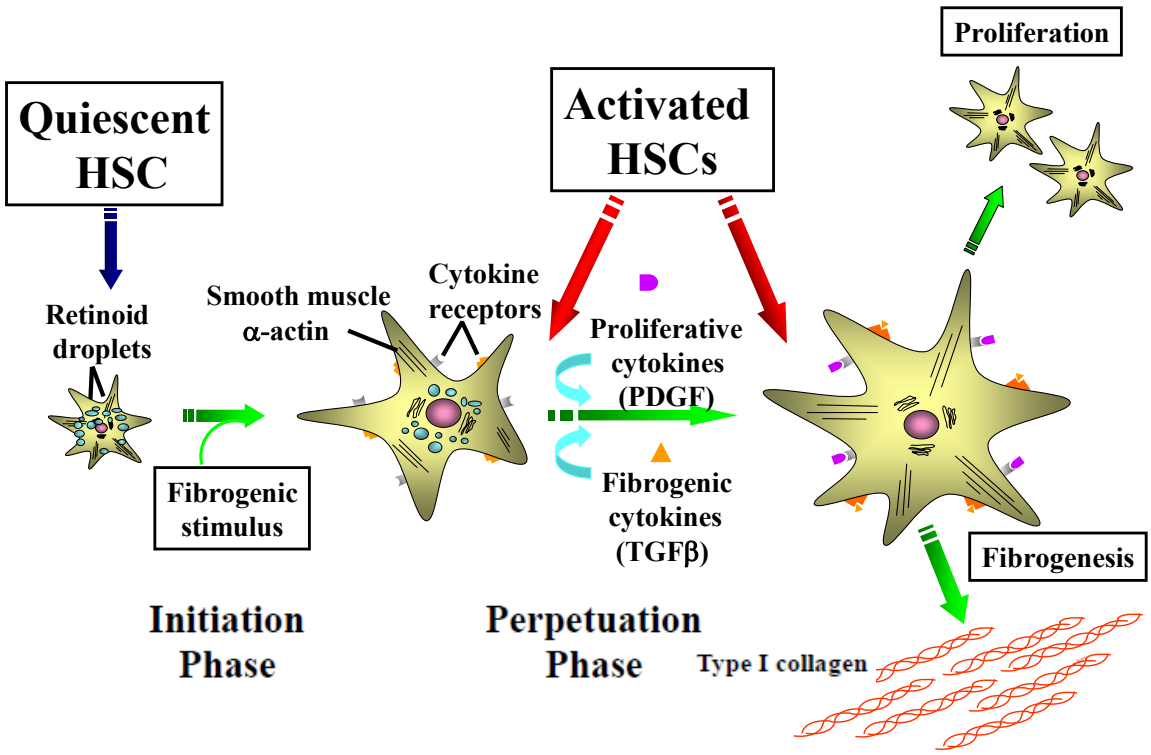

Figure 1.3 Transdifferentiation of HSCs. HSCs reside in the space of Disse in the quiescent phenotype functioning to store vitamin A, regulating normal basement membrane conditions and hepatic microcirculation. Following exposure to a fibrogenic stimulus, HSCs transdifferentiate from quiescent lipid-rich cells to activated myofibroblasts devoid of retinoid droplets and marked by expression of αSMA and a highly proliferative and contractile phenotype. Activated HSCs migrate to sites of injury where they produce and secrete scar matrix components to facilitate wound-healing. (Figure adapted with permission from Rippe, RA)

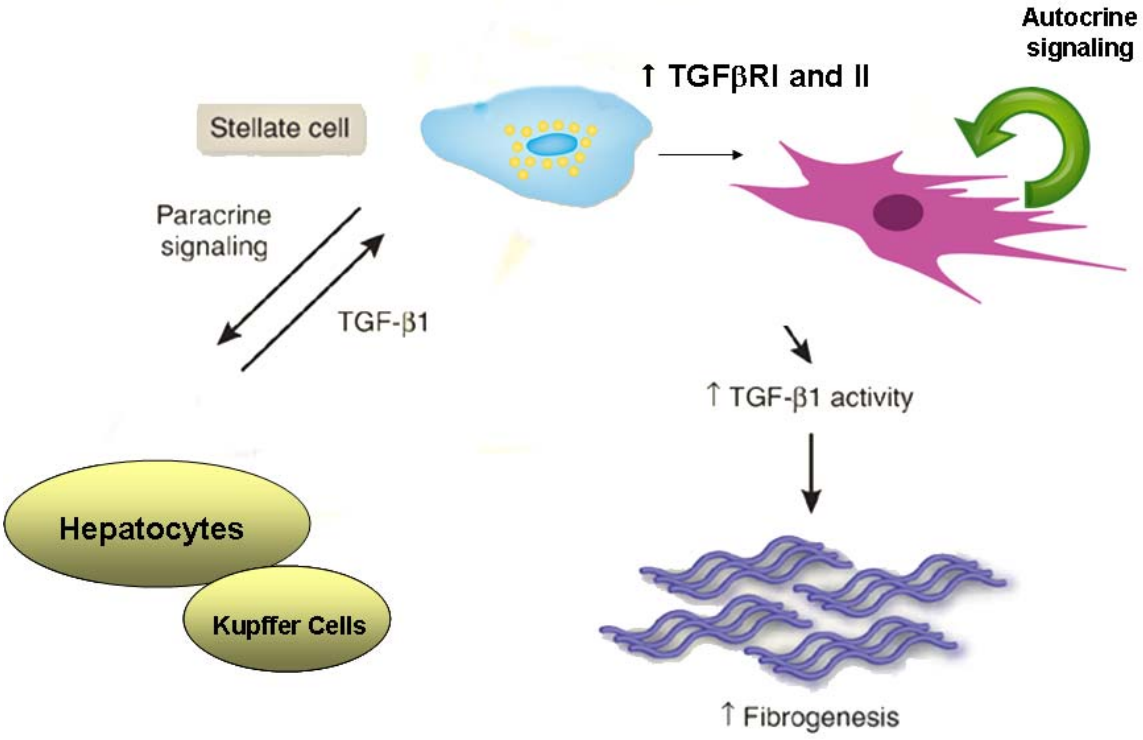

Figure 1.4 TGFβ signaling stimulates and perpetuates HSC transdifferentiation. Tissue and blood levels of TGFβ are elevated following injury. Increased paracrine signals derived from hepatocytes and Kupffer cells stimulate transdifferentiation of the HSC from a quiescent (blue cell) to activated (purple cell) phenotype increasing fibrogenesis. Autocrine signals perpetuate inflammatory signaling resulting in increased matrix deposition and wound-healing. (Figure adapted from Friedman, *Nature Medicine*, 2007). [191]

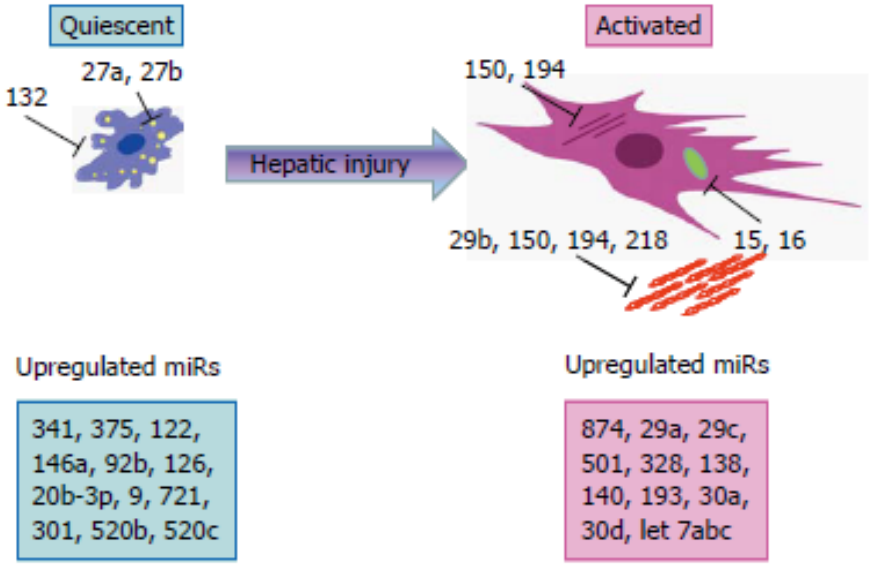

Figure 1.5 miRs involved in HSC transdifferentiation. Functional manipulation studies utilizing mimics and/or antagomirs have demonstrated that the miRs depicted in the above schematic regulate key genes/functions in HSCs. Quiescent HSC: yellow circles represent cytoplasmic lipid droplets; activated HSC: purple lines indicate cytoskeletal protein αSMA; green oval represents bcl-2; red fibrils represent collagen). Additional profiling studies have shown up-regulation of several miRs in both phenotypes, some of which are already associated with hepatic disease (boxes contain a small fraction of published miRs). (Figure from Lakner et al. *World J. Gastro*, 2011). [184]

CHAPTER 2: MATERIALS AND METHODS

2.1 Chapter 3 materials and methods

HSC isolation and culture

Primary HSCs were isolated from male Sprague-Dawley retired breeder rats (>600g) (Charles River, Raleigh, NC). In situ liver perfusion using a pronase (Roche Molecular Biochemicals; Chicago, IL)/ type I collagenase (Sigma-Aldrich; St. Louis, MO) digestion was performed followed by Optiprep (Axis-Shield; Oslo, Norway) density gradient centrifugation. Cells were recovered at approximately 95% purity based on autofluorescence and washed with Gray's Balanced Salt Solution (GBSS: 137 mmol/L NaCl, 2.7 mmol/L $NaHCO_3$, 5.0 mmol/L KCl, 1.5 mmol/L $CaCl_2$-$2H_2O$, 1.0 mmol/L $MgCl_2$-$6H_2O$, 0.7 mmol/L Na_2HPO_4, 0.2 mmol/L KH_2PO_4, 0.3 mmol/L $MgSO_4$-$7H_2O$, 5.5 mmol/L glucose, 25 mmol/L HEPES) and either used immediately (termed: freshly isolated, Q or quiescent) or cultured on plastic using Dulbecco's Modified Eagles Medium (Gibco, Grand Island, NY) supplemented with 10% fetal bovine serum (Atlanta Biologicals, Lawrenceville, GA), 2 mmol/L L-glutamine (Gibco), 100 units penicillin/mL, 0.1 mg/mL streptomycin, and 0.25 μg/mL amphotericin B (Sigma-Aldrich, St. Louis, MO) in 5% CO_2 humidified atmosphere at 37 °C. Growth media was changed every 2 days unless otherwise noted. All animal procedures were performed under the guidelines set by the University of North Carolina at Charlotte Institutional

Animal Care and Use Committee and are in accordance with those set by the National Institutes of Health.

Treatment of HSCs

HSCs were either harvested immediately (day Q or quiescent) or were grown in culture for the designated number of days (every 24 hours from the time of plating is considered 1 day). Cells were treated continually with 100 μmol/L AG490, a JAK2 inhibitor (CalBiochem, San Diego, CA). Media during treatments was changed every 24 hours.

Isolation of RNA and quantitative PCR

Total RNA was isolated from HSCs using TRIzol reagent (Gibco-BRL, Gaithersburg, MD). RNA isolated from Q through day 3 was then cleaned using the RNEasy Clean-Up (Qiagen) following manufacturer's recommendations. Total RNA was reverse-transcribed using Superscript II reverse transcriptase (Promega, Madison, WI) following manufacturer's recommendations. qPCR was run at 94^{o}C 15 s; 58^{o}C 25 s; 72^{o}C 20 s, read 5s (Table 3.1). Reaction mixture consisted of 1 μl each of cDNA, forward and reverse primers at 5 nmol/L, 2 μl DEPC water, and 5 μl of SYBR Green Master Mix (Qiagen). Primers listed in Table 3.1 were all designed for rat. cDNA concentration was used as a reference to normalize samples since the expression of housekeeping genes was modulated through days in culture. Data were reported as cross-point, the point at which the detectable level of SYBR green fluorescence was detected above the background. All experiments were performed a minimum of three times, as noted.

Microscopy

For microscopic images, cells were visualized with transmission light microscopy at 200X magnification. A second exposure was taken under fluorescent light with a DAPI filter to image the fluorescent retinyl esters within the HSC using an Olympus IX71 microscope (Olympus America, Inc.; Hamburg, Germany). The white light image was overlaid with the fluorescent image to produce the final image.

Author contributions

Dr. Alyssa A. Gulledge was responsible for generation of data and study design with guidance from Dr. Laura W. Schrum.

Data analysis

Data are presented as mean ± SEM. One way repeated measures ANOVA was used for determination of statistical significance between the control and treatment groups using SigmaStat version 2.0. A p value of less than 0.05 was considered significant. AMADA 2.0.7 software was used to perform cluster analyses using Spearman correlation and average linkage [192].

2.2 Chapter 4 materials and methods

miRNA isolation, purification and microarray

Total RNA was isolated from samples using Trizol Reagent (Invitrogen, Carlsbad, CA) per manufacturer's instructions. The integrity of the RNA was verified by an Agilent 2100 Bioanalyzer profile (Agilent Technologies Inc., Santa Clara, CA). The RNA was Poly (A) tailed and ligated to biotinylated signal molecules using the FlashTag™ Biotin RNA labeling Kit (Genisphere, LLC, Hatfield, PA). An Enzyme Linked Oligosorbent Assay (ELOSA) QC assay was performed to verify labeling prior to array hybridization.

Hybridization, washing, staining and scanning were performed using Affymetrix GeneChip® system instruments (Affymetrix, Santa Clara, CA). Affymetrix GeneChip® Operating Software (GCOS) version 1.4 was used to analyze microarray image data and to compute intensity values. Affymetrix .CEL files containing raw, probe-level signal intensities were analyzed using Partek Genomics Suite (Partek, St. Louis, MO). Robust multichip averaging (RMA) was used for background correction, quantile normalization and probeset summarization with median polish [193]. Statistical difference was calculated by two-way ANOVA analysis with false discovery rate (FDR). Partek miRNA workflow was used to access TargetScan target prediction database [194] to perform miRNA - mRNA target integration.

Primary hepatic stellate cell isolation, culture and imaging

Male Sprague Dawley rats (> 500g) were purchased from Charles River Laboratories (Wilmington, MA) and housed in facilities approved by the National Institutes of Health. All surgical procedures were reviewed and approved by Carolinas Medical Center Institutional Animal Care and Use Committee. Primary rat HSCs were isolated by pronase/collagenase perfusion digestion followed by subsequent density gradient centrifugation as previously described [195]. Cell purity and viability were confirmed by autofluorescence and trypan blue staining, respectively. HSCs were maintained in Dulbecco's modified Eagle medium supplemented with 10% fetal bovine serum (FBS), 100 U/ml penicillin and 100 μg/ml streptomycin. Culture medium was replaced every 48 hours unless otherwise described and cells incubated at 37°C with 5% CO_2. To document morphological changes, representative images were captured using an Olympus IX71 microscope (Olympus America Inc., Center Valley, PA).

Quantitative Real-Time polymerase chain reaction and immunoblotting

For miRNA analysis, first-strand complementary DNA synthesis was performed using TaqMan® MicroRNA Reverse Transcription Kit primed with miR-specific primer (Applied Biosystems, Foster City, CA). Real-time quantitative RT-PCR (qRT-PCR) was performed using the TaqMan® MicroRNA Assays (Applied Biosystems), following the manufacturer's recommendations, with an ABI Prism 7500 Sequence Detection System using TaqMan® Universal Master Mix (Applied Biosystems). Fold change values were calculated by comparative Ct analysis and normalized to 4.5S rRNA concentrations [196]. For mRNA analysis, total RNA was isolated from primary HSCs, and cDNAs were synthesized as previously described [94]. mRNA expression was measured by the CFX96 Real-Time PCR Detection System using 50 ng cDNA, gene-specific oligonucleotide primers (Supplementary Table 4.S1) and IQ SYBR Green Supermix (BIO RAD, Hercules, CA). The ddCt method was used to calculate mRNA expression levels as normalized to β-actin [94]. Proteins were isolated and subject to SDS-PAGE electrophoresis and transferred to nitrocellulose membranes as previously described [195]. Bradford assays were used to measure protein concentration and Ponceau S staining verified equal protein loading. After blocking, membranes were incubated with primary antibodies (β-actin and TGFβRII, Santa Cruz Biotechnology, Inc, Santa Cruz, CA; MeCP2, Abcam, Cambridge, MA; Type I Collagen, Meridian Life Sciences, Saco, ME) overnight at 4°C followed by incubation with HRP-conjugated secondary antibodies. Chemiluminescence was used to visualize immunoreactivity as previously described.

Transient transfection

Activated HSCs (day 6) were subject to transfection with mature miR 19b and negative control probes using Lipofectamine 2000 (Invitrogen; Carlsbad, CA) according to manufacturers' instructions. Briefly, cells were plated at a density of 1-4 x 10^5 cells/ml in standard culture medium following isolation. Cells were washed 3X with Opti-MEM I Reduced Medium prior to addition of transfection complexes. Lipofectamine-mimic complexes were incubated for 20 minutes and added to HSCs in Opti-MEM at final concentrations of 25, 50 and 75 nM. After 6 h, transfection medium was aspirated and replaced with standard culture medium supplemented with 5% FBS. Recombinant TGFβ (Sigma-Aldrich; St. Louis, MO) was added at a concentration of 5 ng/ml after the 6 h period. Dual luciferase vector (pEZX-MT01) containing the full length 3'UTR of TGFβRII was purchased from GeneCopoeia, Inc (Rockville, MD). Following standard restriction digestion confirmation of control and TGFβ 3'UTR containing vectors, HSCs were co-transfected in 100 mm dishes with 4.8 μg of reporter plasmids and mature miR 19b or negative control (75 nM) using Lipofectamine 2000 as described above. 48 h post-transfection culture medium was aspirated, protein was harvested and luciferase activity was analyzed using the GeneCopoeia Luc-Pair miR Luciferase Assay system. Firefly luciferase was normalized to Renilla luciferase activity and ratios normalized to total protein as determined by Bradford assay.

Immunocytochemistry and in situ hybridization

Prior to transfection culture-activated HSCs were seeded onto glass coverslips. Cells were transfected as described above and fixed with 4% paraformaldehyde and

stained with anti αSMA antibody from Millipore (rabbit monoclonal). Slides were visualized using a Carl Zeiss confocal microscope (LSM 710) with 200X magnification. Liver tissues were obtained from following fibrotic models: bile duct-ligation/sham [Schrum lab, unpublished data], ethanol/lipopolysaccharide [88]. Sections (6 μm) were cut from all paraffin embedded tissues (RNase free). In situ hybridization was performed using mercury LNA^{TM} detection probes, 5'-DIG and 3'-DIG labeled miR 19b according to manufacturer's instructions (Exiqon, Woburn, MA).

Human tissue samples

Human fibrotic (Metavir score of 3 or 4) liver biopsy samples (n=21) were obtained from the Liver-Biliary-Pancreatic Program Repository at Carolinas Medical Center (Charlotte, NC). Informed consent forms were signed by each patient from which samples were collected and approval from the Institutional Review Board was obtained. Normal controls (n=7) were obtained from the Liver Tissue Cell Distribution Center (LTCDS) specimen bank (Minneapolis, MN).

Statistical analysis

Data are presented as mean ± SE as determined from at least three independent experiments. Statistical analyses were performed using one way analysis of variance or student's t-test where appropriate, with p values < 0.05 considered significant and denoted by *.

2.3 Chapter 5 materials and methods

Animals

Male Sprague-Dawley rats (Charles River; Raleigh, NC, 650-750g) were used in these studies. All experiments were approved by the Institutional Animal Care and Use Committee at UNCC.

Materials

Type IV collagenase, Dulbecco's Modified Eagles Medium (DMEM), and $HgCl_2$, were purchased from Sigma-Aldrich (St. Louis, MO). Gliotoxin (GTx) was purchased from BIOMOL International (Plymouth Meeting, PA). TRIzol reagent, Superscript III, Image-iT FX Signal Enhancer and ProLong Gold with DAPI were purchased from Invitrogen (Carlsbad, CA). Antigen Retrieval Citra Solution was purchased from BioGenex (San Ramon, CA). The Bradford assay was purchased from BioRad Laboratories (Hercules, CA). Antibodies against AQP 0, 1, 5, 8, and 9 were purchased from Santa Cruz Biotechnology (Santa Cruz, CA), and antibodies against AQP 11 and 12 were purchased from FabGennix (Frisco, TX). The antibody against Poly (ADP-ribose) polymerase (PARP) was purchased from Abcam (Cambridge, MA). Antibodies against α-SMA, glial fibrillary acidic protein (GFAP), donkey anti-rabbit fluorescein and donkey anti-goat rhodamine were purchased from Millipore (Billerica, Massachusetts). The CaspACE^{TM} Assay System was purchased from Promega (Madison, WI).

HSC isolation and culture

Primary HSCs were isolated from male Sprague-Dawley rats following in situ liver perfusion-pronase/type I collagenase digestion as previously reported [88]. Typical cell purity following isolation was ≥ 95%. Cells were either used immediately (quiescent;

dQ; 4 hours), or cultured on plastic using DMEM supplemented with 10% FBS, L-glutamine (2 mM) and antibiotics for 14 days (activated; d14) as previously described [88]. Culturing HSCs on plastic is routinely used to mimic the in vivo activation process.

Treatment of HSCs and morphological assessment

Quiescent (4 hours) and activated (d14) HSCs were treated with GTx [0.15 or 1.5 μM (final medium concentration), 20-90 minutes] or vehicle (DMSO) in the absence or presence of $HgCl_2$ pre-treatment (100 μM; 15 minutes). Mercurials, including $HgCl_2$, through steric hindrance prohibit AQP pore formation and thus inhibit water/solute movement [197]. At the end of the experimental period, cells were assessed for morphological changes and representative images captured using an Olympus IX71 microscope (Olympus America, Inc., Center Valley, PA). Cell number was assessed by direct cell counts. Additionally, cell viability was determined by trypan blue exclusion assay.

Reverse transcription PCR (RT-PCR) and RealTime PCR

Total RNA was isolated from dQ and d14 HSCs using TRIzol, DNase treated and reverse transcribed with Superscript III according to the manufacturer's directions. RT-PCR was performed using primers specific against rat AQP homologs (Table 5.S1) for 92^{o}C 30s; 58^{o}C 30s; 72^{o}C 30s for 35 or 40 (AQP 0, 4, 5) cycles. Two sets of primers for each AQP homolog were utilized to confirm results. PCR products were visualized on ethidium bromide gels and sequences verified. All experiments were performed in triplicate. RealTime PCR was run at 94^{o}C 15 s; 58^{o}C 25 s; 72^{o}C 20 s, read 5s. Reaction mixture consisted of 1 μL each of cDNA, forward and reverse primers at 5 nmol/L, 2 μl DEPC water, and 5 μL of SYBR Green Master Mix (Qiagen). Data were reported as

cross-point, the point at which the detectable level of SYBR green fluorescence was detected above the background.

Cell lysate preparation and immunoblotting

dQ and d14 HSCs were washed with PBS and whole-cell extracts prepared using ice-cold RIPA buffer [1% (v/v) NP-40, 0.5% (v/v) deoxycholate, 0.1% (w/v) SDS, 0.5mM phenylmethylsulfonyl fluoride, 0.05 mM Na_3VO_4, 2 μg/mL aprotinin in PBS] and sonicated. Total protein concentrations were determined and samples corrected to equal concentration prior to loading. Western blot analysis and detection were performed using antisera specific against the AQP homologs as previously described [162]. Primary antibodies were used at a dilution of 1:1000 (AQP 0, 1, 8 and 9), 1:500 (Cleaved PARP), or 1:250 (AQP 5 and 11) and incubated overnight at 4°C. Secondary antibody (anti-goat-HRP, anti-rabbit-HRP) was used at a dilution of 1:2000-1:5000 and incubated for 1 hour at room temperature.

Osmotic challenge and cell swelling analysis

Cell size was analyzed using a Becton Dickinson FACSCalibur (San Jose, CA) as previously reported [162]. Briefly, to measure basal (untreated) cell membrane water permeability, dQ and d14 HSCs were re-suspended in culture medium (10^6 cells/ml). Cells were then incubated at 37°C for 15 minutes and cell size analyzed by forward scatter. Cells were next subjected to osmotic challenge whereby culture medium osmolality was adjusted to 210 mOsM for 30 seconds. At the end of this period, cell size distribution was measured and histograms overlaid for comparison. In parallel experiments, dQ and d14 HSCs were pre-treated with $HgCl_2$ (100 μM; 2 minutes), and cell size distribution was measured prior to and after osmotic challenge.

Caspase activity

dQ HSCs (10^6 cells) were allowed to adhere in culture for 4 hours using DMEM supplemented with FBS [10% (*v/v*)] prior to treatment. In parallel d14 HSCs were seeded onto 6-well plates (10^6 cells) one day prior to treatment. Cells were either untreated or pre-treated with $HgCl_2$ (100 μM; 15 minutes) and stimulated to undergo apoptosis by the addition of GTx, a fungal metabolite that induces apoptosis in human and rat HSCs in vitro and in vivo [170, 173] [GTx; 0.15 or 1.5 μM (final concentration)]. In a parallel series of studies the pan-caspase inhibitor Z-VAD-FMK (Z-VAD; 50μM) was added simultaneously to GTx-treated HSCs as a negative control. After 20, 45 or 60 minutes culture medium and adherent HSCs were harvested, pelleted by centrifugation (450 x g 10 minutes; 4^{o}C), and HSCs lysed by freeze-thaw. The lysates were then centrifuged (15000 x g 20 minutes; 4^{o}C), and the supernatant collected and analysis performed using a CaspACE^{TM} Assay System according to the manufacturer's instructions. Activity levels were normalized to protein concentration.

Dual fluorescent immunohistochemistry

Liver tissue was obtained from an ethanol/LPS (ELPS) fibrotic animal model [88]. Four micron sections from formalin fixed paraffin embedded tissues were cut and deparaffinized with three changes of xylene (10 minutes), cleared with two changes of 100% ethanol and rehydrated with two changes of 95% and 70% ethanol and water. Cross-linked proteins were exposed using heat-induced epitope retrieval solution. Slides were washed and incubated with signal enhancer to quench background fluorescence. PBS containing donkey serum was used to block slides for 20 minutes. Slides were then incubated with primary antibody cocktail and allowed to incubate overnight at 4^{o}C (AQP

8 1:25/GFAP 1:500, AQP 8 1:25/SMA 1:200, AQP 9 1:50/GFAP 1:500, AQP 9 1:50/SMA 1:200). Slides were washed with PBS then dark incubated with secondary antibody cocktail (rhodamine 1:400, fluorescein 1:400) for one hour. Slides were rinsed with PBS and coverslipped with ProLong Gold with DAPI and allowed to cure overnight. Fluorescent staining was visualized using the Olympus IX71. Images of AQPs 8, 9, GFAP and α-SMA were taken separately at identical exposures and color channels merged using Image-Pro software (Media Cybernetics, Inc., Bethesda, MD).

Statistical analysis

Data are presented as mean ± SEM. One way repeated measures ANOVA with Tukey's post hoc test was used for determination of statistical significance between groups using SigmaStat version 2.0 (Ashburn, VA). A $p < 0.05$ was considered significant.

CHAPTER 3: DAILY GENETIC PROFILING INDICATES JAK/STAT SIGNALING PROMOTES EARLY HEPATIC STELLATE CELL TRANSDIFFERENTIATION

Introduction

Hepatic stellate cells (HSCs) play an important role in the development of liver fibrosis. Following exposure to a fibrogenic stimulus (e.g. virus, toxins, alcohol), the quiescent HSC transdifferentiates into an activated myofibroblast-like cell. During this process the HSC undergoes morphological changes (i.e. stellate cell to a stretched-polygon morphology), becomes hypercontractile and increases expression of fibrillar collagens and cytokines [15]. Increased collagen deposition leads to accumulation of scar matrix, a major cause of liver dysfunction during hepatic fibrosis [23]. The transdifferentiation process, while very difficult to monitor in vivo [198], can be seen and studied in vitro. HSCs in vivo undergo transdifferentiation when exposed to an altered microenvironment (e.g. increased type I collagen deposition as seen in fibrosis). This process can be mimicked in vitro by culturing these cells on a plastic substrate. Several groups have performed microarray analyses on both in vitro and in vivo HSC activation [199-200]; however, little is known about the daily genetic alterations that occur. To understand this complex process, it is necessary to know the sequential activation of key genes, as well as the rise and fall of expression levels. Therefore, based on known gene expression profiles of the quiescent and activated HSC, several genes were selected to follow throughout the transdifferentiation process.

HSCs are an important source of cytokines, and cytokine cross-talk is the main pattern of cellular communication in the injured liver. Specifically, continual wound-healing perpetuated by HSC transdifferentiation is associated with increased IL-6 expression, an important cytokine involved in the acute phase response observed post-liver injury [16]. IL-6 initially binds to specific receptor IL-6R (gp80) and subsequently two molecules of gp130 are recruited leading to activation of down-stream signaling. Classically, for induction of pro-inflammatory target genes, canonical JAK/STAT signaling is activated leading to increased inflammation as well as degradation of ECM [76]. Signaling pathways such as the MAP kinase (MAPK) pathway are also transduced with the activation of soluble IL-6R [201]. However, studies have shown that JAK/STAT signaling is the primary pathway for up-regulation of pro-inflammatory mediators/genes during acute phase response II, the body's innate immune response provoked as a result of liver injury [201]. JAK/STAT downstream signaling affects expression of numerous genes including those involved in cellular proliferation and migration. Additionally, JAK/STAT signaling is associated with down-regulation of anti-apoptotic genes, including bcl-2 family proteins [202]. Stimulation of proliferative pathways (MAPK) and increased cellular differentiation by JAK/STAT signaling promotes the fibrotic response and leads to increased activation of HSCs [23]. Additionally, our lab has shown (unpublished data; Schrum lab) JAK/STAT signaling increases collagen expression at both mRNA and protein levels supporting that this pathway is critical in modulating fibrosis.

To determine the daily genetic profile during normal transdifferentiation in HSCs, the expression of a mini-array of 21 genes (including members of the IL-6 JAK/STAT

signaling pathway) across 10 days in culture was examined. Our results clearly demonstrate unique genetic profiles during different days of transdifferentiation and select days of activation showed similar patterns of gene expression. Results of the genetic and day cluster analyses suggest responsiveness of the cell to different signals will depend upon the temporal state of transdifferentiation. Inhibition of JAK/STAT signaling impeded the progression of HSC transdifferentiation as assessed morphologically and by gene expression. Thus, our data indicate that JAK/STAT signaling may play a key role in the initiation of HSC transdifferentiation and that the changes in gene expression during a precise time period within the activation phase may determine the response of the HSC during this process.

Results

Gene expression profile time-course

To generate a daily profile for gene expression, 21 genes were selected as representatives of cellular behavior exhibited by HSCs. They included standard housekeeping genes (β-actin, G3PDH, HPRT), markers of quiescence (GFAP, PPARγ), markers of activation (SMA, Desmin), matrix remodeling genes (col α1(I), col α2(I), MMP13), mitotic and migratory associated genes (CycD, FAK, RhoA, PDGFR), and pro-fibrotic cytokines, including the IL-6 JAK/STAT signaling pathway (IL-6, IL6R, JAK2, SOCS3, STAT3, TGFβ, TGFβR). Total RNA was harvested at day Q and days 1-10 at exact 24 hour intervals (n=4) and converted to cDNA for quantitative PCR analysis. These data were graphed as raw mRNA expression based on cycle number and subsequently normalized to total cDNA concentration. In order to examine relative fluctuations in gene expression, all genes were normalized to day Q (Figure 3.1A).

Since wide variations existed in mRNA expression of G3PDH, HPRT and β-actin based on total cDNA content (Figure 3.1A), a housekeeping gene was not used for normalization. For example, when IL-6 was normalized to a housekeeping gene (G3PDH, β-actin or HPRT), large variations in gene expression were observed (Figure 3.1B). Therefore, total cDNA concentration was used for normalization to quantitate daily changes in gene expression.

Due to the extensive amount of data generated from the mini-array, AMADA software was used to detect significant relationships in gene expression patterns. Genes with similar expression patterns over 10 days of culture were clustered together (Figure 3.2A). Genes incorporated in the same bracket have a more comparable expression pattern than those outside that bracket. The degree of correlation decreases with the distance between bifurcations [203]. Further examination identified that SMA and collagen α1(I) and α2(I) were similarly regulated, while FAK, TGFβR and Desmin displayed a similar yet not identical regulation as they were positioned on adjacent brackets. Conversely, GFAP, IL-6, JAK2, MMP13 and SOCS3 had distinctly different expression patterns as they were separated by multiple bifurcations. Additionally, PPARγ demonstrated the least amount of relatedness to any other gene. Interestingly, a majority of IL-6 signaling pathway constituents (IL-6, JAK2, SOCS3) were clustered together indicating a high degree of correlation in expression pattern, while STAT3 and IL-6R exhibited a divergent expression pattern from these three IL-6 signaling components.

Clustering software was utilized to demonstrate which days of culture-activation were most closely linked based on gene expression profile (Figure 3.2B). Day Q is

distinct from all other days in culture. Days 1, 2 and 3 were closely linked, with day 1 having a more comparable gene expression profile to day 2 than day 3. Days 5 and 6 were also well-coupled as were days 7-10; however, as in all hierarchal clustering dendrograms, ordering within the bracket is arbitrary and thus does not contribute to the relatedness. Day 4, like day Q, exhibited a distinct expression profile that did not directly correspond with other days in culture indicating these days may be important cellular transition points.

Markers of gene expression

After examining gene expression by mini-array, we further dissected distinct markers of quiescence (GFAP, PPARγ; Figure 3.3A), markers of early activation (MMP13, IL-6; Figure 3.3B), markers of late activation (SMA, Desmin, col α1(I), col α2(I), Figure 3.3C), pro-fibrotic markers (TGFβ, TGFβR, MMP13, PDGFR; Figure 3.3D) and constituents of the IL-6 JAK/STAT signaling pathway (IL-6, IL6R, JAK2, SOCS3, STAT3; Figure 3.3E). Classic quiescent markers were clustered closely and decreased steadily over days in culture (Figure 3.3A), while markers of early activation increased sharply on day 1 and fell to basal levels over time (Figure 3.3B). Consistent with previous findings in our lab, we observed approximately a 10^3-fold induction in MMP13 mRNA and a 100-fold induction in IL-6 mRNA expression from day Q to day 1. Markers of HSC activation increased steadily for the first seven days of activation then plateaued (Figure 3.3C). PDGFR, TGFβ and TGFβR expression increased after day 2 and remained constant (Figure 3.3D). Notably, five genes in the IL-6 JAK/STAT signaling pathway were coordinately regulated during early HSC transdifferentiation (Figure 3.3E). Although differences in gene expression magnitude existed, the

overarching pattern remained consistent. These data suggest the IL-6 JAK/STAT signaling pathway may be linked to regulation of HSC transdifferentiation which warrants further investigation.

JAK/STAT pathway in early HSC transdifferentiation

Since gene expression analysis indicated early transient spikes in IL-6, JAK2 and STAT3 mRNAs (Figure 3.3E), contribution of this signaling pathway to the initiation of HSC transdifferentiation was examined. A specific JAK2 inhibitor, AG490, was used to block JAK/STAT signaling within the cell to determine if inhibition of this pathway could alter changes seen in transdifferentiation. Cells were exposed continually to AG490 over a five day period and assessed morphologically at days 1, 3 and 5. Culture-activated HSCs lose retinyl esters and cytoplasmic processes, and proliferate vigorously. As indicated by black arrows, cytoplasmic processes were only evident at day 1 in control cells (Figure 3.4) compared to day 3 and 5 which exhibited stretched-polygon morphology characteristic of the activated phenotype. However, HSCs treated with AG490 retained these cytoplasmic processes over five days in culture indicating an inhibition of the activated phenotype and suggesting the importance of the JAK/STAT signaling pathway in early HSC transdifferentiation.

AMADA software was again used to cluster days based on gene expression profiles of the AG490-treated cells (Figure 3.5). Cluster analysis indicated that the expression profile of the HSCs treated with the inhibitor on days 1, 3 and 5 shared a high degree of relatedness to day Q as opposed to later days in culture. Specific gene expression associated with HSC activation was also examined. Inhibiting the JAK/STAT pathway with AG490 clearly showed a significant decrease in expression of markers of

activation (collagen, SMA, PDGFR and TGFβR) thereby impeding early HSC activation (Figure 3.6). Day 3 showed the most prominent reduction of gene expression compared to day 1 and day 5. Even though significant decreases in gene expression were observed on day 5, a less dramatic effect was seen compared to day 3 suggesting JAK/STAT may be involved in early transdifferentiation and plays a lesser role during later stages.

Discussion

The process of HSC transdifferentiation is key in understanding and eventually ameliorating liver fibrosis. During the course of HSC transdifferentiation there are several genes/proteins that are altered in expression. Genes involved with lipid/vitamin A regulation [97, 115, 117], such as peroxisome proliferator activated receptor gamma (PPARγ) [116, 204], are lost, while cytoskeletal genes are shifted, decreasing glial fibrillary acidic protein (GFAP) but increasing desmin and smooth muscle-α actin (SMA) [205-208]. Manipulation of PPARγ expression by adenoviral expression in activated cells leads to a reversal of the activated phenotype (flattened polygonal morphology with prominent actin stress fibers) to the quiescent phenotype (retracted cytoplasm and appearance of processes) [209]. These phenotypic changes are also correlated with decreased expression of HSC activation marker genes such as collagen and TGFβ [209]. Extracellular matrix components change from normal basement matrix components, such as type IV collagen, to a fibrotic matrix, including type I collagen [210-212]. In all previous studies, quiescent HSCs or HSCs in early activation have been compared to activated cells. Although continuous changes throughout the transdifferentiation process have been observed, changes in gene expression/profiles have not been tracked in a daily manner defining which days show similar phenotype and which days serve as a

transition. While individual components of HSC phenotypes have been identified, there has been no concerted attempt to demonstrate the interplay of relevant genes as they coordinate the transition from a quiescent to a fully activated phenotype.

The initial stimulus of the transdifferentiation process has not been identified; however, several cytokines including TGFβ, TNF-α and IL-6 have been implicated [213]. Several labs have previously used microarray analysis to examine differential expression of genes in HSCs [199, 214]. However, these studies examined two or three specific time points, rather than daily changes or gene relationships that could play a role in the initiation of transdifferentiation. In a study by DeMinicis et al., HSCs cultured for 20 hours represented the quiescent phenotype and day 5 culture-activated cells were considered fully activated [199] and in another study, days 0, 4 and 7 were the selected populations [214]. Further, other studies examined cells at days 0 and 15 along with a third time point where cells were cultured until they had been passaged six or seven times [215]. The aforementioned studies are not consistent with days HSCs are considered to be quiescent (ranging from freshly isolated to day 1 or 2) or activated (ranging from days 5 to 15 of culture-activation). Varying degrees of quiescence and activation can lead to inconsistent results and misinterpreted data. None of these studies followed the transdifferentiation process on a daily basis. Therefore, these previous studies could not pinpoint transitions and steady-state profiles. Additionally, because of the multitude of time points, data generated in these studies are not comparable to each other. Therefore, for the first time, our study analyzed an array of 21 genes over consecutive days in culture to identify candidate signaling pathways and genes which peak in expression to initiate and commit the HSC to activation/transdifferentiation.

Using AMADA software, genotypic clustering was performed to profile genes that are modulated in quiescence, early and late activation, and pro-fibrotic conditions. This analysis demonstrated that day Q was clearly divergent from all other days during transdifferentiation, while days 1-3 were significantly different from days 5-10 (Figure 3.2B). Further, day 4 is genetically distinct from other days in culture, suggesting this may be the commitment point to the activated phenotype. Although no dramatic changes in gene expression were seen at day 4, commitment to expression patterns was observed suggesting day 4 is a critical point of transition (Figure 3.3). Additionally, components of IL-6 JAK/STAT signaling pathway appeared to be crucial in the first 72 hours of HSC transdifferentiation.

Our results also demonstrated that blocking the JAK/STAT signaling pathway inhibited phenotypic changes seen during activation as indicated by retention of cytoplasmic projections (Figure 3.4) and significantly decreased pro-fibrotic gene expression (Figure 3.6). JAK/STAT signaling can be transduced by numerous factors/ligands including IL-6, leptin and interferon gamma (IFN-γ) which are also associated with HSC activation [54, 213].

IL-6 is up-regulated in liver disease, with positive effects on liver regeneration and protection from hepatotoxins. IL-6 is an important cytokine in the regulation of immune and acute phase responses during bacterial infections or damage [216]. It can be synthesized by a variety of liver cells, including Kupffer cells (KCs), hepatocytes [81] and HSCs [217-220], as well as infiltrating lymphocytes, monocytes/macrophages, endothelial cells, smooth muscle cells and fibroblasts [216, 221]. Conversely, IL-6 signaling can also be detrimental. In the case of liver fibrosis, it is pro-fibrotic causing

perpetual type I collagen stimulation by the HSCs [216]. Thus, fibrogenic effects of autocrine and paracrine IL-6 signaling and the specific contribution of each on initiation of HSC activation and perpetuation warrants further investigation.

The pro-fibrotic hormone, leptin, binds to OB-R_L transducing its signal through the JAK/STAT complex. Culture-activated but not quiescent HSCs express leptin [222] resulting in significant increases in α2(I) collagen mRNA [223] and suppression of PPARγ [224]. Inhibition of JAK2 with AG490 impeded leptin signaling thereby ameliorating the fibrotic response [225]. In contrast IFNγ is considered to be anti-fibrotic and also signals through the JAK/STAT pathway. Pro-fibrotic cytokine TGFβ increases ECM deposition from activated HSCs contributing to disruption of liver architecture in fibrosis. IFN-γ has been shown to abrogate the activation of TGFβ and diminish the excessive wound-healing response [226]. While it is clear that JAK/STAT signaling is important in the fibrotic response of HSCs, the specific ligand initiating trandifferentiation is yet to be elucidated. Numerous studies have demonstrated that signaling through the MAP kinase (MAPK) pathway leads to increased HSC proliferation promoting the fibrotic response [23, 201]. However, JAK/STAT signaling is the primary pathway for up-regulation of pro-inflammatory mediators/genes during liver injury [201], and no studies to date have examined the significance of JAK/STAT signaling during early HSC transdifferentiation.

We describe here that freshly isolated HSCs are distinct from all days of culture-activation and that these cells should not be equated with or used interchangeably with early days in culture. Based on our daily genetic profile assessment, the day of culture-activation used could significantly impact studies examining different cellular processes

including transdifferentiation, proliferation, gene expression and migration of the HSCs. It would be interesting to determine if other fibrogenic stimuli such as alcohol or acetaldehyde could also initiate HSC activation through JAK/STAT, particularly given that commitment to the activated phenotype perpetuates the fibrotic response. Overall, these data demonstrate the daily changing genetic profile of the HSC results in differentiation into a unique phenotype rendering the cell sensitive to ligands which signal through JAK/STAT. Since inhibition of the JAK/STAT signaling pathway impedes the progression of HSC transdifferentiation/activation, this may serve as a potential therapeutic target to inhibit or slow the development of liver fibrosis.

Table 3.1 Primers used in this study.

Table 1 Primers used in this study

Gene	Forward	Reverse	Size (bp)	Read (℃)
β-actin	GAGCTATGAGCTGCCTGACG	GGATGTCAACGTCACACTTC	154	80
Collagen α1(I)	CACTGCAAGAACAGCGTAGC	ATGTCCATTCCGAATTCCTG	200	82
Collagen α2(I)	AAGGCATTCGAGGACACAAC	TTACCAACAGGCCCAAGTTC	296	84
Cyclin D1	TGGAAAGAAAGTGCGTTGTG	TGCAAATGGAACTGCTTCTG	291	82
Desmin	TACACCTGCGAGATTGATGC	ACATCCAAGGCCATCTTCAC	209	81
Focal adhesion kinase	TTACCCAGGTCAGGCATCTC	GGAATCGCTCTTCCTTTTCC	218	80
Glyceraldehyde 3 phosphate dehydrogenase	ATCCCGCTAACATACCCTGG	ACTGTGGTCATGAGCCCTTC	292	80
Glial acidic fibrillary protein	AGAAAACCGCATCACCATTC	TTGGGCCTAGCAAACAAGAC	264	81
Hypoxanthine-guanine phosphoribosyltransferase	CGCCAGCTTCCTCCTCAG	CCAGCAGGTCAGCAAAGAAC	288	80
Interleukin 6	CCCACCAGGAACGAAAGTC	TTTTCTGACAGTGCATCATCG	240	76
Interleukin 6 receptor/gp80	CAGGTGCCTTGCCAGTATTCT	AACTGACTTTGAGCCAACGA	228	79
Janus Kinase 2	GGTGCCCTAGGATTTTCTGG	CGACCAGCACTGTAGCACAC	284	79
Matrix metalloproteinase 13	CATACGAGCATCCATCCCGAGAC	GCATCTACTTTGTCGCCAATTCC	290	78
Platelet-derived growth factor receptor β	ATGCAGTGCAGACTGTGGTC	CCGTGGTCATTCACACTCAC	247	82
Peroxisome proliferator-activated receptor γ	CGAGGACATCCAAGACAACC	CCGTCTTCTTGATCACATGC	161	81
Ras homolog gene family, member A	CGGAATGATGAGCACACAAG	GCACCCCGACTTTTTCTTC	207	80
Smooth muscle α-actin	CATCAGGAACCTCGAGAAGC	TCGGATACTTCAGGGTCAGG	247	81
Signal transducer and activator of transcription 3	TATCTTGGCCCTTTGGAATG	GTGGGGATACCAGGATGTTG	284	80
Transforming growth factor β	ATGACATGAACCGACCCTTC	TGGTTGTAGAGGGCAAGGAC	283	82
Transforming growth factor β receptor 1	GCTCCTGGGTGTTTTGGAG	CCAGCTCCTTCACCCTACAG	288	80

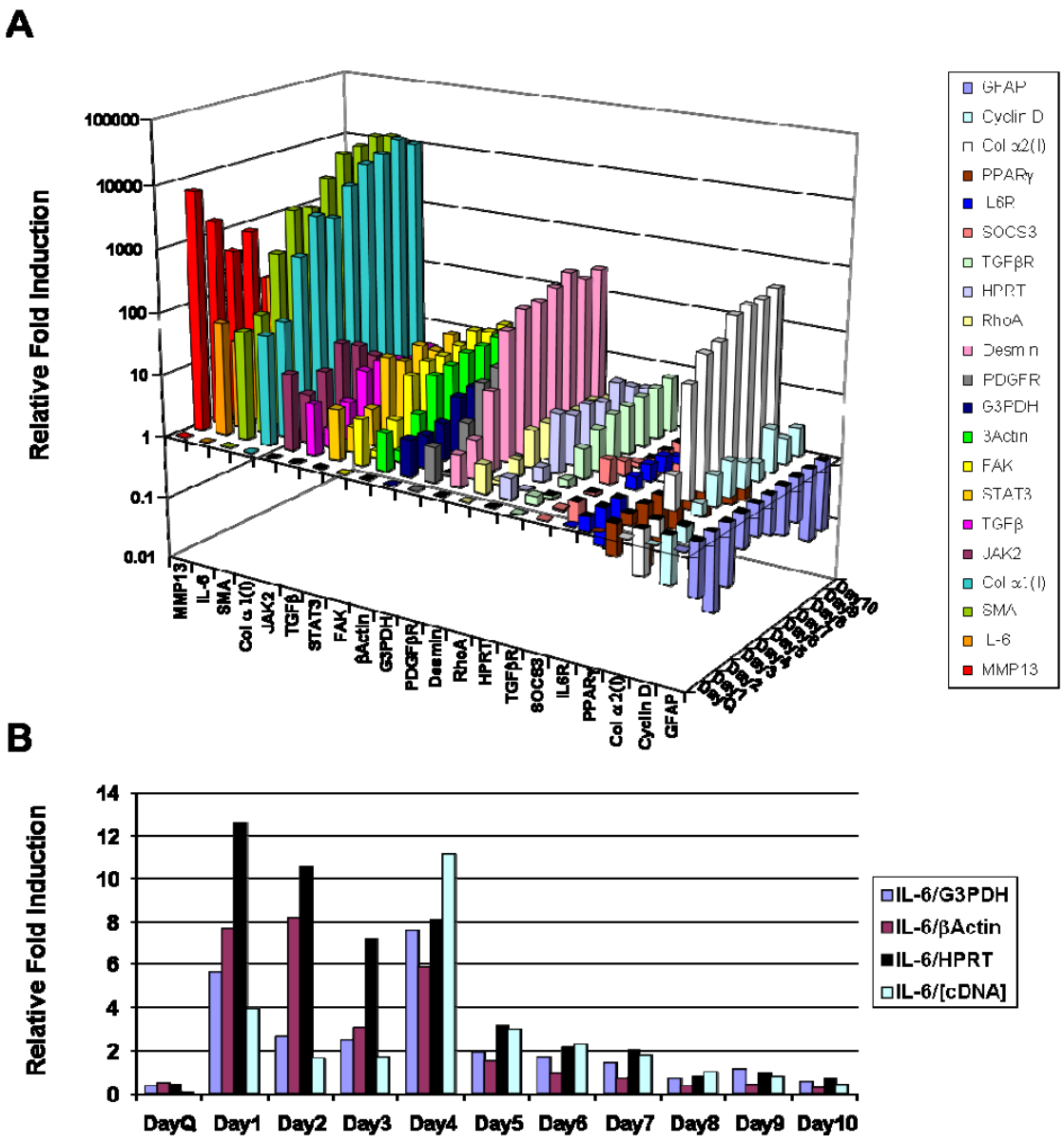

Figure 3.1 Gene expression profile time course. (A) Mini-array of 21 genes across 10 days in culture as analyzed by RealTime PCR. Results are averages from three separate experiments. Quiescent time point was set to 1 for all genes. (B) Classic housekeeping markers (G3PDH, β-actin and HPRT) fluctuated over days in culture-activation, thus they served as unreliable normalization markers.

Figure 3.2 Clustered genetic and day analyses. (A) The genes were grouped based on the degree of relatedness in their expression patterns over time using AMADA software. Distance relationships were calculated using Spearman rank correlation (D = 0 - 2). The shorter the distance between two genes, the more similar the expression profile over days in culture. (B) The clustering tree demonstrated which days in culture were most coordinately regulated. As expected, day Q branches alone, while culture-activated HSCs are more closely regulated. Unexpectedly, day 4 also branched alone.

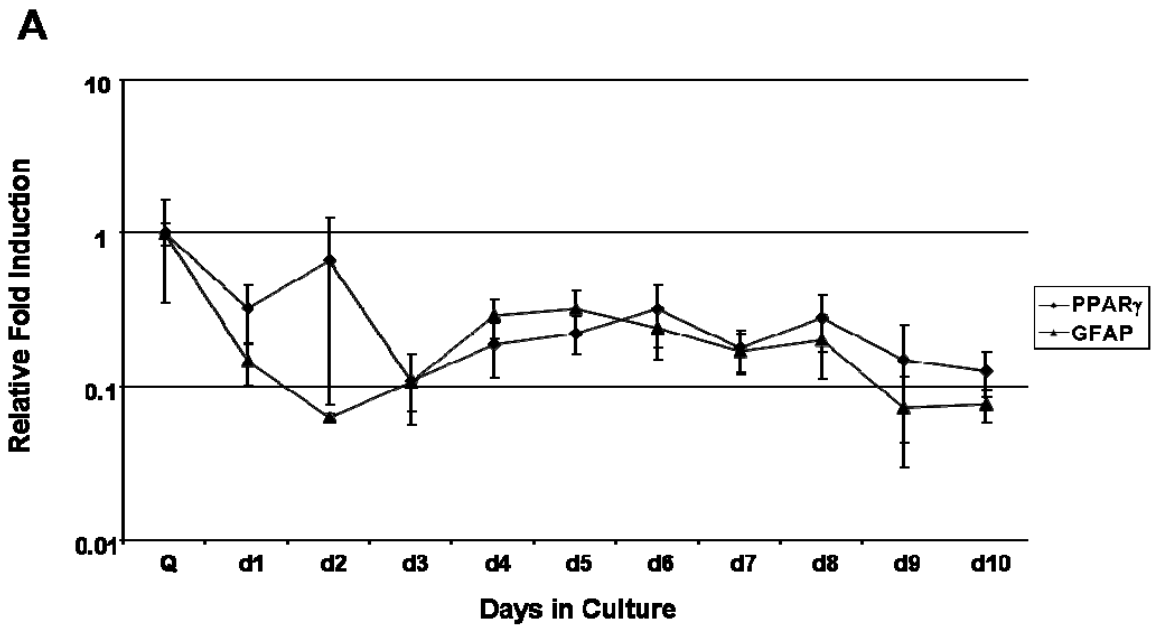
A
10
1
0.1
0.01
Relative Fold Induction
Q
d1
d2
d3
d4
d5
d6
d7
d8
d9
d10
Days in Culture
PPARγ
GFAP

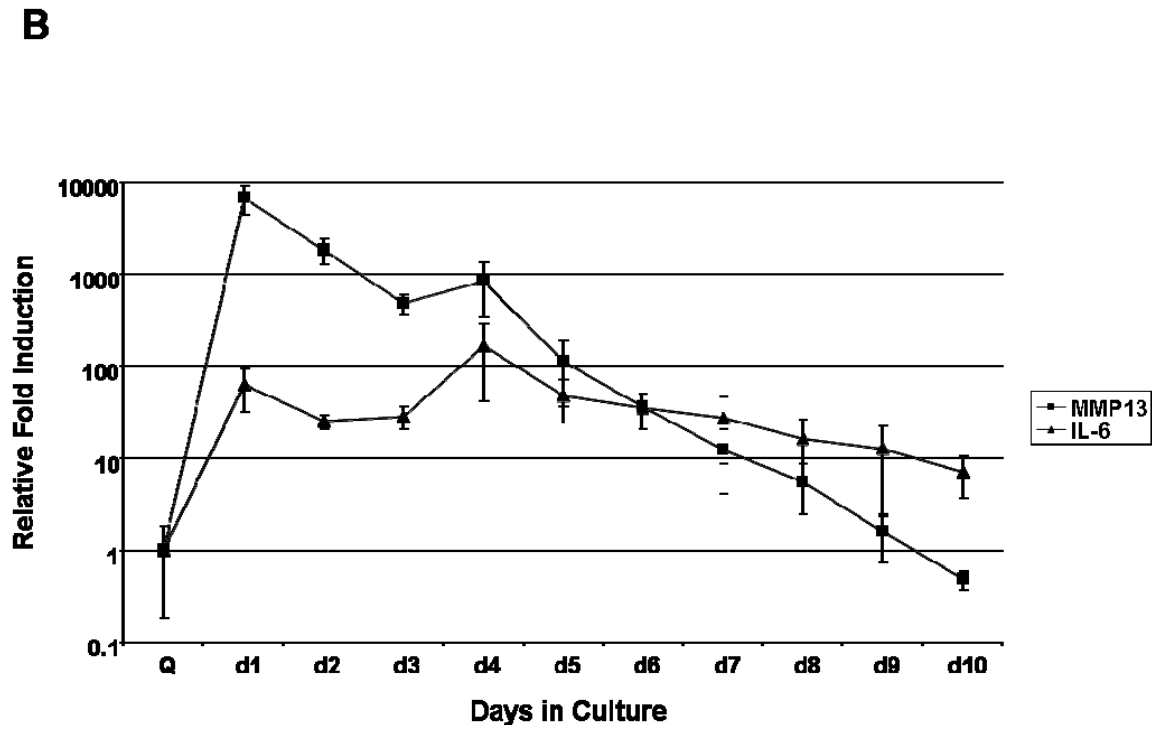
B
10000
1000
100
10
1
0.1
Relative Fold Induction
Q
d1
d2
d3
d4
d5
d6
d7
d8
d9
d10
Days in Culture
MMP13
IL-6

C

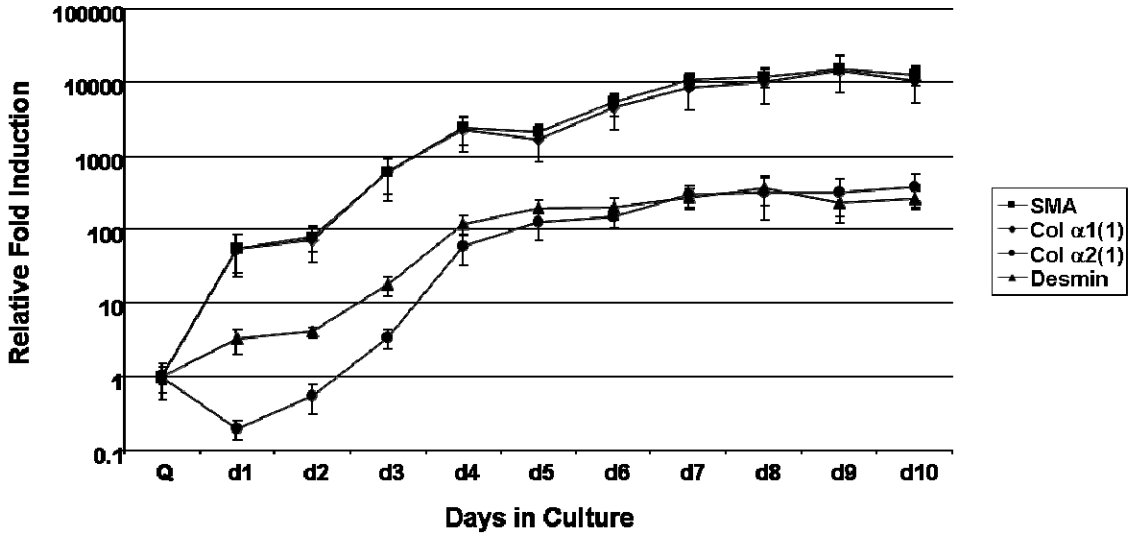
100000
10000
1000
100
10
1
0.1
Relative Fold Induction
Q
d1
d2
d3
d4
d5
d6
d7
d8
d9
d10
Days in Culture
SMA
Col α1(1)
Col α2(1)
Desmin

D

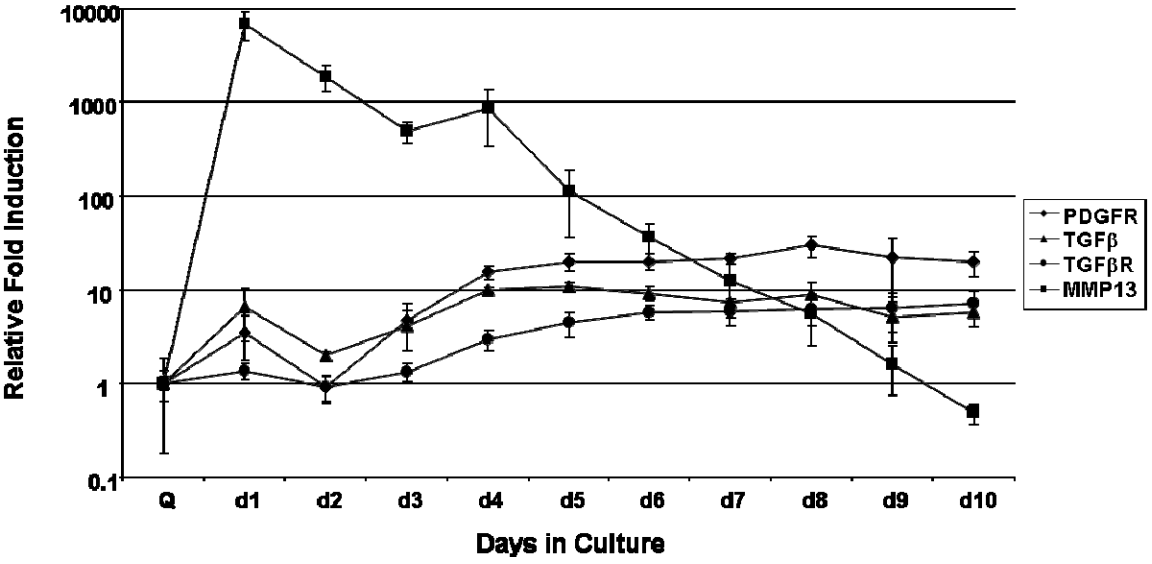
10000
1000
100
10
1
0.1
Relative Fold Induction
Q
d1
d2
d3
d4
d5
d6
d7
d8
d9
d10
Days in Culture
PDGFR
TGFβ
TGFβR
MMP13

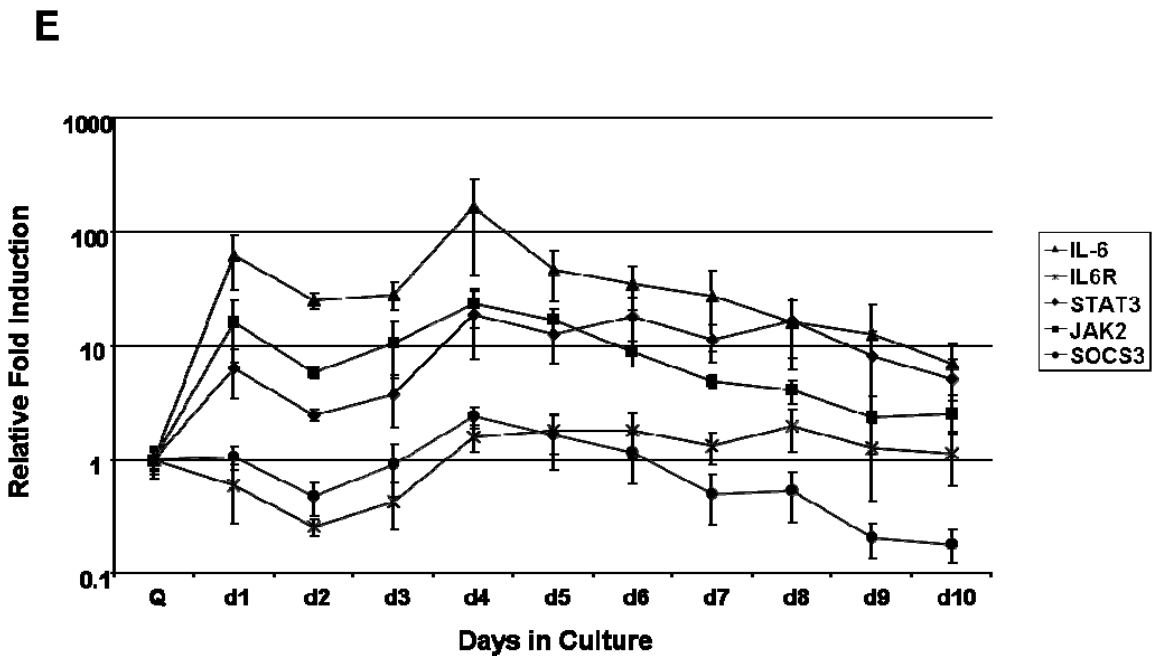

Figure 3.3 Gene expression markers during different stages of HSC activation. Markers of quiescence, early and late activation, fibrosis and the IL-6 signaling pathway (A-E respectively) were examined over ten days in culture. RealTime PCR was used to analyze gene expression. Fold induction was relative to the day Q expression levels. Data are presented as mean ± SEM.

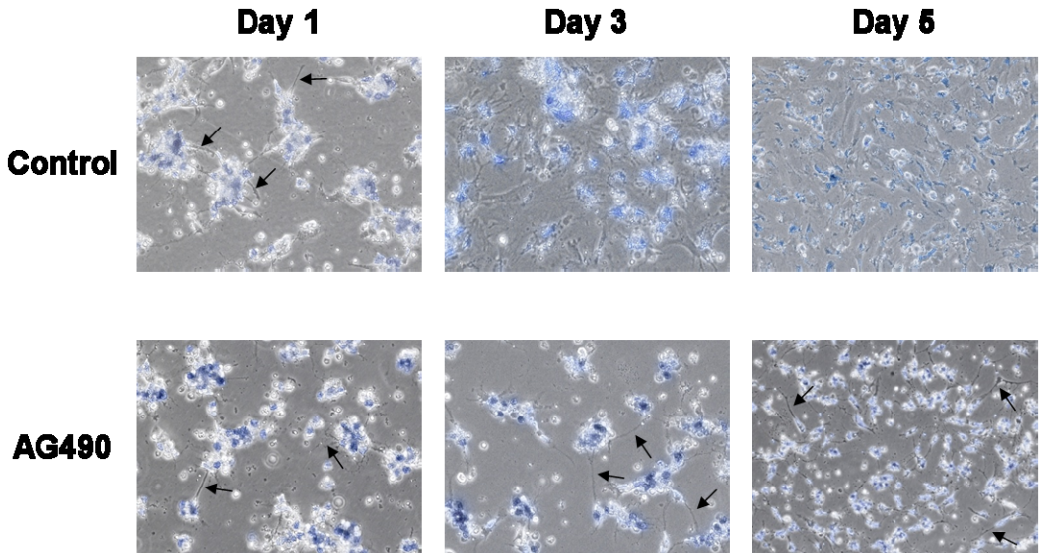

Figure 3.4 Inhibition of JAK/STAT signaling pathway: morphological alterations. Culture-activated HSCs were treated continually with AG490 throughout a five day period and subsequently analyzed morphologically at days 1, 3 and 5. Cells treated with AG490 maintained their cytoplasmic projections (black arrows) throughout the five days of culture-activation, whereas the control cells lost these processes as early as day 3.

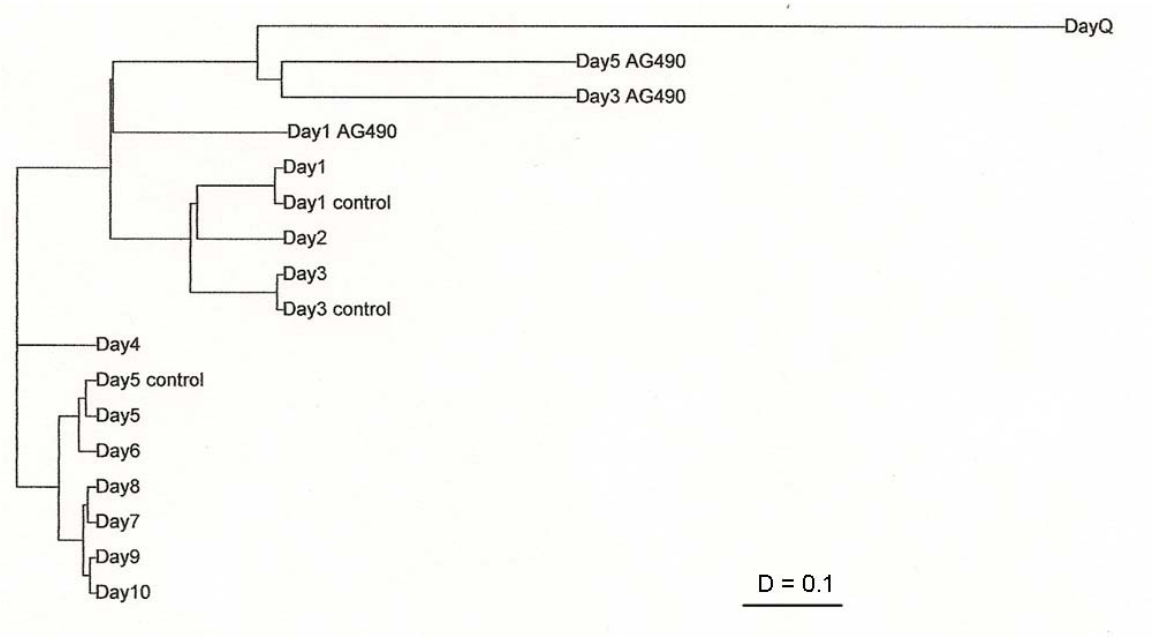

Figure 3.5 Inhibition of JAK/STAT signaling pathway: cluster analyses. AMADA software was used to detect any relationships between the days in culture treated with or without AG490 over a 5 day period. Distance relationships were calculated using Spearman rank correlation (D = 0 - 2). The shorter the distance between two genes, the more similar the expression profile over days in culture. Data from the treated cells (day 1, 3 and 5) were incorporated with the previous data for days in culture (day Q – day 10) to demonstrate days of similarity based on gene expression. The clustering showed the gene expression profile of HSCs treated with AG490 was highly related to the expression profile of the day Q HSCs.

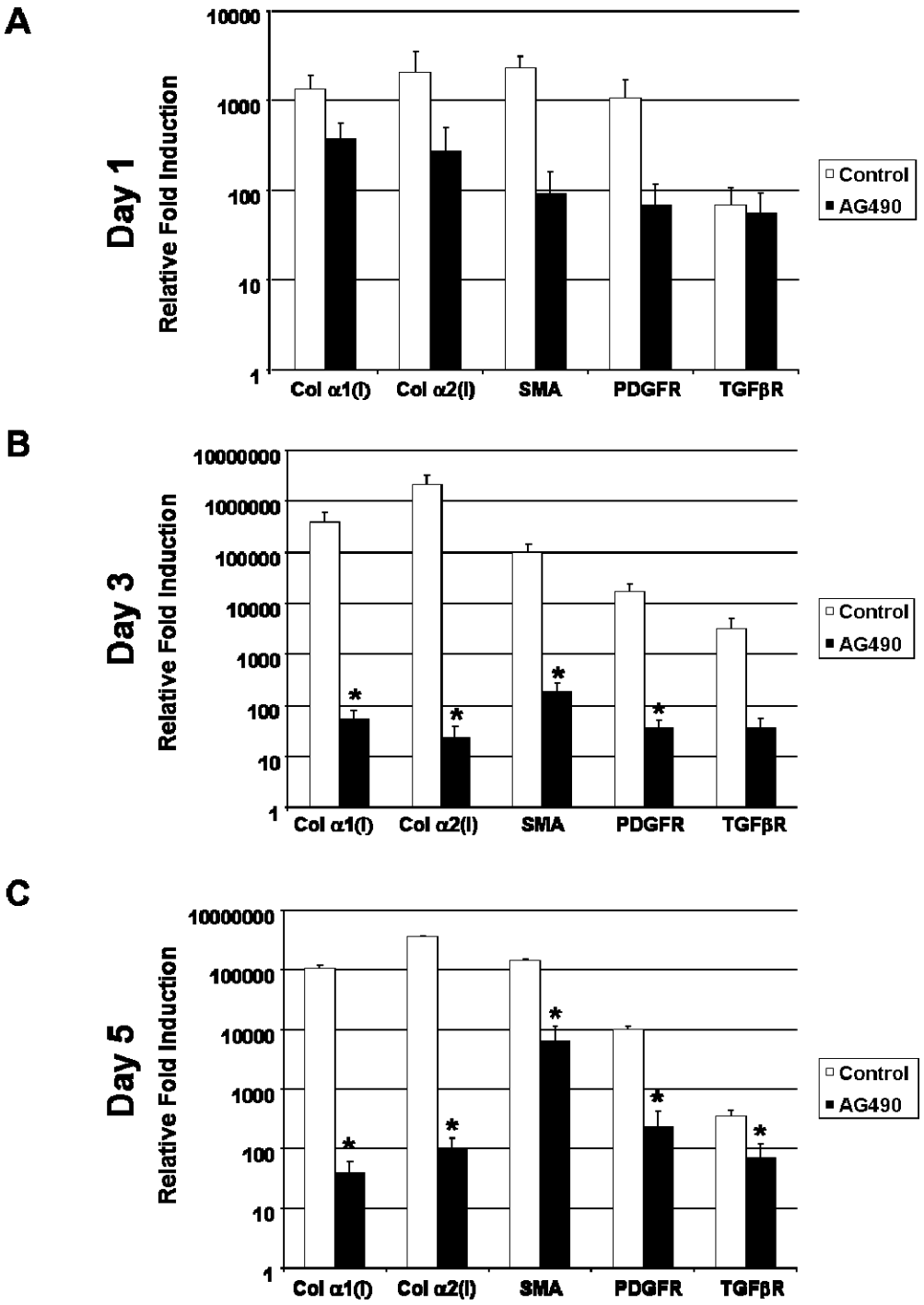

Figure 3.6 Inhibition of JAK/STAT signaling pathway: genetic alterations of fibrotic markers. mRNA expression of fibrotic genes from day 1, 3 and 5 (A-C respectively) culture-activated HSCs treated with or without AG490 were analyzed by RealTime PCR. Data were presented as mean ± SEM. * $p<0.05$ compared to control.

CHAPTER 4: MIRNA 19B: NOVEL BIOMARKER AND INHIBITOR OF HEPATIC STELLATE CELL-MEDIATED FIBROGENESIS

Introduction

Fibrosis of the liver is characterized by excessive deposition of extracellular matrix (ECM) components, predominantly type I collagen. Disproportionate deposition of fibrillar collagens disrupts normal liver architecture and hepatic function, and if left untreated, progresses to cirrhosis. Cytokine signaling predominates during fibrogenesis initiating activation of resident immune and hepatic stellate cells (HSCs) promoting wound repair [83]. Activated HSCs are the principal cell type promoting synthesis and deposition of ECM proteins in response to increased levels of circulating inflammatory signals derived from damaged parenchymal cells. These resident vitamin A storing cells are found within the perisinusoidal space of Disse in a quiescent state, but upon hepatic injury, HSCs transdifferentiate into myofibroblast-like cells marked by expression of smooth muscle-α actin (αSMA) [16], loss of retinyl ester stores and neural marker glial fibrillary acidic protein (GFAP), and increased proliferation and contractility. Myofibroblastic HSCs respond to and secrete a variety of profibrogenic cytokines including connective tissue growth factor, tissue inhibitor of metalloproteinases and transforming growth factor-β (TGFβ). Of these, TGFβ is recognized as the most potent fibrogenic cytokine regulating HSC collagen production via autocrine and paracrine signaling [32]. Numerous in vitro and in vivo studies report the importance of TGFβ signaling and that inhibition of TGFβ and/or its receptors decreases hepatic fibrosis and

HSC activation [85, 227]. In addition to induction of TGFβ signaling, numerous morphological and gene expression profile changes are acquired during transdifferentiation [94]. Recent epigenetic profiling of the transdifferentiation process highlighted a role for methyl CpG binding protein MeCP2, which was significantly up-regulated upon culture-activation. Mechanistically, MeCP2 is reported to aid in the epigenetic reprogramming of the HSC through recruitment of silencing complexes to the promoter region of PPARγ (known to maintain HSC quiescence) [128].

microRNAs (miRNAs, miRs) are small non-coding RNAs which negatively regulate target gene expression through base pairing with 3'UTRs inducing mRNA cleavage or translational repression. With multiple and diverse targets, miRs exert control over key cellular developmental processes including differentiation and proliferation. Specific contribution of select miRs in hepatic disease development and progression has been described [184]. Recent studies report the process of HSC transdifferentiation is governed by differential miRNA expression. Specifically, down-regulation of miRNAs that control fat accumulation and adipocyte programming and up-regulation of miRNAs that promote sustained activation of the cell concurrent with increased proliferation and suppression of apoptotic responses are observed [149, 228-229]. Forced expression of miRs 150 and 194 in activated HSCs resulted in suppression of the fibrotic phenotype and inhibition of ECM production through downstream regulators of collagen expression [147]. Additional studies by Ogawa et al. reported direct regulation of collagen synthesis via binding of miR 29b to the 3'UTR of collagen and transcriptional regulator Sp1 in a human HSC line [150]. While the field continues to advance, studies to date have lacked accurate miR profiling of the divergent HSC

phenotypes in primary cells. Additionally, no studies have identified any miRs that have a global effect on profibrotic TGFβ signaling in the liver which could be more efficient than targeting a single gene.

Herein, we report a set of differentially expressed miRs in quiescent (freshly isolated) vs activated HSCs, among which, miRNA 19b (miR 19b) directly inhibited fibrotic TGFβ signaling. Specifically, we validated computational prediction of miR 19b binding to the 3'UTR of TGFβRII by luciferase reporter assay. miR 19b mimic significantly decreased expression of TGFβRII as well as downstream target gene collagen, with additional suppression of markers of HSC activation (αSMA and MeCP2) and concurrent increases in quiescent characteristics. In vitro findings translated to in vivo studies with decreased levels of miR 19b evident in fibrotic rat and human liver tissue compared to normal controls. These results identify miR 19b as a novel regulator of TGFβ signaling in HSC-mediated fibrogenesis and suggest a potential therapeutic approach for treating hepatic fibrosis.

Results

miRNA profiling in quiescent and activated hepatic stellate cells

A total of 55 significantly differentially expressed miRs were identified by array analyses of quiescent (freshly isolated) and activated (day 14 of culture) HSCs. Validation of previously described miR expression levels was obtained, with miRs 16, 29a/b/c, 150 and 194 all significantly down-regulated during culture activation (Figure 4.1A, Table 4.S2). These experiments also identified ~20 differentially expressed miRs not previously reported in published array data available at the time of manuscript preparation (Table 4.S2). Analysis of differentially expressed miRs revealed members of

the miR-17-92 cluster (19a, 19b, 92a) were significantly down-regulated in the profibrotic activated phenotype. Based upon previous literature and in silico analyses (TargetScan and miRanda prediction databases), which predict putative seed match sites for miR 19b in the 3'UTR of TGFβRII, this miR was selected for further analysis. qRT-PCR confirmed array data, verifying a significant decrease of miR 19b in activated compared to quiescent HSCs (Figure 4.1B). Expression profile of miR 19b and predicted target mRNA TGFβRII were followed over 14 days in culture and a significant inverse relationship was observed (Figure 4.1C) with a dramatic decrease seen in expression of the miR from quiescence to day 3 and a significant up-regulation of TGFβRII.

miR 19b negatively regulates profibrotic TGFβ signaling

Activated HSCs were transfected with synthetic miR 19b (19b) or a miRNA mimic negative control (SCR) and following 24 or 48 h of transfection, RNA and protein were analyzed. Preliminary studies validated the SCR sequence did not significantly affect TGFβRII expression or invariant control β-actin compared to mock transfection or untransfected cells (Lipofectamine 2000 alone) (data not shown). Additionally, effective transfection of primary cells was verified by qRT-PCR and consistent concentration dependent increases were observed in miR 19b relative to 4.5S rRNA expression (Supplementary Figure 4.S1). TGFβRII mRNA levels at both 24 and 48 h post-transfection were significantly decreased compared to control, with greatest reduction seen when transfected with 75 nM 19b (Figures 4.2A and B). Similar results were observed in human HSCs (LX-2) (data not shown). Protein expression of the receptor was also significantly blunted by forced expression of miR 19b (Figure 4.2C).

Fibrotic TGFβ signaling propagates through the SMAD family of transcriptional activators, and like TGFβRII, SMAD2 and SMAD3 are up-regulated following fibrotic liver injury [230]. While R-SMAD2/3 3'UTRs do not harbor putative miR 19b binding sites (as predicted by TargetScan and miRanda), mRNA expression of SMAD3 is significantly down-regulated after 48 h of miR 19b transfection (Figure 4.2D). miR 19b is also predicted to bind to the 3'UTR of Co-SMAD4, but no significant changes were observed in SMAD4 mRNA expression following transfections (Supplementary Figure 4.S2). Computational prediction of miR 19b binding to the 3'UTR of TGFβRII was validated by luciferase reporter assay (Figure 4.2E). Addition of miR 19b mimic induced a 50-60% reduction in luciferase activity compared to controls.

miR 19b decreases expression of TGFβ target genes

Effects of increasing miR 19b on downstream TGFβ signaling target procollagen mRNA and protein were measured. Forced expression of miR 19b dampened mRNA expression of both procollagen Col α1(I) and Col α2(I), with more significant effects observed on the transcription of Col α2(I) (Figures 4.3A and B). Translation of the fibrillar collagen is also markedly decreased after 48 h miR 19b treatment as denoted by a 40% decrease in intracellular protein expression observed after 48 h (Figure 4.3C), confirming negative regulation of TGFβRII signaling by miR 19b as both procollagen 3'UTRs lack predicted binding sites (TargetScan). Additionally, functional secretion of this protein is disrupted by miR 19b as determined by immunoblot utilizing proteins concentrated from harvested culture medium (48 h) (Supplementary Figure 4.S3).

miR 19b Inhibits Paracrine TGFβ Signals

Recombinant TGFβ1 was added to activated HSCs transfected with miR 19b mimics and levels of procollagen mRNA determined. Verification of collagen stimulation by addition of recombinant TGFβ1 protein was performed (data not shown). After 24 h Col α2(I) mRNA expression was decreased even in the presence of exogenous TGFβ and both procollagens were significantly decreased after 48 h of treatment as compared to respective control (Figure 4.4), indicating a powerful role for miR 19b in the inflammatory hepatic microenvironment.

Markers of HSC activation are suppressed by miR 19b

Forced expression of miR 19b blunted the activated HSC phenotype as denoted by shrunken cytoplasm, decreased polygonal shape and increased spindle shaped cellular protrusions (characteristic of the quiescent phenotype) (Figure 4.5A). Morphological changes indicative of suppression of the activated phenotype correlated with levels of αSMA mRNA, which were significantly decreased after 48 h of transfection (Figure 4.5B). Immunoctyochemical analysis of αSMA protein expression corroborated the visible reduction in activated phenotype as visualized by markedly reduced red fluorescence as well as by disorganization and disorientation of actin fibers (Figure 4.5C). Further, miR 19b restored quiescent gene expression as evidenced by increased GFAP (Figure 4.5D). Levels of MeCP2 mRNA and protein were significantly reduced with increased expression of miR 19b (Figures 4.5E and F), highlighting a broad antifibrotic role for miR 19b.

miR 19b is decreased following fibrotic liver injury in vivo

Next, we assessed whether decreased miR 19b also occurs in vivo (or in intact animals), in rat models of hepatic fibrosis. Tissue sections from BDL and sham operated control rats were subjected to in situ hybridization experiments to assess expression of miR 19b. miR 19b was markedly decreased in fibrotic liver tissue compared to controls (Figure 4.6A and B, Supplementary Figure 4.S4). miR 19b specific staining (dark blue chromagen) in control tissue appears outside of the parenchymal cells and higher magnification inspection is indicative of perisinusoidal (HSC-specific location) expression. Co-localization of miR 19b and HSC specific markers (GFAP and αSMA) was attempted, but due to the nature of the punctate miR cytoplasmic expression and more dominant expression of HSC markers, chromagen-based co-localization was unsuccessful (paired IHC staining for HSC quiescent and activated markers appears in Supplementary Figure 4.S5). Interestingly, the decrease of miR 19b does not appear to be stimulus-specific, because in another rat model of liver injury/fibrosis (ethanol/lipopolysacchardide, ELPS [88]) hepatic miR 19b levels were also decreased (Figure 4.6C and D), strengthening the conserved importance of decreased miR 19b in hepatic fibrosis.

Hepatic fibrosis is associated with decreased miR 19b in human liver

Total RNA was isolated from fibrotic (Metavir fibrosis score of 3 or 4 due to varying etiologies including PBC, HCC and HCV) and normal control livers. qRT-PCR was used to determine relative expression levels of miR 19b. As observed in the rodent fibrotic injury models, levels of miR 19b were also significantly decreased by approximately 80% in human patients with fibrotic livers (Figure 4.7).

Discussion

This study provides the first evidence that miR 19b has a functional role in rat and human liver fibrosis. Mechanistically, miR 19b acts as a novel inhibitor of fibrotic TGFβ signaling in the HSC and holds clinical promise as a therapeutic molecule and/or biomarker for fibrosis. Significant down-regulation of miR 19b was observed in activated HSCs as well as in rodent models of fibrosis and in human disease. Forced expression of mature miR 19b in activated HSCs significantly reduced expression of TGFβRII, which is vital for efficient activation of downstream profibrotic gene expression. Expression of procollagen mRNAs and secreted type I collagen were also markedly reduced by miR 19b, even in the presence of exogenous TGFβ. In addition to regulating profibrotic gene expression, miR 19b impeded HSC activation and produced reversion to a more quiescent phenotype. miRs also exert indirect inhibitory actions on transdifferentiation through modulating epigenetic machinery [128]. Increased miR 19b significantly decreased MeCP2 expression, a factor necessary to suppress the quiescent phenotype of the cell.

Although pathologies of chronic hepatic disease (ALD, HCV, HCC) are variable, fibrosis is an underlying commonality [2]. The exacerbated wound-healing response is characterized by excessive deposition of ECM components, predominantly type I collagen, by the activated HSC [3]. Fibrotic ECM remodeling disrupts normal hepatic architecture leading to organ dysfunction. Following exposure to a fibrogenic stimulus, numerous changes in cellular organization, gene expression and overall organ function can be observed. Damage to liver parenchyma results in hepatocyte necrosis and apoptosis with subsequent release of transforming growth factor beta (TGFβ). Following

liver injury, blood and tissue TGFβ levels are elevated stimulating collagen gene expression and additional downstream profibrotic targets including matrix degrading proteins. TGFβ is the most potent stimulus for HSC-mediated fibrogenesis [2, 231] as it plays a critical role in initiation of the transdifferentiation process. In addition to paracrine sources of the cytokine, TGFβ synthesis is markedly increased as a result of activation, further perpetuating the fibrotic phenotype. Inhibition of TGFβ receptors (soluble TGFβRII and knock-out models) and/or signaling components decreases HSC activation and dramatically blunts chronic wound-healing in experimental animal models [31-32, 84, 90]. These findings have established HSC-mediated TGFβ signaling as a pivotal mechanism in hepatic fibrogenesis and disruption of HSC activation and collagen deposition via inhibition of TGFβ signaling as a mechanism to ameliorate and/or reverse fibrosis.

miRs have emerged as key regulatory molecules in chronic liver disease, including hepatic fibrosis [232-234]. Array profiling studies report differential miR expression in normal vs. fibrotic liver tissue in a variety of rodent injury models including BDL and CCl_4 [235]. miRs 150, 187, 194 and 207 were significantly down-regulated in HSCs isolated from BDL animals compared to sham controls, while let7 family members were significantly up-regulated. Recently we have seen evidence that these small non-coding RNAs modulate fibrogenesis and HSC activation [184]. Overexpression of miRs 150 and 194 in human HSCs (LX-2) resulted in inhibition of proliferation as well as decreases in type I collagen and αSMA [147].

miR profiling in human and murine liver fibrosis, and additional published in vitro manipulation studies, have highlighted a role for the miR 29 family in fibrosis via

regulation of collagen expression [150, 235]. While fibrosis underlies most chronic liver diseases, including HCV and ALD, when expression of miR 29 was examined in human samples, Roderburg et al. found expression of the miR highly variable amongst patients with viral vs alcohol-induced fibrosis, indicating the role of miR 29 in fibrosis may be stimulus specific [235]. Here we report that miR 19b levels are down-regulated in two experimental animal models of hepatic fibrosis (BDL, ELPS), and these results were confirmed in fibrotic human patients despite variable underlying etiology, supporting a highly conserved role of this miR in fibrosis. Moreover, success in identifying target genes of dysregulated miRs in liver disease has been limited. Herein, we report that miR 19b binds to the 3'UTR of TGFβRII directly inhibiting fibrotic HSC activation. Previous studies report miR expression patterns are organ and tissue specific, making systemic miR targeting problematic. However, recent reports have shown that miRs derived from the miR-17-92 cluster directly regulate TGFβ signaling in non-liver cell types, including neuroblastoma cells [236] and colonocytes [237]. Additionally, miR 19b levels are down-regulated in fibrosis and ECM remodeling of other tissue/organs (pulmonary, cardiac) [238-239], indicating a highly conserved role of miR 19b in TGFβ-mediated fibrogenesis.

In addition a very direct role in fibrogenesis through induction of pro-fibrotic target genes, TGFβ signaling may also be regulating expression profiles on a global level. miRs are processed from precursors molecules into pre-miRs within the nucleus. Once exported to the cytoplasm, the hairpin is cleaved by Dicer and strand selection occurs producing a mature miR available to associate with the RNA-induced silencing complex (RISC) [151]. Seminal studies have demonstrated miR biogenesis and processing are

directly controlled by constituents in the TGFβ pathway. Several miRs are post-transcriptionally induced by TGFβ and nuclear accumulation of R-SMAD proteins promotes Drosha-mediated miR processing [152-153]. It would be of interested for future studies to investigate if increased levels of TGFβ observed in fibrosis affect disease pathology through HSC-mediated actions as well as by affecting global miR biogenesis/expression.

Currently there are no FDA-approved treatments for fibrosis. As the field of miR research is rapidly developing, pioneering advances have emphasized there are critical changes in miR expression profiles during development of fibrosis which regulate wound-healing transcripts. While acknowledged that therapeutic modulation of single miRs in vivo has aimed to inhibit expression via antisense oligos/antagomirs, miR over-expression strategies are also ongoing and hold great promise to restore delicate genetic programs vital to normal organ function. Adenoviral delivery of miR-17-92 cluster inhibited HCV replication in cell culture propogated HCV [240]. Additionally, recent reports in HCC demonstrate miR 26a administration is capable of repressing tumorigenesis without significant systemic effects [241], indicating that over-expression of miR 19b may be a useful therapeutic agent for TGFβ-mediated fibrosis.

In addition to use as a therapy, miR 19b may also serve as an accurate biomarker of liver fibrosis and/or HSC activation. Several studies in settings of chronic liver disease with underlying fibrosis have shown strong correlations between specific miR expression patterns and responses to drug treatments as well as disease progression/prognostic outcome [184]. Plasma levels of miR 122 are elevated in both HBV and HCV patients as well as in models of alcohol and drug-induced liver damage reinforcing a role for miRs

as biomarkers [242]. Recent studies have also shown inverse correlations between tissue and plasma miR levels [242-243]. In fact, miR 19b was up-regulated 4.3-fold in serum of individuals with cirrhotic livers compared to normal controls [244] suggesting a potentially non-invasive route for diagnosing hepatic fibrosis. Future studies are needed to carefully monitor plasma miR 19b expression in relation to tissue from healthy individuals compared to varying fibrotic stages and etiologies.

HCV represents the major cause of hepatic fibrosis on a global scale and is the most frequent indication of liver transplantation [245]; however, recurrent hepatitis C occurs in 80% of patients by 3 year post-transplant [246] and up to 20% advance to bridging fibrosis or cirrhosis within 2 years [247] due to TGFβ signaling and HSC activation [248-249]. Antiviral therapy with interferon and ribavirin in transplant recipients is only 10-30% effective, and therapy may not be well-tolerated. Identifying liver transplant recipients at greatest risk for rapid development of fibrosis from recurrent hepatitis C would target those recipients most urgently in need of antiviral therapy and defer treatment to those at less risk for disease progression [249]. In support of our findings, miR 19b levels were significantly higher in HCV responder vs non-responder patient populations, underscoring the importance of this specific miR [250]. Examining expression levels of miR 19b in HCV transplant patients could lead to development of a reliable marker to identify rapid progressors of fibrosis.

Overall these systematic studies indicate that miR 19b is a novel regulator of fibrotic TGFβ signaling and indicates that the loss of miR 19b following HSC activation perpetuates the fibrotic response. Restored miR 19b expression in activated HSCs indicated this miR may be a possible therapy for the treatment or reversion of fibrosis, and patient data indicates this

powerful miR may prove to be an accurate biomarker for the fibrotic condition. These studies provide novel insight into the global regulation of a key signaling pathway which promotes hepatic fibrosis, and more importantly, provides a new avenue to be explored for translational research.

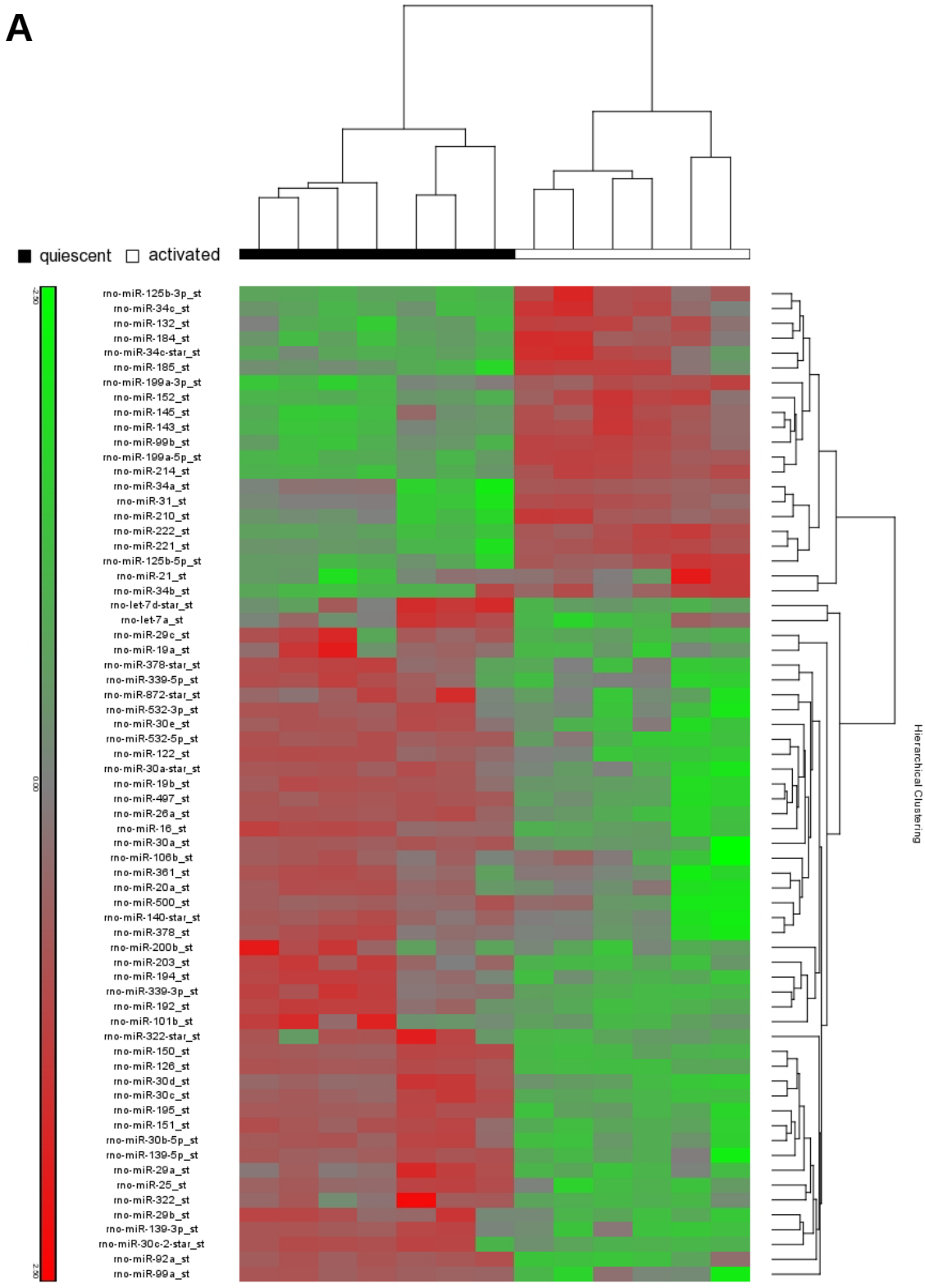
A
quiescent
activated
rno-miR-125b-3p_st
rno-miR-34c_st
rno-miR-132_st
rno-miR-184_st
rno-miR-34c-star_st
rno-miR-185_st
rno-miR-199a-3p_st
rno-miR-152_st
rno-miR-145_st
rno-miR-143_st
rno-miR-99b_st
rno-miR-199a-5p_st
rno-miR-214_st
rno-miR-34a_st
rno-miR-31_st
rno-miR-210_st
rno-miR-222_st
rno-miR-221_st
rno-miR-125b-5p_st
rno-miR-21_st
rno-miR-34b_st
rno-let-7d-star_st
rno-let-7a_st
rno-miR-29c_st
rno-miR-19a_st
rno-miR-378-star_st
rno-miR-339-5p_st
rno-miR-872-star_st
rno-miR-532-3p_st
rno-miR-30e_st
rno-miR-532-5p_st
rno-miR-122_st
rno-miR-30a-star_st
rno-miR-19b_st
rno-miR-497_st
rno-miR-26a_st
rno-miR-16_st
rno-miR-30a_st
rno-miR-106b_st
rno-miR-361_st
rno-miR-20a_st
rno-miR-500_st
rno-miR-140-star_st
rno-miR-378_st
rno-miR-200b_st
rno-miR-203_st
rno-miR-194_st
rno-miR-339-3p_st
rno-miR-192_st
rno-miR-101b_st
rno-miR-322-star_st
rno-miR-150_st
rno-miR-126_st
rno-miR-30d_st
rno-miR-30c_st
rno-miR-195_st
rno-miR-151_st
rno-miR-30b-5p_st
rno-miR-139-5p_st
rno-miR-29a_st
rno-miR-25_st
rno-miR-322_st
rno-miR-29b_st
rno-miR-139-3p_st
rno-miR-30c-2-star_st
rno-miR-92a_st
rno-miR-99a_st
-2.50
0.00
2.50
Hierarchical Clustering

B

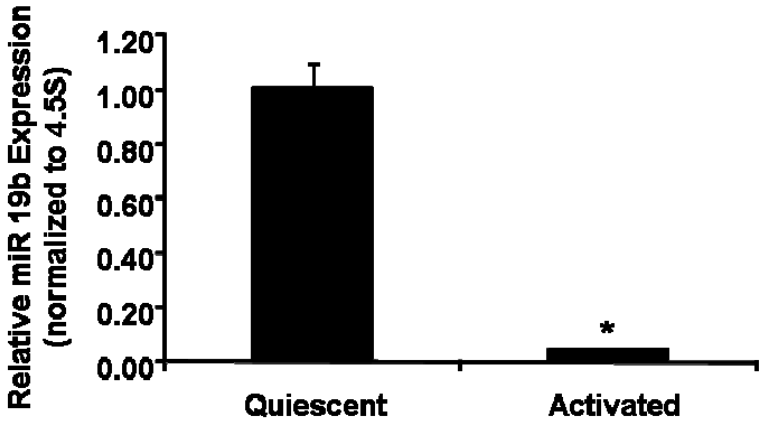
Relative miR 19b Expression
(normalized to 4.5S)
1.20
1.00
0.80
0.60
0.40
0.20
0.00
*
Quiescent
Activated

C

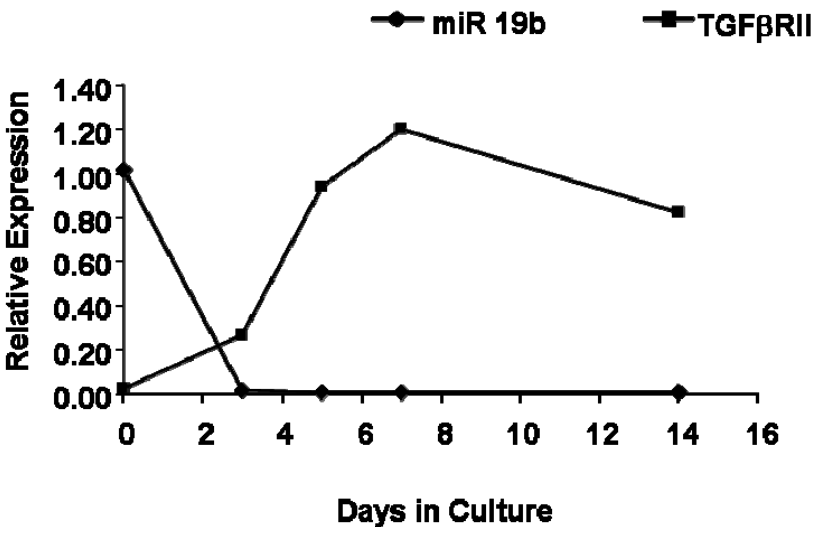
miR 19b
TGFβRII
Relative Expression
1.40
1.20
1.00
0.80
0.60
0.40
0.20
0.00
0
2
4
6
8
10
12
14
16
Days in Culture

Figure 4.1 Differential miRNA expression in quiescent vs activated HSCs. (A) Microarray analysis for miRNA was performed with RNA extracts from primary quiescent (n=7) and activated (n=6) HSCs. Hierarchical cluster analysis of significantly differentially expressed miRs: bright green, underexpression; gray, no change; bright red, overexpression. (B) Cells were harvested and miR 19b expression was determined in quiescent (n=7) and activated (day 14, n=6) HSCs as assessed by qRT-PCR. (C) qRT-PCR analysis of miR 19b and TGFβRII expression levels over days in culture (n=3) as normalized to 4.5S rRNA and β-actin, respectively. Data are presented as mean ± SE. *Differs from quiescent vs activated, $p<0.05$.

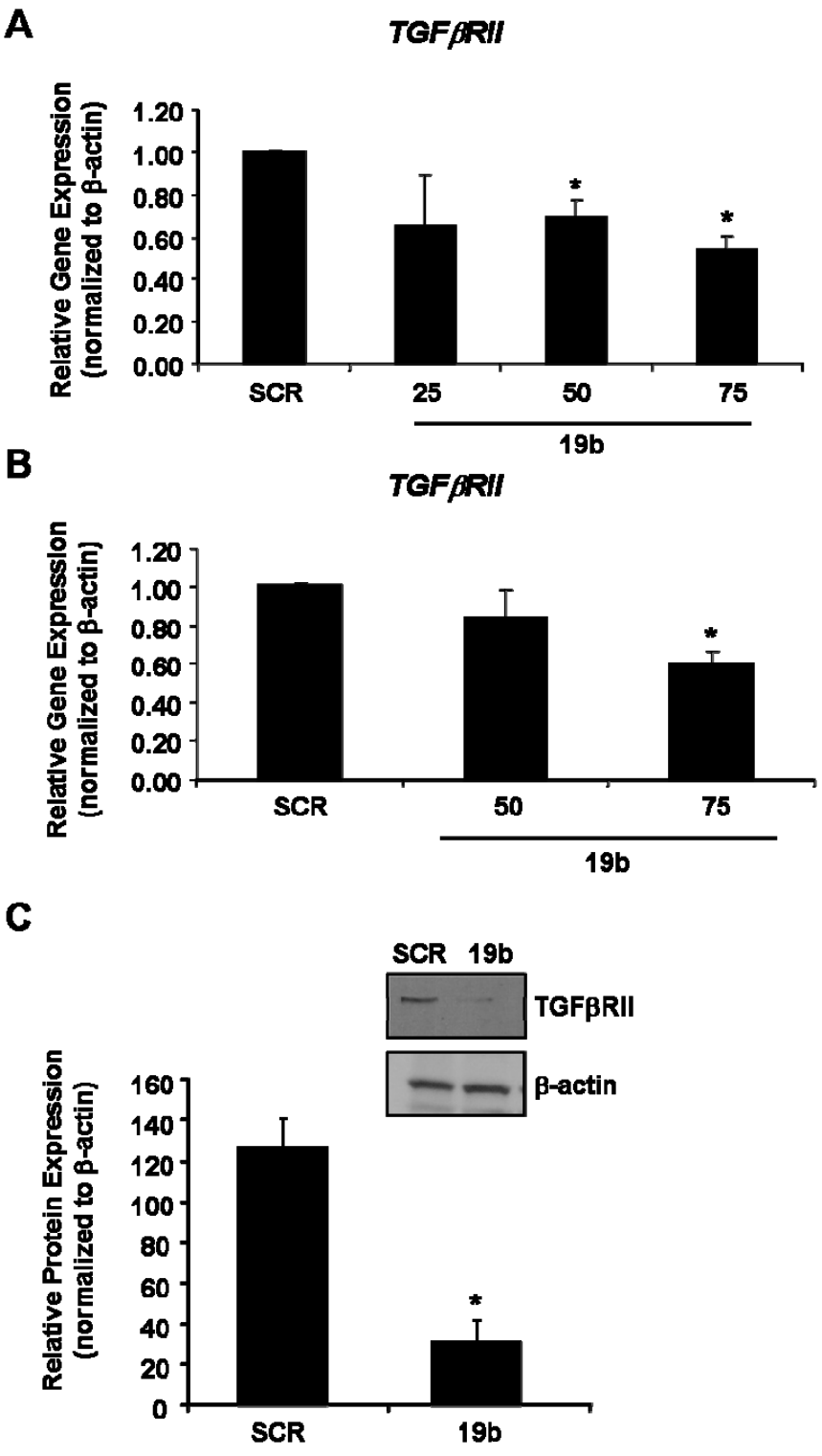
A
TGFβRII
Relative Gene Expression (normalized to β-actin)
1.20
1.00
0.80
0.60
0.40
0.20
0.00
SCR
25
50
75
19b
B
TGFβRII
Relative Gene Expression (normalized to β-actin)
1.20
1.00
0.80
0.60
0.40
0.20
0.00
SCR
50
75
19b
C
SCR 19b
TGFβRII
β-actin
Relative Protein Expression (normalized to β-actin)
160
140
120
100
80
60
40
20
0
SCR
19b

D

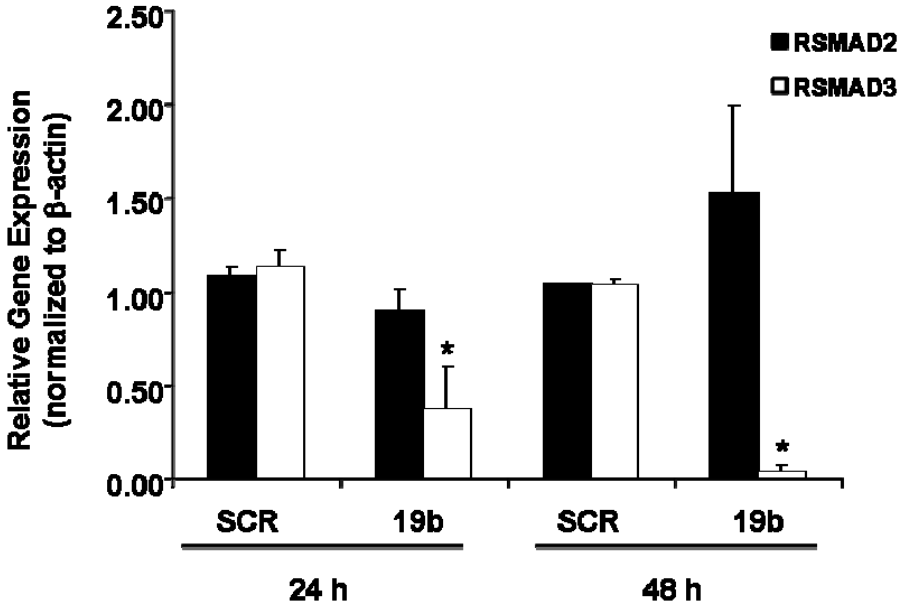
Relative Gene Expression
(normalized to β-actin)
2.50
2.00
1.50
1.00
0.50
0.00
RSMAD2
RSMAD3
*
*
SCR
19b
SCR
19b
24 h
48 h

E

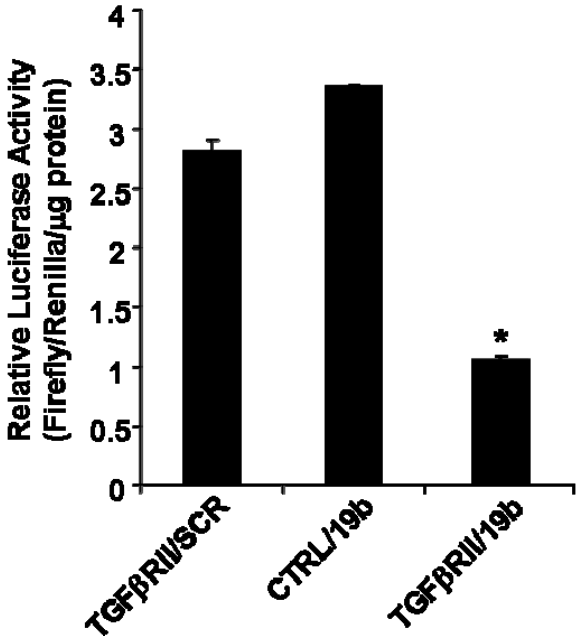
Relative Luciferase Activity
(Firefly/Renilla/µg protein)
4
3.5
3
2.5
2
1.5
1
0.5
0
*
TGFβRII/SCR
CTRL/19b
TGFβRII/19b

Figure 4.2 miR 19b negatively regulates TGFβRII expression. Day 6 HSCs were transiently transfected with miR 19b mimic (25-75 nM) and TGFβRII gene expression was measured by qRT-PCR at (A) 24 h and (B) 48 h (n=4). Expression was normalized to β-actin. (C) Representative immunoblot and quantitative densitometry of TGFβRII protein expression 48 h post-transfection (miR 19b, 75 nM) (n=3). Expression was normalized to β-actin. (D) R-SMAD gene expression in activated HSCs (day 6) transfected with mature miR 19b for 24 and 48 h was determined by qRT-PCR. (E) Inhibition of firefly luciferase activities of pEZX-TGFβRII reporter by miR 19b mimic. LX-2 cells were co-transfected with 4.8 μg of pEZX-TGFβRII reporter plasmid or empty vector and 75 nM miR 19b mimic or SCR using Lipofectamine 2000. Data are presented as mean ± SE. *Differs from SCR, $p<0.05$.

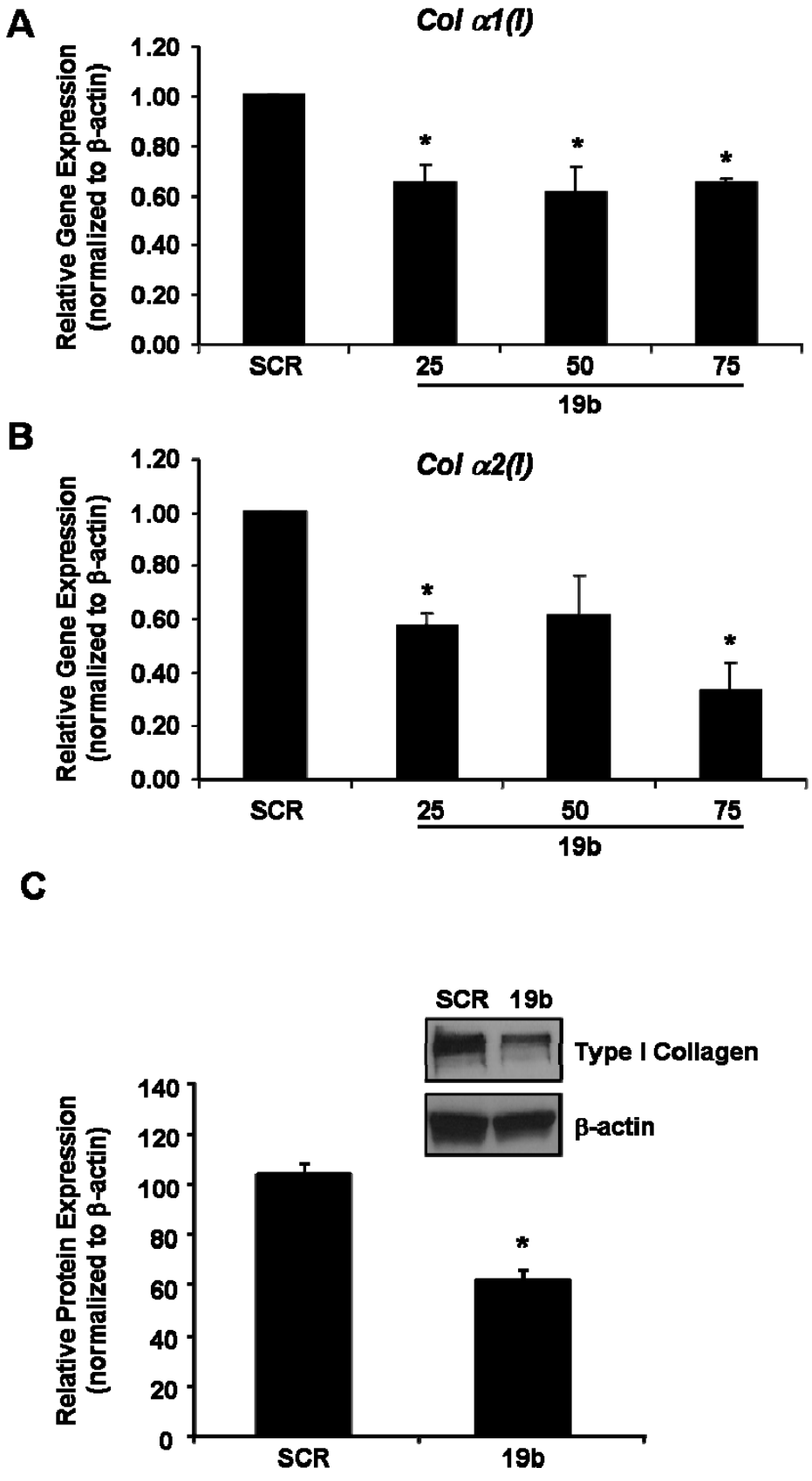
A
Col α1(I)
Relative Gene Expression (normalized to β-actin)
1.20
1.00
0.80
0.60
0.40
0.20
0.00
*
*
*
SCR
25
50
75
19b
B
Col α2(I)
Relative Gene Expression (normalized to β-actin)
1.20
1.00
0.80
0.60
0.40
0.20
0.00
*
*
SCR
25
50
75
19b
C
SCR 19b
Type I Collagen
β-actin
Relative Protein Expression (normalized to β-actin)
140
120
100
80
60
40
20
0
*
SCR
19b

Figure 4.3 miR 19b exerts inhibitory effects on TGFβ target gene collagen. Day 6 HSCs were transiently transfected with miR 19b mimic (25-75 nM) and Col α1(I) and Col α2(I) gene expression was assessed by qRT-PCR at (A) 24 h and (B) 48 h (n=4). Expression was normalized to β-actin. (C) 48 h post-transfection cells were harvested and immunoblot performed on whole cell lysates for type I collagen expression. Expression was determined by quantitative densitometry and normalized to β-actin (n=3). Data are presented as mean ± SE. *Differs from SCR, $p<0.05$.

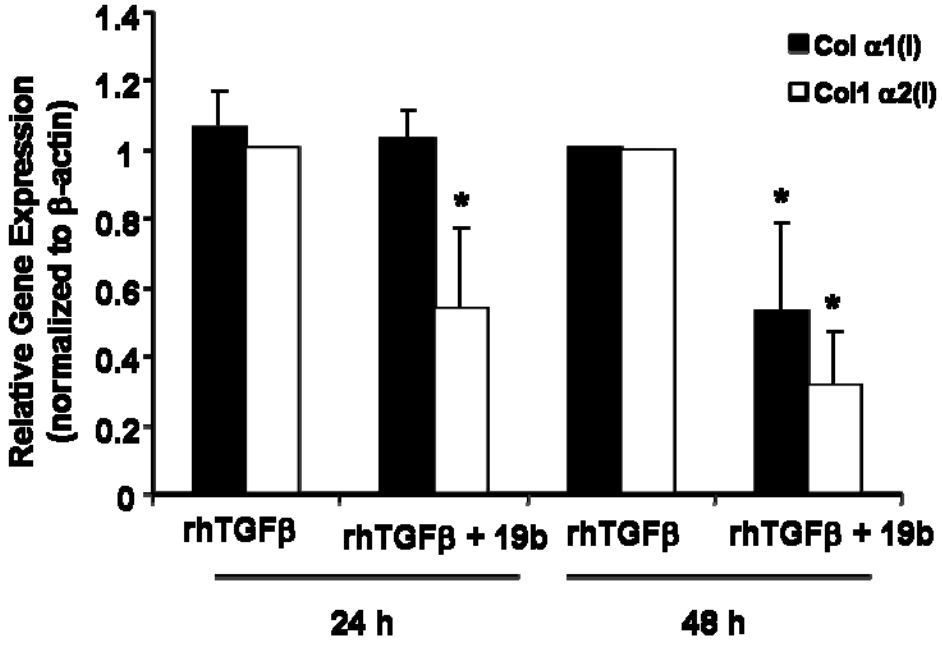

Figure 4.4 miR 19b inhibits paracrine TGFβ signals. Day 6 activated HSCs were transfected with or without miR 19b mimic (75 nM) and following standard 6 h incubation, transfection medium was removed and fresh culture medium devoid of antibiotic was added that contained 5 ng/mL of recombinant TGFβ (rhTGFβ) for a period of 48 h. Cells were harvested and mRNA levels of Col α1(I) and Col α2(I) were assessed by qRT-PCR (n=3). Data are presented as mean ± SE. *Differs from rhTGFβ control, $p<0.05$.

A

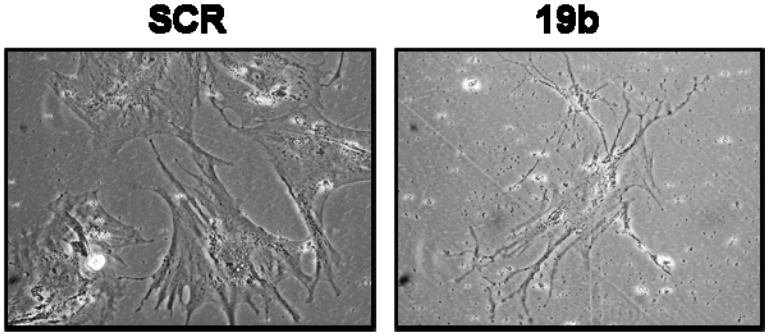
SCR
19b

B

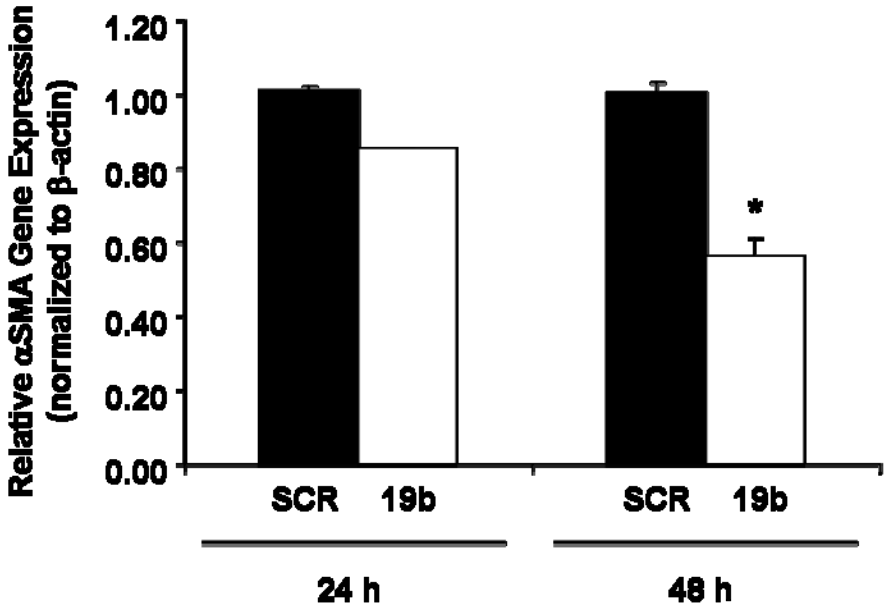
Relative αSMA Gene Expression
(normalized to β-actin)
1.20
1.00
0.80
0.60
0.40
0.20
0.00
*
SCR
19b
SCR
19b
24 h
48 h

C

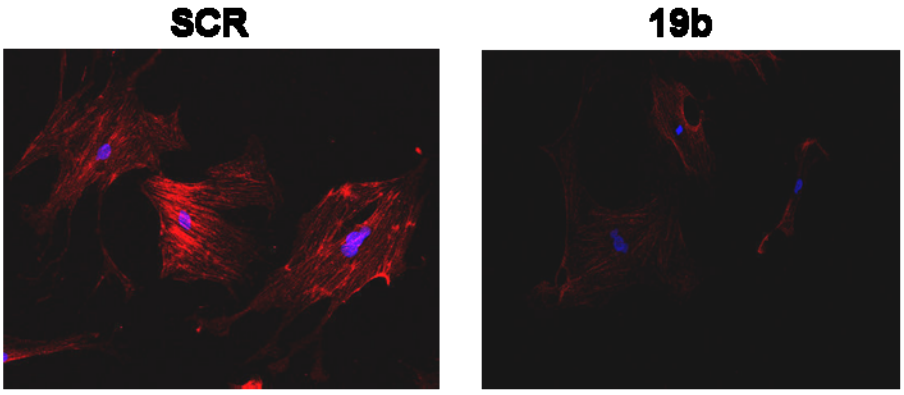
SCR
19b

D

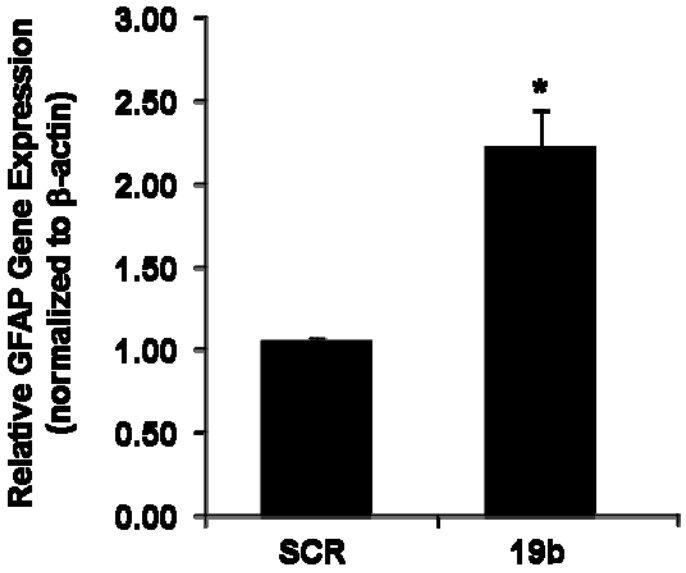
Relative GFAP Gene Expression
(normalized to β-actin)
3.00
2.50
2.00
1.50
1.00
0.50
0.00
*
SCR
19b

E

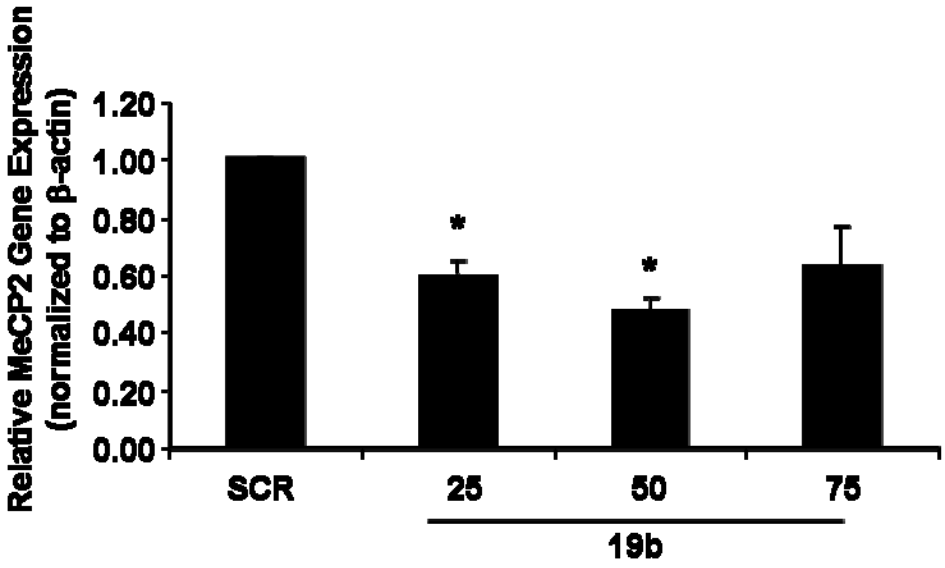
Relative MeCP2 Gene Expression
(normalized to β-actin)
1.20
1.00
0.80
0.60
0.40
0.20
0.00
*
*
SCR
25
50
75
19b

F

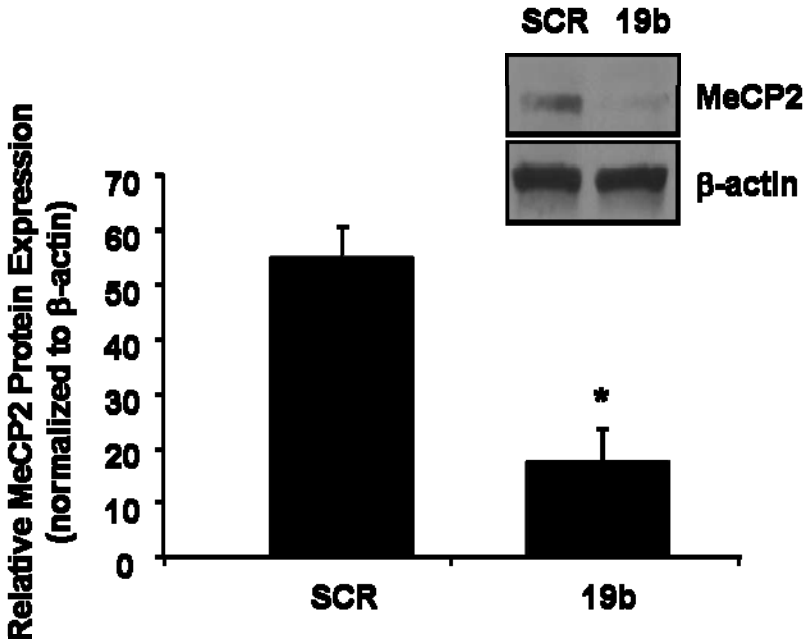
SCR 19b
MeCP2
β-actin
Relative MeCP2 Protein Expression
(normalized to β-actin)
70
60
50
40
30
20
10
0
*
SCR
19b

Figure 4.5 HSC activation is inhibited by miR 19b. (A) Activated HSCs (day 6) were transfected with negative control (SCR) or miR 19b (75 nM) for 48 h. Cell morphology was visually assessed and representative light micrographs (40X) are shown. (B) Day 6 HSCs were transiently transfected with miR 19b mimic (75 nM) and αSMA gene expression was assessed by qRT-PCR at 24 h and 48 h (n=4). (C) Representative images (40X) of fluorescent immunocytochemical analysis of αSMA expression (red) in activated HSCs following 48 h of transfection with SCR or miR 19b mimic (75 nM); dapi staining (blue) was used to indicate cell nuclei (n=3). (D) Day 6 HSCs were transiently transfected with miR 19b mimic (75 nM) and GFAP expression was assessed by qRT-PCR at 48 h (n=4). (E) MeCP2 gene expression as measured by qRT-PCR following 24 h of miR 19b transfection in activated HSCs (day 6) (n=4). (F) Representative immunoblot and quantitative densitometry of MeCP2 protein expression in HSCs (day 6) following 48 h of miR 19b (75 nM, n=3). Expression was normalized to β-actin. Data are presented as mean ± SE. *Differs from SCR, $p<0.05$.

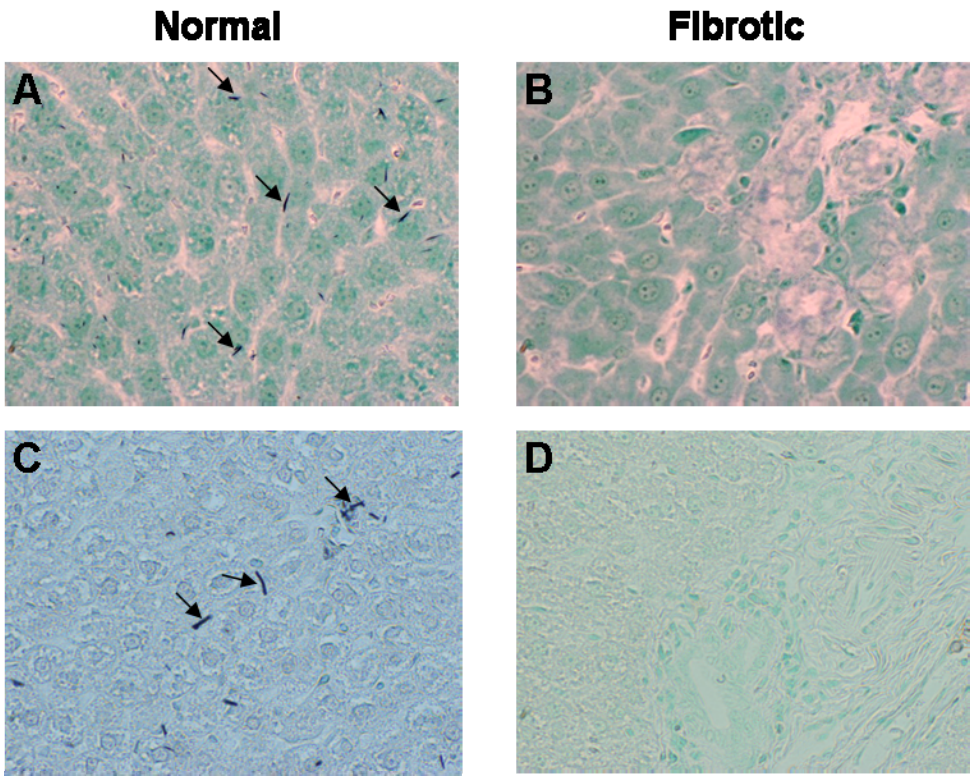

Figure 4.6 Down-regulation of miR 19b in rodent models of hepatic fibrosis. Representative light micrographs (40X) of liver tissue sections following in situ hybridization with double DIG labeled LNA miR 19b probes. miR 19b expression levels are marked by dark blue chromagen staining (denoted by black arrows). (A-D) miR 19b expression in normal and fibrotic liver tissues. (A and B) Liver tissues harvested from rats which underwent BDL or sham surgeries (tissue harvested at 2 weeks). (C and D) Liver tissue harvested from controls and rats fed ethanol with bi-weekly injections of LPS [88].

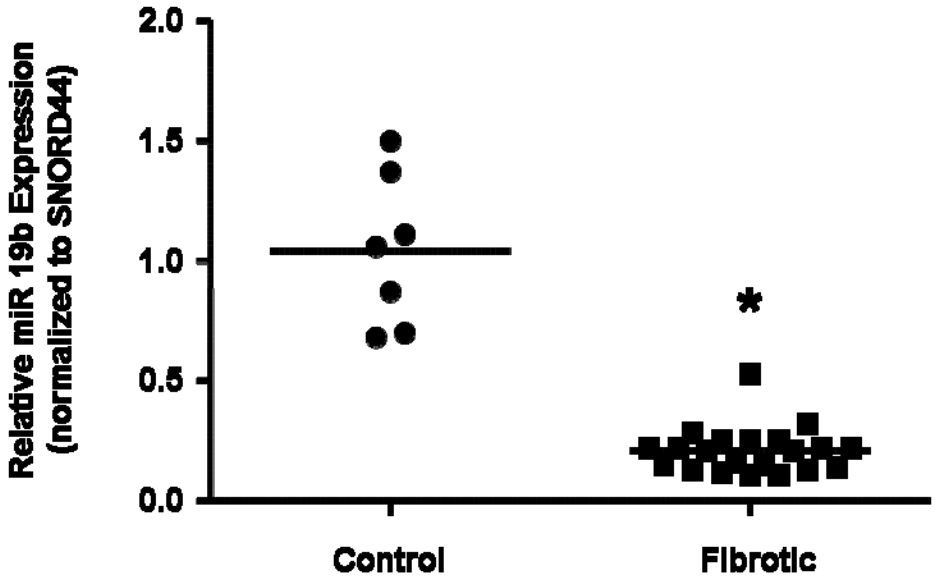

Figure 4.7 miR 19b is a putative biomarker for human hepatic fibrosis. RNA was harvested from normal (n=7) and fibrotic (n=21) human liver tissue and miR 19b expression was assessed by qRT-PCR. Expression was normalized to SNORD44. Data are presented as mean ± SE. *Differs from control, $p<0.05$.

Table 4.S1 Primers used in this study.

Gene	Forward	Reverse
β-actin	GAGCTATGAGCTG CCTGACG	GGATGTCAACGTC ACACTTC
Collagen α1(I) **(col α1(I))**	CACTGCAAGAACA GCGTAGC	ATGTCCATTCCGAA TTCCTG
Collagen α2(I) **(col α1(I))**	AAGGCATTCGAGG ACACAAC	TTACCAACAGGCCC AAGTTC
Glial fibrillary acidic protein **(GFAP)**	AGAAAACCGCATC ACCATTC	TTGGGCCTAGCAA ACAAGAC
Methyl CpG binding protein 2 **(MeCP2)**	TGCTGCTGCCTTTG GTCT	TTGAAAAGGTGGG AGACA
SMAD2	TGGTAAGAAAATG TCGTCCATC	TTTCAGAGCAAGTG CTTGGTAT
SMAD3	GTGACACTCCTGAA GGCCATAC	GGCCAACAAAGAG GGTTCTAGT
SMAD4	AAGGACAGCCATC CTTACCC	GCCCTGAAGCTATC TGCAAC
Smooth muscle-α actin **(αSMA)**	CATCAGGAACCTC GAGAAGC	TCGGATACTTCAGG GTCAGG
Transforming growth factor β receptor II (**TGFβRII**)	TCACTAGGCACGTC ATCAGC	AGGACAACCCGAA GTCACAC

Table 4.S2 List of differentially expressed miRs detected in activated vs. quiescent HSCs.

Probeset ID	p-value(activated vs. quiescent)	Fold-Change (activated vs. quiescent)
rno-miR-122_st	7.3E-05	-3.7E+02
rno-miR-126_st	5.4E-10	-6.7E+01
rno-miR-139-3p_st	2.1E-04	-7.5E+00
rno-miR-139-5p_st	1.0E-04	-6.8E+00
rno-miR-140-star_st	3.4E-03	-2.5E+00
rno-miR-150_st	8.2E-09	-7.5E+01
rno-miR-151_st	3.9E-07	-2.1E+00
rno-miR-16_st	5.3E-06	-2.2E+00
rno-miR-192_st	9.3E-05	-7.8E+01
rno-miR-194_st	9.0E-05	-6.7E+01
rno-miR-195_st	8.2E-07	-1.7E+01
rno-miR-19a_st	2.2E-03	-1.5E+00
rno-miR-19b_st	2.8E-05	-6.3E+00
rno-miR-203_st	1.9E-05	-3.1E+00
rno-miR-25_st	2.5E-05	-4.2E+00
rno-miR-26a_st	2.8E-06	-2.7E+00
rno-miR-29a_st	1.9E-04	-2.5E+00
rno-miR-29b_st	1.2E-04	-5.2E+00
rno-miR-29c_st	5.1E-04	-3.1E+00
rno-miR-30a-star_st	3.1E-04	-6.3E+00
rno-miR-30a_st	2.1E-04	-4.1E+00
rno-miR-30b-5p_st	4.4E-06	-6.9E+00
rno-miR-30c-2-star_st	6.9E-04	-6.4E+00
rno-miR-30c_st	1.6E-07	-4.8E+00
rno-miR-30d_st	3.4E-05	-3.3E+00
rno-miR-30e_st	1.2E-04	-8.2E+00
rno-miR-322-star_st	2.8E-03	-3.8E+00
rno-miR-322_st	9.5E-04	-3.6E+00
rno-miR-339-3p_st	1.5E-05	-5.7E+00
rno-miR-378-star_st	3.0E-03	-5.0E+00
rno-miR-378_st	3.8E-03	-4.5E+00
rno-miR-497_st	9.5E-06	-1.8E+01
rno-miR-532-3p_st	6.4E-04	-3.7E+00
rno-miR-532-5p_st	2.5E-05	-1.8E+01
rno-miR-872-star_st	1.0E-03	-2.2E+00
rno-miR-92a_st	3.1E-05	-2.0E+00
rno-miR-99a_st	1.7E-03	-3.3E+00
rno-miR-125b-3p_st	1.6E-06	7.4E+00
rno-miR-125b-5p_st	9.0E-06	2.0E+00
rno-miR-132_st	2.4E-05	1.3E+01
rno-miR-143_st	1.5E-05	3.0E+00
rno-miR-145_st	2.6E-04	2.6E+00
rno-miR-152_st	1.5E-06	3.3E+00
rno-miR-184_st	2.7E-05	1.5E+01
rno-miR-185_st	8.7E-04	2.7E+00
rno-miR-199a-3p_st	1.1E-04	3.8E+00

rno-miR-199a-5p_st	3.4E-08	6.0E+00
rno-miR-210_st	1.9E-04	1.2E+01
rno-miR-214_st	3.9E-08	8.0E+00
rno-miR-221_st	1.5E-05	1.1E+01
rno-miR-222_st	2.7E-07	1.7E+01
rno-miR-31_st	2.1E-03	1.5E+01
rno-miR-34b_st	1.6E-03	2.2E+00
rno-miR-34c-star_st	6.7E-04	9.4E+00
rno-miR-34c_st	6.7E-05	2.7E+01
rno-miR-99b_st	1.9E-06	2.4E+00

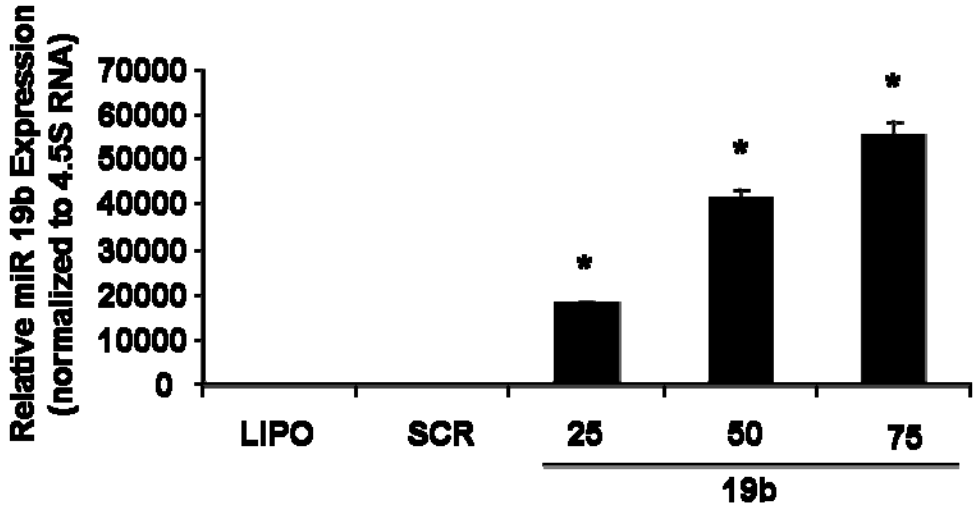

Figure 4.S1 Efficient transfection of miR 19b in activated HSCs. Representative qRT-PCR analysis of miR 19b expression in HSCs transfected with Lipofectamine 2000 alone (LIPO), negative control (SCR) or mature miR 19b (25-75 nM) for 24 h. Expression was normalized to r RNA. Data are presented as mean ± SE. *Differs from SCR, $p<0.05$.

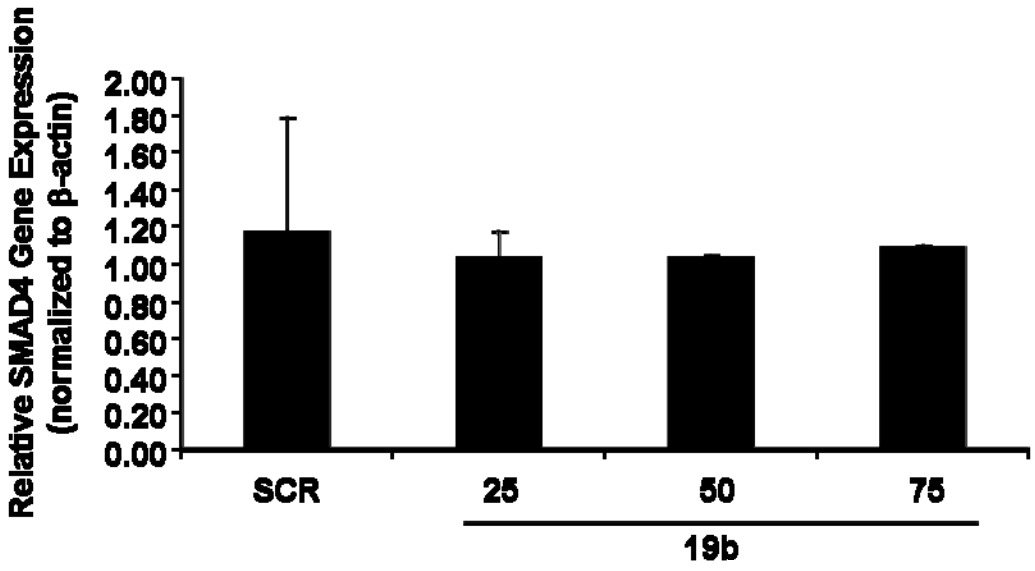

Figure 4.S2 miR 19b does not affect SMAD4 gene expression in activated HSCs. qRT-PCR analysis of SMAD4 gene expression following 24 h of miR 19b transfection studies as normalized to levels of β-actin (n=3).

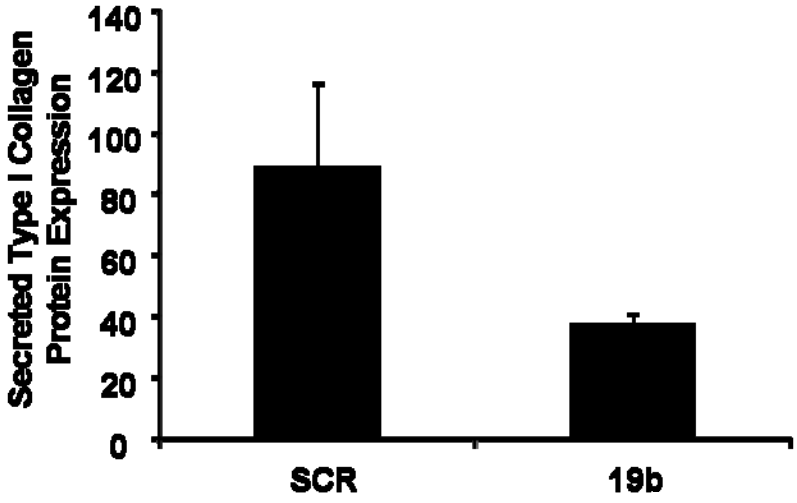

Figure 4.S3 Collagen secretion is inhibited by miR 19b in activated HSCs. Quantitative densitometry of immunoblot analyses of secreted type I collagen protein expression following 48 h of miR 19b (75 nM) transfection in HSCs (day 6). Culture medium was harvested following 48 h and proteins concentrated using Nanosep tubes (Pall Corporation; Ann Arbor, MI). Concentrated protein (10 μg) was used for standard immunoblotting analysis. Quantitative densitometry of secreted type I collagen was performed and normalized to total protein (n=3). Data are presented as mean ± SE.

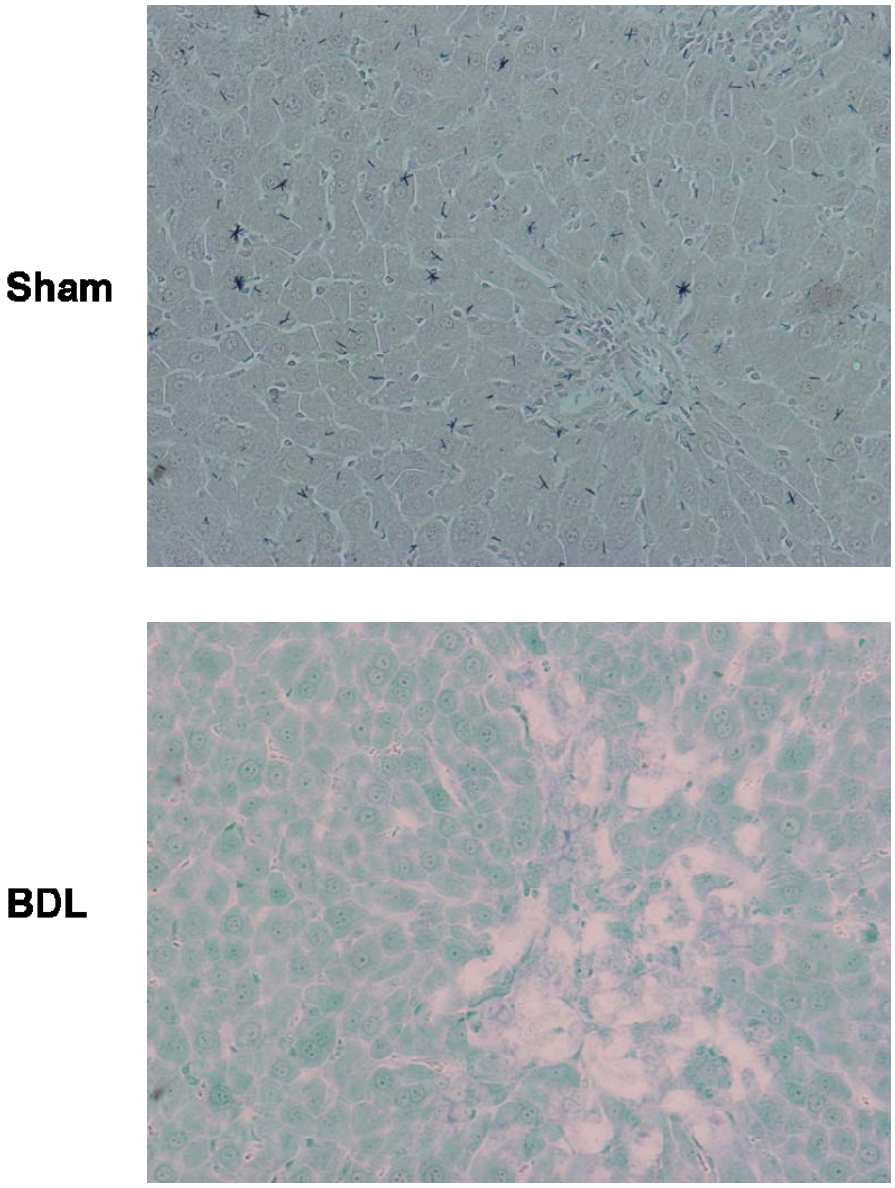

Figure 4.S4 In situ hybridization of miR 19b in normal and fibrotic rat liver. Liver sections from a BDL model of hepatic fibrosis (sham, top panel; BDL, bottom panel). miR 19b expression levels are marked by dark blue chromagen staining. Representative light micrographs (20X) of liver tissue sections.

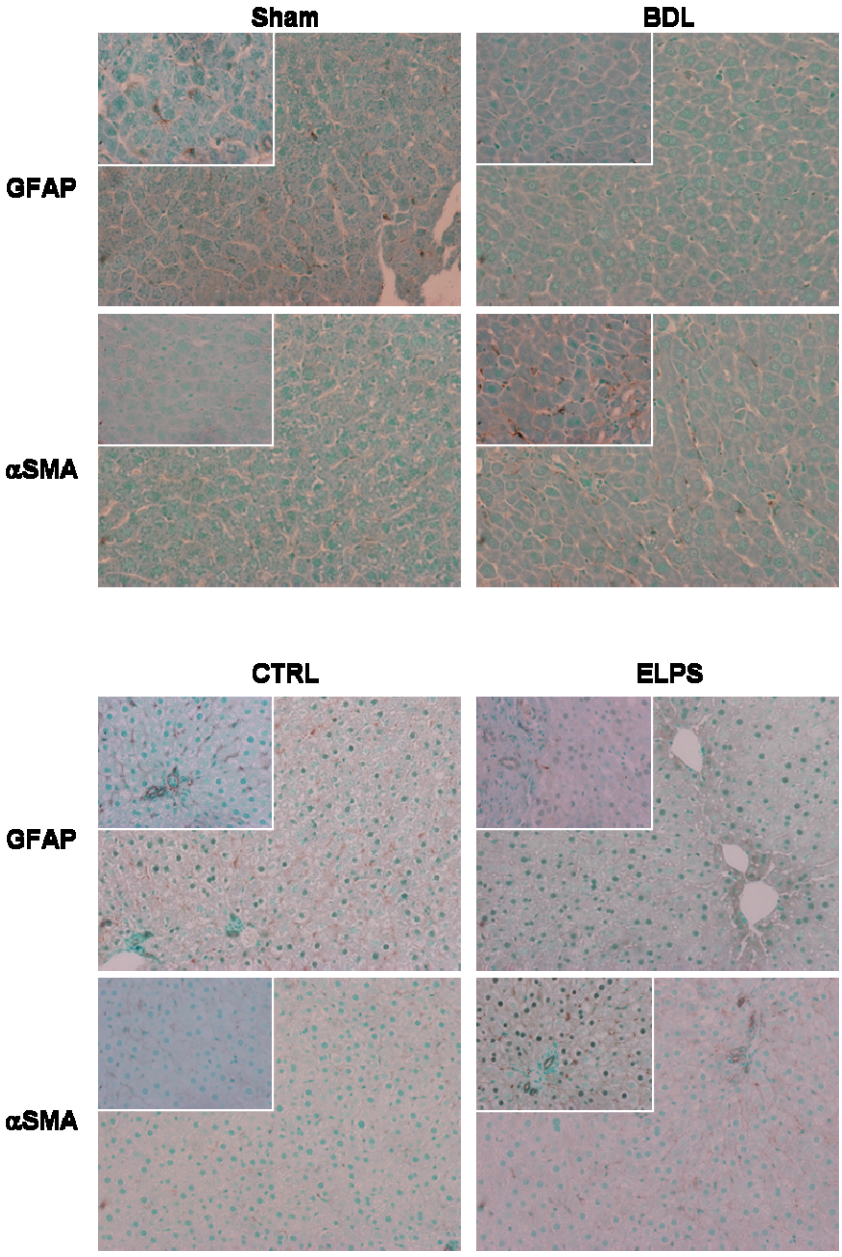

Figure 4.S5 Immunohistochemistry of quiescent and activated markers of HSCs. Liver sections from two models of hepatic fibrosis [BDL; top panels, Ethanol/LPS (ELPS); bottom panels]. Quiescent and activated HSCs were detected by GFAP and αSMA staining, respectively (brown chromagen) and counterstained with methyl green.

CHAPTER 5: ALTERED AQUAPORIN EXPRESSION AND ROLE IN APOPTOSIS DURING HEPATIC STELLATE CELL ACTIVATION

Introduction

Hepatic fibrosis is characterized by an accumulation of secreted type I collagen by hepatic stellate cells (HSCs) [15-16]. Within the liver, fibrosis is mediated by a number of factors including viral infection, genetic disease, and/or xenobiotic-induced damage. In the normal liver HSCs reside in a quiescent state, functioning to store vitamin A, modulate the microcirculation, and regulate extracellular matrix production. Following injury, the HSCs transdifferentiate into an activated myofibroblast-like cell characterized by loss of vitamin A droplets, increased smooth muscle-α actin expression (α-SMA), and decreased sinusoidal blood flow. Continued HSC transdifferentiation leads to collagen deposition, persistent activation, increased proliferation, and diminished responsiveness to apoptotic stimuli [52]. Reversal of hepatic fibrosis has been reported and is dependent, at least in part, on the induction of HSC apoptosis [48].

Apoptosis is characterized by a highly conserved series of biochemical and morphological events initiated by the apoptotic volume decrease (AVD). During the AVD intracellular K^+ levels decrease from 140mM to < 35mM, a pre-requisite for downstream caspase and nuclease activation [159-160]. These, and other, changes in intracellular solute concentrations, result in the creation of a sustained osmotic gradient and net water loss from the cell resulting in the cell "shrinkage" characteristic of all apoptotic cells [159, 161].

Aquaporins (AQPs) are a family of transmembrane proteins that are ubiquitously expressed in plant and animal cells [163]. To date 13 mammalian AQP homologs (AQP 0-12) have been identified, which have been functionally subdivided based on solute transported (e.g. aquaporins and aquaglyceroporins) [165, 251]. Studies using knockout mice demonstrate the importance of AQPs in regulating a wide array of cell functions in a range of organ systems including the liver [167, 252-253]. Previous studies demonstrate water movement during the AVD occurs via AQPs [159-160, 162], and inhibition of AQP-dependent water movement during the AVD significantly slows apoptotic progression [160-161, 164]. At least 7 AQP homologs have been identified in the liver and play important roles in hepatobiliary physiology and patho-physiology [162, 167].

No studies, to our knowledge, have addressed the expression or function of AQPs in HSCs. Given the importance of AQPs during the initiation and progression of apoptosis [159-160, 162], and the role of HSC apoptosis during the regression of hepatic fibrosis [48], we hypothesized that sustained HSC activation and increased cell survival in activated HSCs may be due to changes in AQP expression and/or function.

Results

Decreased AQP expression in activated versus quiescent HSCs

Analysis by RT-PCR detected the expression of AQP 0, 1, 5, 8, 9, 11, and 12 mRNAs in dQ HSCs. In contrast, culture-activated (d14) HSCs were characterized by the presence of AQP 0 and 11 mRNA and a failure to detect AQP 1, 5, 8, 9 or 12 mRNA (Figure 5.1A). mRNA for the remaining AQP homologs (AQP 2, 3, 4, 6, 7, and 10) were detected in positive control samples but not detected in either dQ or d14 HSCs (data not shown). Since AQP 8 and 9 are prominently expressed in dQ HSCs and represent two subclasses of proteinacious AQP channels, gene expression of both homologs was

determined over 10 days in culture to measure changes in expression during HSC activation. Consistent with RT-PCR, RealTime analyses showed dQ HSCs to have significantly higher expression of AQPs 8 and 9 compared to all other days in culture, with the most dramatic decline in expression occurring from dQ to d1 (Figure 5.1B).

To determine AQP protein expression Western blot analyses were performed for those AQPs detected at the mRNA level in dQ and/or d14 HSCs. Using this approach, we failed to detect AQPs 0, 1, 8, and 9 protein in d14 HSCs (Figure 5.1C) (albeit at very long exposures a faint band appeared for AQP 8 and 9, data not shown). Conversely, AQP 11 was clearly detectable in d14 HSCs, an effect not evidenced in dQ HSCs. Despite detecting AQP 5 mRNA and protein in control tissue (rat kidney) and AQP 5 mRNA in dQ HSCs, we were unable to detect AQP 5 protein expression in either dQ or d14 HSCs, even following prolonged film exposure times (20-25 minutes, Figure 5.1C). Finally, we were unable to detect AQP 12 protein expression in either HSCs (dQ or d14) or positive control tissue (rat pancreas) extracts using commercially available antibodies (data not shown).

Plasma membrane water permeability is AQP-dependent in HSCs

To ascribe AQP functionality in HSCs, we next determined cell membrane water permeability with or without AQP inhibitor pre-treatment; $HgCl_2$ (100μM; 2 minutes), concomitant with rapid osmotic challenge (210 mOsm; 30 seconds). In dQ HSCs osmotic challenge significantly increased cell swelling as evidenced by increased mean cell size and a "shift" in cell distribution/forward scatter (Figure 5.2A and B, $p<0.005$). The effect of osmotic challenge on dQ HSCs was abrogated by pre-treatment with $HgCl_2$ (100 μM; 2 minutes, Figure 5.2A and B). Conversely, d14 HSCs demonstrated a failure to

significantly respond to osmotic challenge compared to freshly isolated HSCs, an observation that was not significantly affected by pretreatment with $HgCl_2$ (100 μM; 2 min, Figure 5.2A and B).

AQP-dependent morphological responses to apoptotic stimulus

Treatment of dQ HSCs with GTx led to dramatic and rapid (20 minutes) decreases in cell surface attachment, accompanied by loss of cytoplasmic projections at both doses of GTx tested (0.15 or 1.5 μM, Figure 5.3A). In contrast, similar anoikis-like effects in d14 HSCs were only observed after 60 minutes of GTx treatment and only at the higher dose employed (1.5 μM) (Figure 5.3B). To determine if the effects of GTx were dependent on AQP expression/function, dQ and d14 HSCs were treated in parallel with $HgCl_2$ (100μM; 15 min) prior to GTx exposure. Under these experimental conditions no cell detachment was observed following 0.15 or 1.5 μM GTx treatment. Furthermore, dQ HSCs pre-treated with $HgCl_2$ maintained morphological integrity, as characterized by the presence of cytoplasmic projections, indicating the maintenance of a quiescent/early activation phenotype. Pre-treatment of d14 HSCs with $HgCl_2$ did not stimulate changes in cell morphology/phenotype (myofibroblast-like) either in the absence or presence of GTx (Figure 5.3A and B). Direct cell counts and trypan blue exclusion assay during treatment with 1.5 μM GTx showed significantly decreased cell viability in dQ HSCs 20 min after GTx compared to d14; $HgCl_2$ pre-treatment abrogated this effect (Figure 5.3C and D). Trypan blue exclusion studies confirmed pre-treatment with $HgCl_2$ did not adversely affect HSC viability (93 ± 4 % and 95 ± 2% viability 60 minutes after $HgCl_2$ treatment, dQ and d14 HSCs, respectively).

Inhibition of AQP channels decreases apoptotic response

To further elucidate the morphological response to apoptotic challenge, caspase-3 activity was measured. Treatment of dQ HSCs with GTx (1.5 μM) led to significant increases in caspase-3 activity 20 minutes after GTx stimulation before decreasing over the following 40 minutes (Figure 5.4A). In contrast, no significant increase in caspase-3 activity was observed in d14 HSCs until 45 minutes after GTx stimulation, and the increase in caspase-3 activity was transient (Figure 5.4A). Pre-treatment of dQ and d14 HSCs with $HgCl_2$ (100 μM; 15 minutes) abrogated the effect of GTx on caspase-3 activity at all of the time points measured (Figure 5.4A, $p<0.05$). Pre-treatment of dQ and d14 HSCs with Z-VAD (pan-caspase inhibitor) demonstrated that subsequent GTx treatment failed to significantly stimulate caspase-3 activity in either dQ or d14 HSCs (Figure 5.4A). Western blot analyses confirmed these results, PARP cleavage being decreased in d14 HSCs as compared to dQ HSCs, effects that were abolished by $HgCl_2$ pre-treatment (Figure 5.4B).

Decreased AQP expression in activated versus quiescent HSCs in a model of liver injury

Dual fluorescent immunohistochemical staining was performed to measure AQP expression in activated and quiescent HSCs in vivo. GFAP and α-SMA were used as markers of quiescent and activated HSCs, respectively. Merged images confirmed increased colocalization of quiescent HSCs with both AQP 8 and 9 in control (CTRL) liver tissue as indicated by yellow fluorescence (Figure 5.5A and E). Conversely, in injured liver (ELPS) tissue GFAP positive quiescent HSCs were decreased [as indicated by the lack of green fluorescence in Figure 5.5C and G] while α-SMA (a hallmark of

activated HSCs) expression increased. However, a lack of colocalization of α-SMA positive cells with AQP 8 and 9 expression was observed, as indicated by the lack of yellow fluorescence in merged images (Figure 5.5D and H).

Discussion

Several studies have reported the specific expression of AQP homologs in different hepatic cell populations (as reviewed by Masyuk and LaRusso [167]). However, to our knowledge, no studies have addressed the specific expression, or functional significance, of AQPs in the hepatic stellate cell (HSC). In this report we describe the expression profile of aquaporin (AQP) homologs in HSCs in vitro, and the changes that occur in AQP expression between quiescent and activated HSCs. Specifically we report quiescent HSCs are characterized by AQP 0, 1, 8 and 9 expression at the mRNA and protein level. Conversely, only AQP 11 was detected at both the mRNA and protein level in activated HSCs. Using osmotic challenge, in the absence and presence of a non-specific AQP channel blocker ($HgCl_2$), we demonstrated rapid AQP-dependent water movement across the plasma membrane in quiescent HSCs indicating the presence of functional AQP homologs within the plasma membrane. Conversely, activated HSCs failed to respond to osmotic challenge. We demonstrated that quiescent HSCs (4 hours), expressing multiple AQP homologs, were significantly more responsive to apoptotic stimulation (gliotoxin; GTx) versus activated HSCs. Finally, confirming in vitro studies, fluorescent immunohistochemistry showed strong colocalization between quiescent HSCs and AQPs 8 and 9, while α-SMA positive HSCs found in injured liver tissue exhibit dramatically decreased AQP expression.

The amelioration of hepatic fibrosis has been attributed to decreasing the presence of HSCs at the site of injury through apoptotic cell death [48, 154]. Additionally, upon cessation of the fibrogenic stimulus, activated HSCs are thought to undergo apoptosis, removing the source of continued ECM deposition without eliciting an inflammatory response [173]. There has been considerable interest in determining the molecular events that regulate HSC apoptosis. Activated HSCs have been reported to demonstrate increased resistance to apoptosis due to increased bcl-2 expression [52]. However, activated HSCs are still capable of undergoing apoptosis in response to a variety of stimuli including gliotoxin, superoxide, and tumor necrosis factor-related apoptosis-inducing ligand (TRAIL) [169-170, 173, 254]. In general, studies have been inconsistent when examining the two HSC phenotypes (quiescent and activated) in vitro. Studies either did not compare the rate of apoptosis in the activated state to quiescent HSCs, or if they did, the comparison was made to HSCs 48 hours after initial isolation and culture [169]. In contrast, our studies utilized freshly isolated HSCs for expression analysis or within 4 hours of performing functional studies. Our data demonstrate that quiescent HSCs express more AQP homologs, are more susceptible to osmotic challenge, and respond more rapidly and to lower doses of GTx than do fully activated, 14 day cultured HSCs. Interestingly, studies in a rat model of hepatocellular carcinoma demonstrated increased AQP 8 and 9 expression following isolation from the tumor and culturing in vitro. These changes in AQP expression correlate accordingly with altered responsiveness to osmotic and apoptotic challenge [162].

Several studies that modulated AQP expression demonstrated overexpression of specific homologs leads to increased migratory capacity and cell proliferation [255].

Additionally, AQP 1 and 3 knockout mice exhibited significant impairment in wound-healing and in urinary concentrating function [251, 253]. Our studies demonstrate that while AQPs 0, 1, 8 and 9 were detected at the mRNA and protein level in freshly isolated HSCs, AQP 5 and 11 were only detected at the mRNA level. Conversely, the only AQP we were able to detect at the mRNA and protein level in the activated HSCs was AQP 11. This raises several important questions that require further analysis experimentally. Firstly, what is the endogenous function of AQPs in quiescent HSCs in vivo? The majority of studies of AQP expression and function focus on organ systems that require the regulation of high levels of water movement as an integral part of physiological function (e.g. kidney, eye). Similarly, within the liver, the majority of work to date has focused on the role of hepatocyte AQPs (AQP 8 and 9) in regulating bile synthesis and modification [256-257], no discernable function having been identified for AQP 0, the other AQP homolog reported (ostensibly in the cytoplasm) of pericentral hepatocytes [258]. In contrast, quiescent HSCs in the healthy liver would not appear to require a high physiological demand for rapid water movement; however, AQP expression may be necessary for other functions such as migration and proliferation in response to injury [251] since 4 different AQP proteins and 7 different AQP mRNAs are expressed.

Secondly, AQP 5 and 11 mRNA were detectable in quiescent HSCs, yet we failed to detect the corresponding proteins. One possible explanation for this may lie in the ubiquitous expression and highly conserved nature of AQPs whereby mutation of the gene encoding one AQP homolog may have such dire, and rapid, consequences on cell function that an inherent “redundancy” exists. This does not, however, explain our observation that AQP 11 is clearly expressed in activated HSCs yet appears to play no

discernable role in mediating transmembrane water movement (as attested by the failure of activated HSCs to respond to osmotic or apoptotic stimulation). Interestingly, AQP 11 is characterized by an unusual NPA-pore forming motif [259] and controversy exists as to its water transport capabilities and function [260-262].

In contrast to the quiescent HSC, when stimulated to transdifferentiate, proliferate and undergo activation by culture on plastic, HSCs were characterized by marked decreases in net AQP expression. One possible explanation for this may be an absolute requirement for the activated HSC (in vivo) to demonstrate sustained resistance to apoptosis in the face of severe and/or prolonged hepatic insult. In doing so the HSC would thus maintain the ability to synthesize/secrete ECM as an integral part of the net hepatic protective response. Alternatively, it is possible that the process of matrix protein degradation, cell isolation and purification may also play a part in regulating both AQP expression and/or localization. AQP functionality is regulated by cellular/membrane localization, insertion into the plasma membrane creating an “unregulated”, bi-directional channel for water movement, the net direction of movement being dependent on the osmotic gradient [163, 165]. As such, during the process of removing HSCs from the native, complex 3-dimensional environment of the hepatic sinusoid may be sufficient to initiate changes in AQP mRNA and/or protein expression.

In summary, these data demonstrate that HSCs express AQPs and suggest that regulation of AQP expression/function contributes to HSC susceptibility to an apoptotic challenge. These data indicate it will be of considerable interest to study AQP expression and apoptosis in HSCs using animal models of progressive liver injury in which the magnitude and duration of the hepatic insult can be manipulated. In doing so, direct or

indirect modulation of AQP expression in HSCs may lead to the development of novel therapeutics for the treatment of hepatic fibrosis.

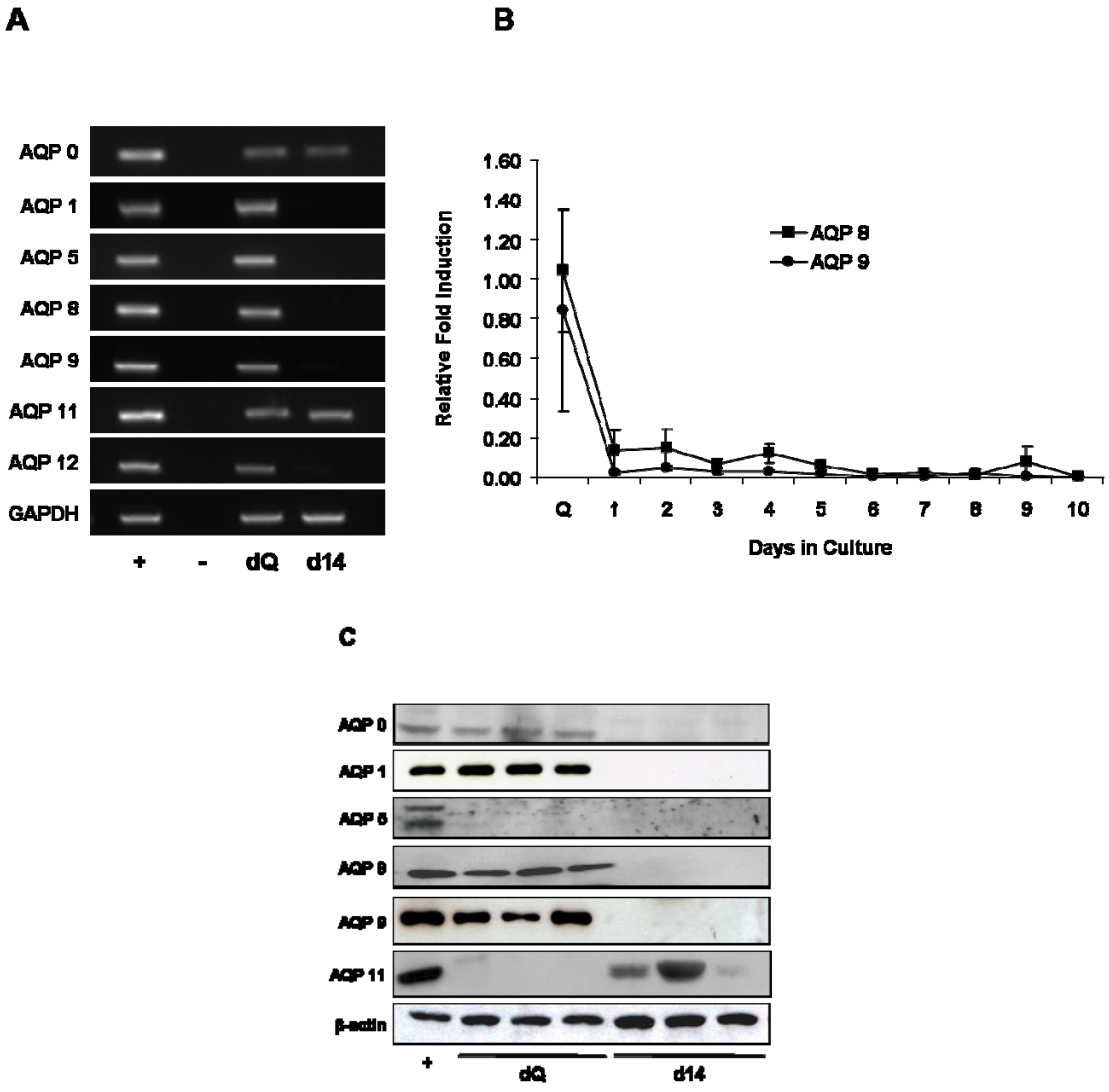

Figure 5.1 Aquaporin expression in quiescent and activated HSCs. (A) Representative RT-PCR analyses of AQP mRNA expression. Analysis of AQPs 2, 3, 4, 6, 7, and 10 revealed no detectable message. (B) Quantitative analysis of AQP 8 and 9 mRNA expression over 10 days in culture assessed by RealTime PCR (relative to dQ); *$p<0.05$ as compared to d1-d10. (C) Representative immunoblot analyses of samples prepared from quiescent (dQ) and activated (d14) HSCs using antibodies specific against AQP 0, 1, 5, 8, 9, and 11. (+) tissue positive control; liver tissue for AQPs 0, 1, 4, 8, 9 and 11; kidney tissue for AQPs 1, 2, 3, 5, 6, 7 and 10; pancreas tissue for AQP 12; small intestine tissue for AQP 10; (-) water (n=3).

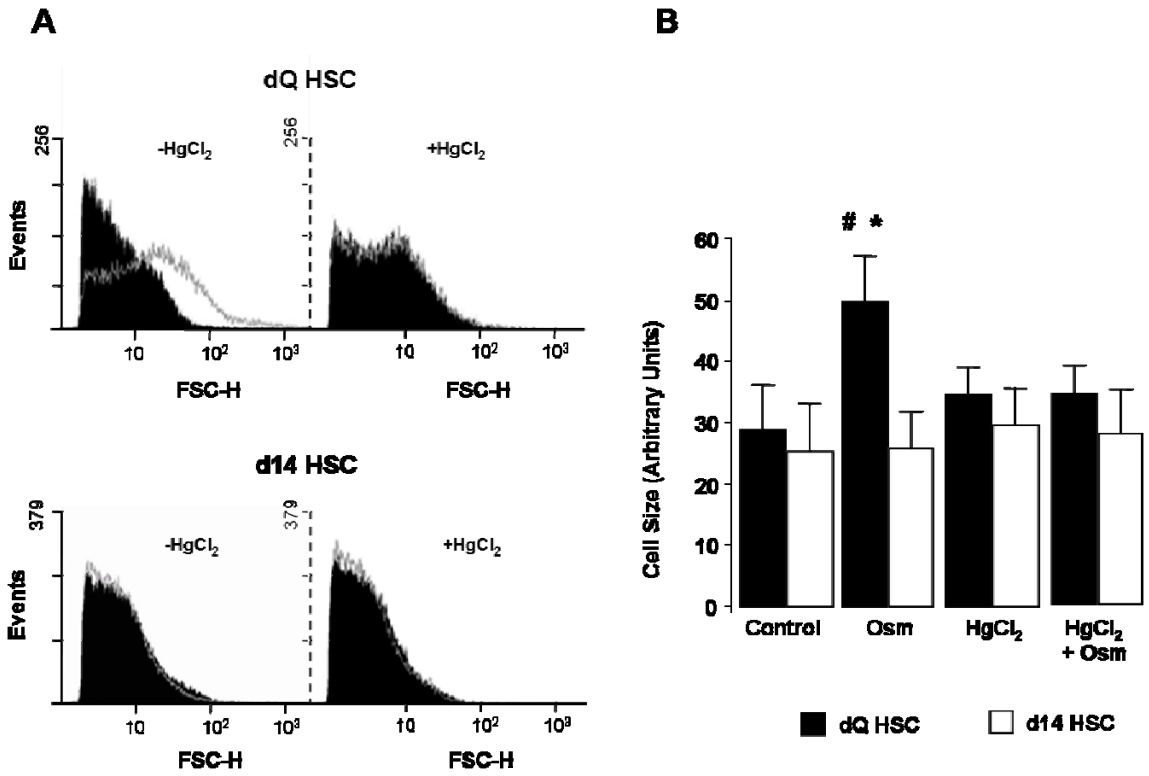

Figure 5.2 HSC plasma membrane water permeability. (A) Representative cell swelling analysis histograms of dQ and d14 HSCs in normotonic (black) and hypotonic (grey line overlay) solutions. Samples were pre-treated with or without the AQP channel blocker $HgCl_2$ (100 μM; 2 minutes). (B) Quantitative analysis of cell swelling in dQ or d14 cells (n=4) * $p<0.05$ as compared to control, #$p<0.05$ versus $HgCl_2$ + Osm (osmotic challenge).

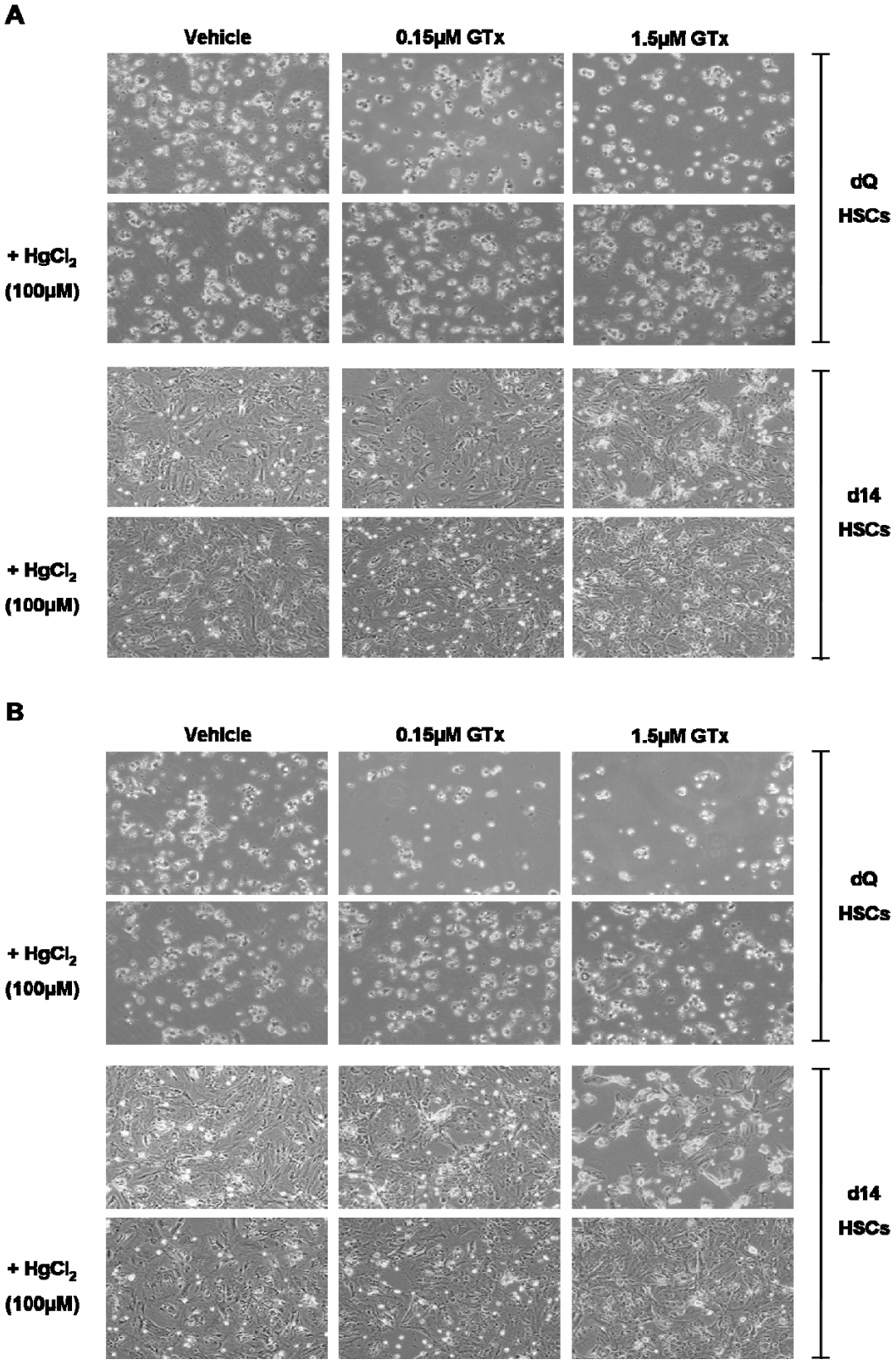
A
Vehicle
0.15μM GTx
1.5μM GTx
dQ HSCs
+ HgCl2 (100μM)
d14 HSCs
+ HgCl2 (100μM)
B
Vehicle
0.15μM GTx
1.5μM GTx
dQ HSCs
+ HgCl2 (100μM)
d14 HSCs
+ HgCl2 (100μM)

C

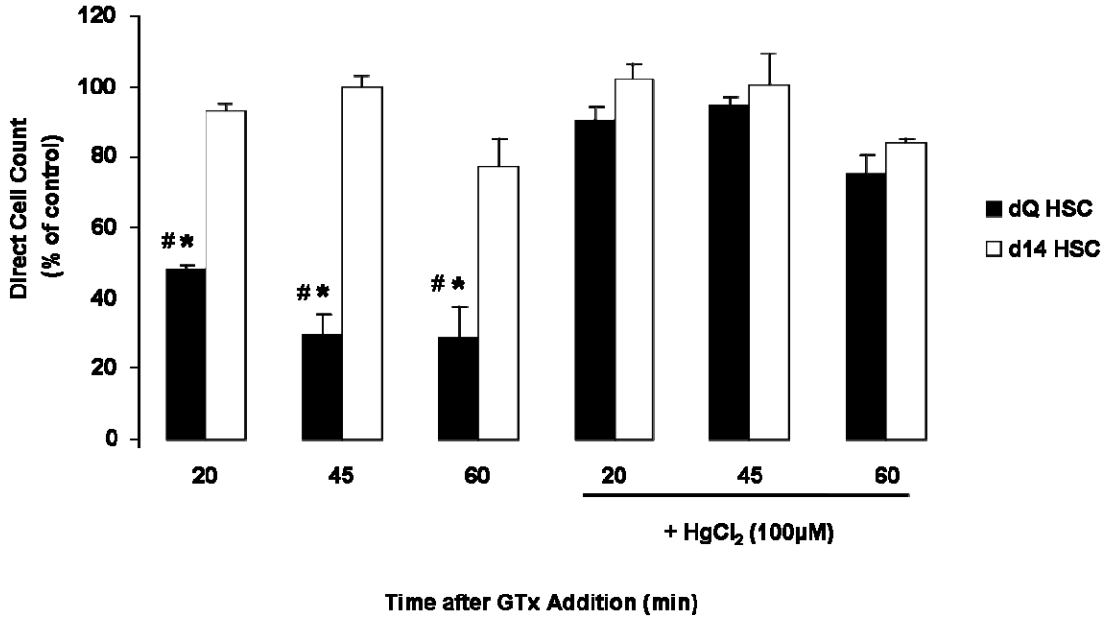
Direct Cell Count
(% of control)
120
100
80
60
40
20
0
#*
#*
#*
dQ HSC
d14 HSC
20
45
60
20
45
60
+ HgCl2 (100µM)
Time after GTx Addition (min)

D

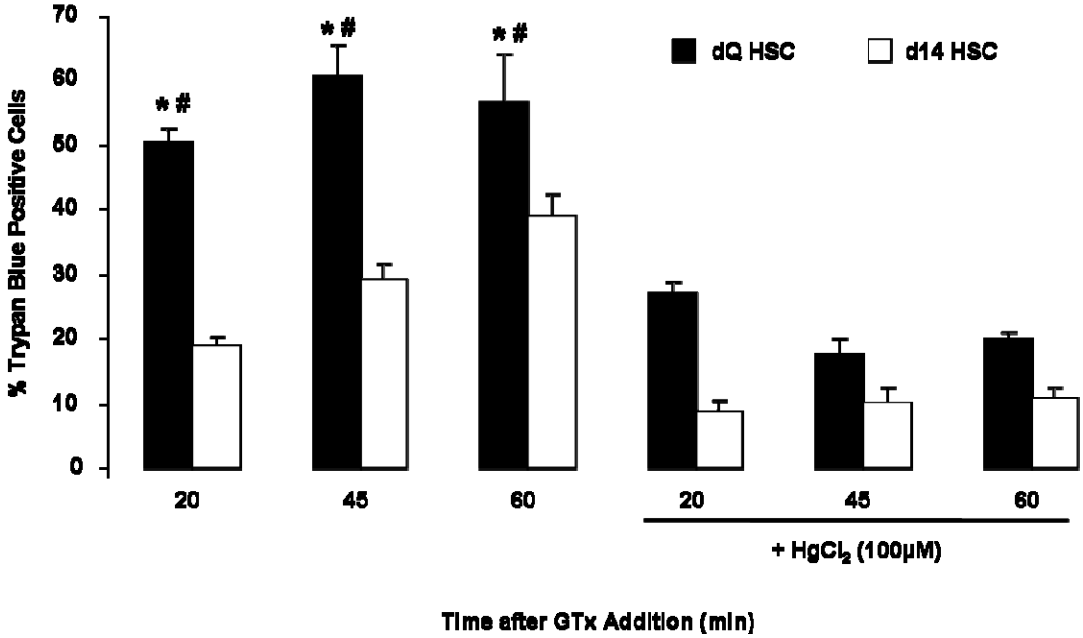
% Trypan Blue Positive Cells
70
60
50
40
30
20
10
0
*#
*#
*#
dQ HSC
d14 HSC
20
45
60
20
45
60
+ HgCl2 (100µM)
Time after GTx Addition (min)

Figure 5.3 Morphological response to an apoptotic stimulus. Cells were treated with gliotoxin (GTx; 0.15 or 1.5 μM) or vehicle alone. Samples were pre-treated with or without the AQP channel blocker $HgCl_2$ (100 μM; 15 minutes). (A) Morphology of dQ (4 hours) and d14 HSCs were assessed after 20 minutes under 20X magnification (n=4). (B) Morphology of dQ (4 hours) and d14 HSCs after 60 minutes (n=4). (C,D) dQ and d14 cell viability was assessed by direct cell counts and trypan blue exclusion assay at the indicated time points following exposure to 1.5 μM GTx. Percent remaining cells was calculated (remaining adherent cell number/vehicle x 100); *$p<0.05$ as compared to $HgCl_2$ treated samples, #$p<0.05$ within treatment group.

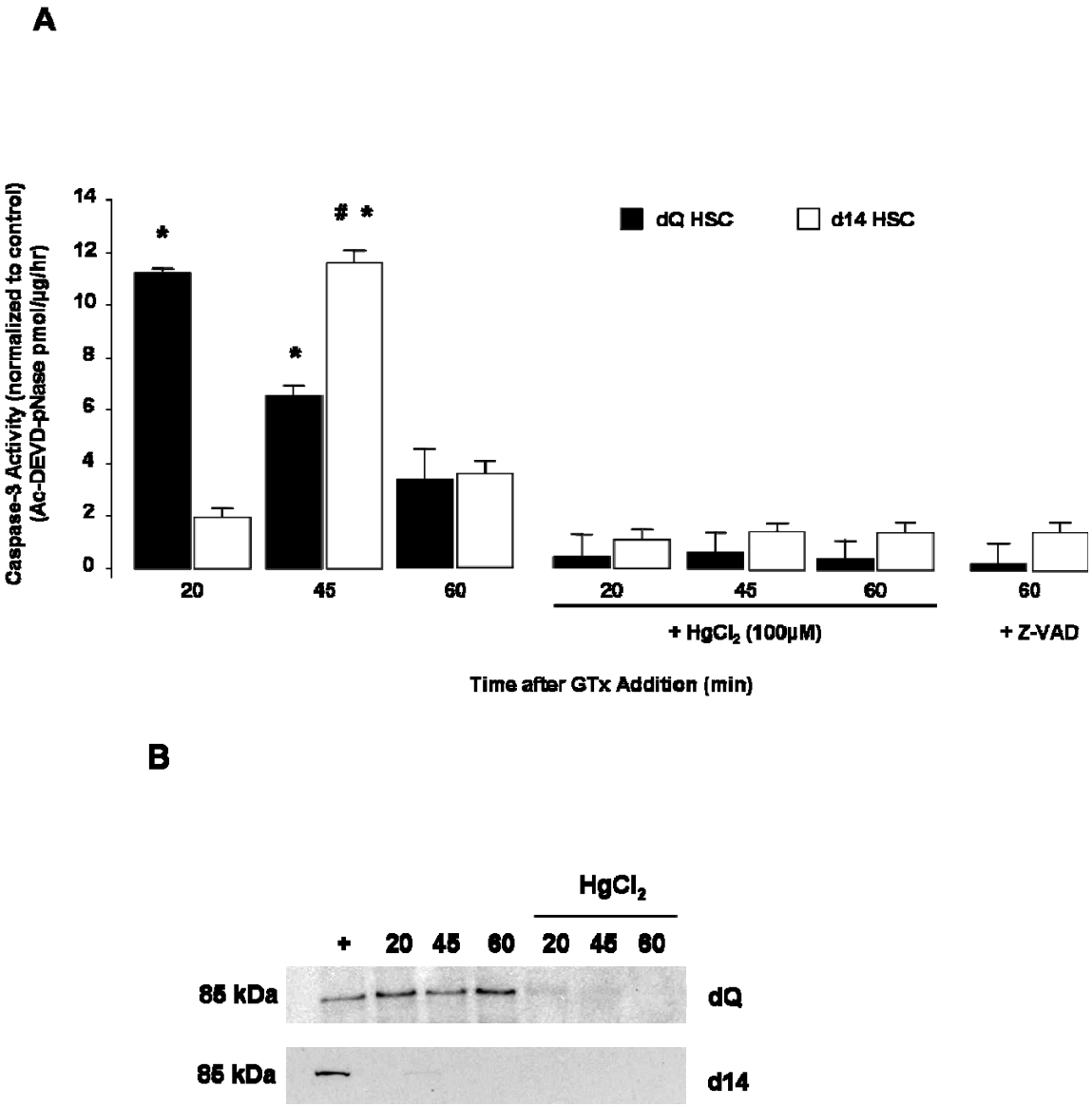

Figure 5.4 Effect of aquaporin channel inhibition on caspase-3 activity. (A) Caspase-3 activity in dQ (4 hours) and d14 HSCs. Cells were treated for 20, 45, or 60 minutes with vehicle or gliotxin (GTx; 1.5 µM). Cells were pre-treated with or without $HgCl_2$ (100 µM; 15 minutes). The pan-caspase inhibitor Z-VAD-FMK (Z-VAD) was added as control (n=3). *$p<0.05$ as compared to $HgCl_2$ treated samples; #$p<0.05$ within treatment group. (B) Representative immunoblot analyses of samples prepared from dQ and d14 HSCs using an antibody specific against the cleaved fraction of PARP (89 kDA). Cells were treated for 20, 45, or 60 minutes with vehicle or gliotxin (GTx; 1.5 µM) and were pre-treated with or without $HgCl_2$ (100 µM; 15 minutes) (n=2).

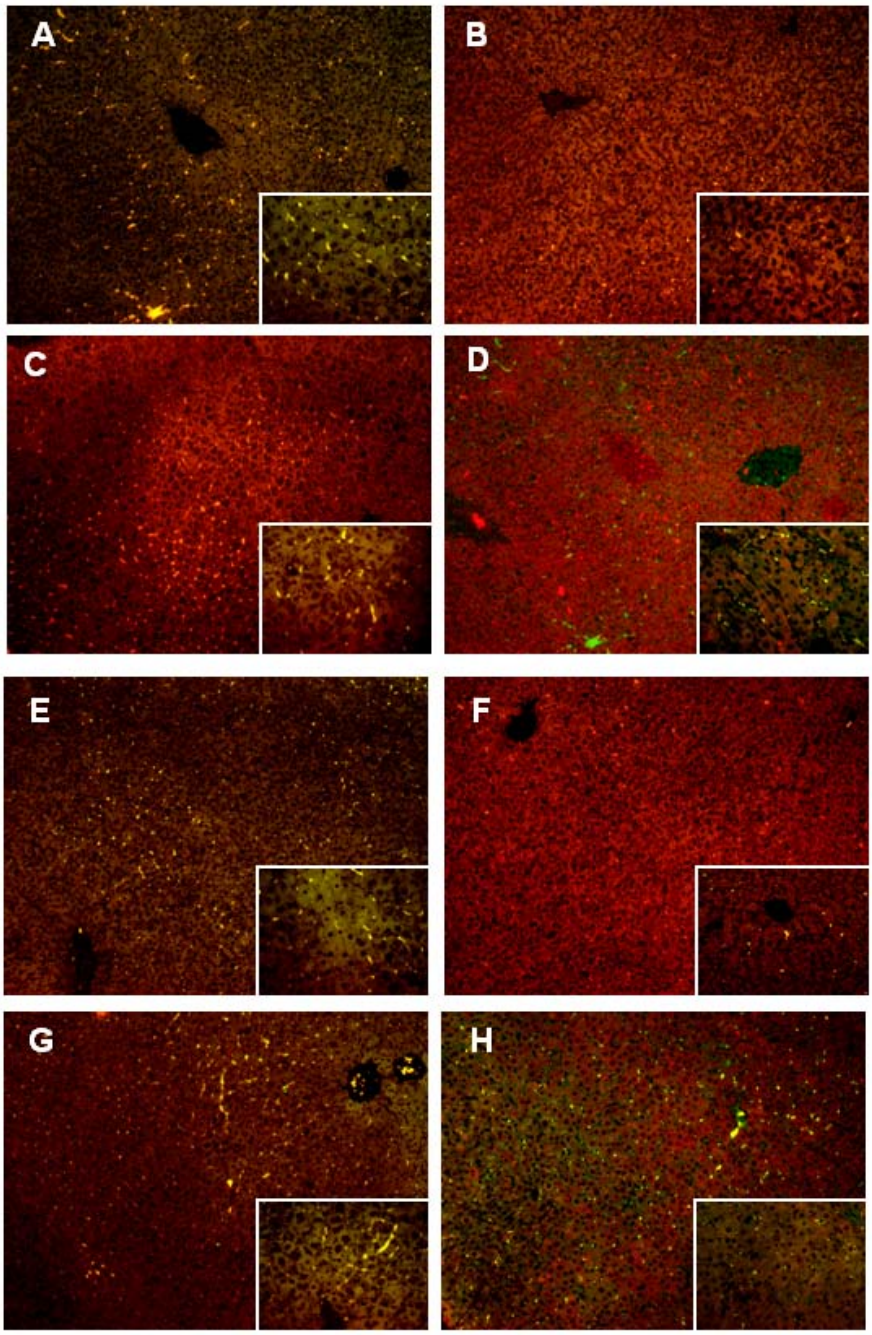

Figure 5.5 HSC aquaporin expression in a model of liver injury. Dual fluorescent immunohistochemistry was performed on liver tissue (20X magnification with 40X insets) using an ethanol/LPS (ELPS) injury animal model. Sections (4μm) from ELPS (C, D, G, H) or control (CTRL, A, B, E, F) were incubated with primary antibody cocktail. Aquaporin immunoreactivity is shown in red (AQP 8 panels A-D, AQP 9 panels E-H); GFAP and α-SMA (shown in green) were used as markers of quiescent and activated HSCs, respectively. Colocalization is indicated by yellow fluorescence.

Table 5.S1 Primers used in this study.

Gene	Forward	Reverse
AQP 1	CATGAAGGTGTGGACCAGTG	CCAGGAAGCTCTGAGACCAG
AQP 2	GGTTCCCAGTGCAGAGTA	GCGGAGACGAGCACTTTTAC
AQP 3	AGGAGTTGATGAACCGTTGC	AAGCCAAGTTGATGGTGAGG
AQP 4	AGAGCATCATGGTGGCTTTC	CGATGCTGATCTTTCGTGTG
AQP 5	TCTGGGTAGGGCCTATTGTG	CAGCTCGATGGTCTTCTTCC
AQP 6	TCAAGAGACCAGGAGGATCG	GCCAGGAACTCAGCAAAAAG
AQP 7	ATCCTTGTTTGCGTTCTTGG	AGAACCCTGTGGTGGTATGC
AQP 8	TCATTGCTACCTTGGGGAAC	GCTCCTGCTCCTGGACTATG
AQP 9	CGCCAGGTGCCTTTGTAG	GAAGACCTCAAACCCCATC
AQP 10	GCGAGCTCTCTGGCTGTTAC	AGGGACAGATATGGGGAAGG
AQP 11	CCTTCCAGCTCTGCTACTGC	GGTACTTGGTCAGGCTCAGG
AQP 12	GGGAGCTCAGCGAACTACAC	AGGTGTTCCCAGAACAGTGG

CHAPTER 6: SUMMARY AND FUTURE DIRECTIONS

In a normal healthy liver, HSCs are found in the quiescent phenotype and reside in the space of Disse. Quiescent HSCs store vitamin A in the form of retinyl esters, regulate hepatic sinusoidal microcirculation, and maintain basement membrane conditions. Following exposure to fibrogenic stimuli, HSCs transdifferentiate to activated myofibroblast-like cells characterized by increased proliferative and hypercontractile properties. The activated phenotype is marked by loss of retinyl ester stores and star-like morphology and expression of myofibroblast marker αSMA [4, 16]. Initiation of HSC activation is driven by increased circulating proinflammatory molecules. Upon migration to sites of injury, HSCs not only respond to, but secrete a wide range of proinflammatory cytokines, most notably TGFβ. In facilitation of wound-healing, HSCs produce and secrete ECM products to repair damaged tissues. Withdrawal of noxious stimuli results in a reduced number of activated HSCs, with the fate of activated cells unknown; speculation has indicated induction of apoptosis or reversion to quiescence [2]. However, in states of chronic injury, accumulation of ECM components, predominately type I collagen, disrupts normal liver architecture impairing nutrient delivery, metabolic/detoxification functions, and sustains the inflammatory milieu, culminating in hepatic fibrosis. With fibrosis unresolved, progression to end-stage liver disease (cirrhosis) is observed. While removal of underlying stimuli or treatment of fibrosis can result in reversion of the disease state, this is not the case for cirrhotic patients. Currently,

there are no FDA-approved treatment regimes for hepatic fibrosis, underscoring the importance of development of novel therapeutic strategies [3, 15].

The process of HSC transdifferentiation has been studied intensely to determine points of therapeutic intervention. While cellular and molecular events characterizing initiation and perpetuation phases have been described, there is still much to be learned about specific properties unique to each HSC phenotype that could be exploited for therapeutic development. Overview of the literature indicates clearly there is not a common cure-all for HSC-mediated fibrosis. Therefore, examination of multiple points of HSC transdifferentiation is necessary to uncover novel targets and/or avenues for combination therapies.

Examining specific genes and/or cellular signaling pathways involved in initiation of HSC transdifferentiation is imperative. However, for these findings to have impact it is of even greater importance that divergent phenotypes of the HSC be clearly defined. While studying the process of HSC transdifferentiation is difficult to monitor in vivo, culturing these cells on plastic substrates to mimic increased matrix stiffness remains a widely accepted technique. Unfortunately, past and ongoing studies examining quiescent and activated HSCs have convoluted the terminology [214, 263]. Isolation of primary HSCs from rodents and subsequent culturing of the cells on plastic leads to a transition from quiescent to fully-activated myofibroblasts [264-265]. However, the term "quiescent" has been utilized to indicate varying stages of HSC activation and culture. While some use the term to describe cells that have been in culture for 24 hours, others state cells are quiescent up to 3 days on plastic. However, it has been shown by our lab and others that plating HSCs on plastic for as few as 24 hours initiates a dramatic change

in gene expression profile more similar to HSCs in later stages of culture (day 10) than freshly isolated cells [94]. Therefore, the aims of chapter 3 of this dissertation were to examine differential gene expression between truly quiescent (freshly isolated) and fully activated (14 days on plastic) HSCs. Several groups have performed mRNA microarray analyses comparing quiescent and activated phenotypes isolated from both in vitro and in vivo settings [199-200]; however, little is known about the daily genetic alterations that occur. To fully understand transdifferentiation, it is necessary to know the sequential activation of key genes, as well coordinate patterns of expression. Therefore, based on known gene expression profiles of quiescent and activated HSCs, several genes were selected to follow throughout transdifferentiation. Our study analyzed an array of 21 genes over 10 consecutive days in culture to identify candidate signaling pathways and genes which peak early in expression to initiate and commit the HSC to activation/transdifferentiation.

Using AMADA software, genotypic clustering was performed to profile genes that are modulated in quiescence, early and late activation, and pro-fibrotic conditions. Analyses demonstrated day Q was clearly divergent from all other days during transdifferentiation, while days 1-3 were significantly different from days 5-10. Further, day 4 is genetically distinct from all other days in culture, suggesting this may be the commitment point to the activated phenotype. Additionally, components of the IL-6 JAK/STAT signaling pathway appeared to be pivotal in the first 72 hours of HSC transdifferentiation. Results also demonstrated chemical inhibition of the JAK/STAT signaling pathway blunted phenotypic changes seen during activation as indicated by retention of cytoplasmic projections and significantly decreased pro-fibrotic gene

expression. Overall, these data demonstrate shifting of genetic profiles during early activation results in differentiation into a unique phenotype rendering the cell sensitive to ligands that signal through JAK/STAT. Since inhibition of the JAK/STAT signaling pathway impedes progression of HSC transdifferentiation/activation, this may serve as a potential therapeutic target to inhibit or slow development of hepatic fibrosis. While not directly confirmed in our experiments, several reports have shown AG490 (100 μmol/L) significantly inhibits the activity of JAK2 with subsequent decreases in STAT3 phosphorylation [266-268], confirming its use as an effective chemical inhibitor. However, as a tyrosine kinase inhibitor, it is possible that AG490 could potentially affect the activity of other similarly structured receptors. Therefore, future studies utilizing specific gene silencing molecules (small interfering RNA or short hairpin RNA) should be performed to confirm our findings. Uncovering the vital function of JAK/STAT in the transduction of signals necessary to initiate HSC transdifferentiation will undoubtedly expand the arsenal of pharmaceutical inhibitors used to treat fibrosis [94].

In addition to JAK/STAT signaling, TGFβ is critical to both initiation and perpetuation phases of transdifferentiation. Post-liver injury both blood and tissue TGFβ levels are elevated stimulating HSC transdifferentiatioin. Increased TGFβ stimulates expression of procollagen and other profibrogenic target genes [84, 226]. In addition to paracrine signals from damaged parenchymal cells, endogenous TGFβ synthesis is significantly increased as a result of transdifferentiation, underscoring the importance of this signaling network in the foundation and progression of hepatic fibrosis. Disruption of TGFβ signaling in activated HSCs both in vitro and in vivo markedly decreased fibrosis in experimental animal models [23, 31-32]. However, no

studies to date have examined global factors regulating TGFβ signaling in HSCs in efforts to design novel therapies against pro-fibrotic signaling. miRs act as key regulatory molecules in hepatic fibrosis controlling gene expression by binding to 3'UTRs of target genes inducing mRNA instability or translational repression [140]. miR-based regulation of genes controlling HSC transdifferentiation has been demonstrated, highlighting a novel area of therapeutic intervention [184]. Microarray analyses showed a significant down-regulation of miR 19b in activated compared to quiescent HSCs. In silico analyses predicts miR 19b binding to the 3'UTR of TGFβRII, a component critical to successful signal transduction, which were validated by dual luciferase reporter assays. Overexpression of miR 19b in activated HSCs suppressed TGFβRII expression with subsequent repression of SMAD3 and downstream target gene, type I collagen. In addition to suppression of pro-fibrotic signaling, marked reduction in HSC activation was also observed. miR 19b mimics induced significant reductions in activated morphology with corresponding decreases in αSMA mRNA and protein. Additionally, forced miR 19b expression decreased epigenetic regulator and suppressor of quiescence MeCP2 accompanied by restoration of quiescent marker GFAP. In vivo studies confirmed decreased miR 19b expression in fibrotic liver tissue. More importantly, miR 19b expression was significantly down-regulated in tissue from human fibrotic patients, highlighting a new role of miR 19b as a novel fibrotic biomarker and possible therapeutic. Significantly decreased levels of miR 19b were detected in liver tissues from fibrotic patients with various underlying etiologies, indicating a highly conserved role of this miR in fibrogenesis.

As HCV represents the major cause of hepatic fibrosis on a global scale, it would be interesting to confirm the in vitro findings in HCV-infected HSCs utilizing a newly developed sub-genomic replicon system. Additionally, as rates of HCV recurrence post-transplant remain high, identifying liver transplant recipients at greatest risk for rapid development of fibrosis from recurrent hepatitis C would target those recipients most urgently in need of antiviral therapy and defer treatment to those at less risk for disease progression. To this end, recent studies have shown inverse correlations between tissue and plasma miR levels [242-243]. In fact, miR 19b was up-regulated 4.3-fold in serum of individuals with cirrhotic livers compared to normal controls [244]. Therefore, examining expression levels of miR 19b in HCV transplant patients could lead to development of a reliable marker to identify rapid progressors of fibrosis.

Modulation of miR 19b expression in fibrotic animal models is necessary to confirm the contributions of this specific miR in HSC-mediated fibrogenesis. While potential clearly exists for miR 19b as a serum biomarker of fibrosis, it is imperative that future studies examine other tissues and cell types for expression of this miR under normal and injured liver conditions to determine if the observed decreased in expression occurs on a global level.

Resolution of hepatic fibrosis has been attributed to inhibition of HSC transdifferentiation, interruption of pro-fibrotic signaling, and induction of HSC apoptosis [49, 170, 269]. However, activated HSCs have been reported to demonstrate increased resistance to apoptosis due to increased bcl-2 expression [52]. Still, activated HSCs are capable of undergoing apoptosis in response to a variety of stimuli including gliotoxin, superoxide radicals, and tumor necrosis factor-related apoptosis-inducing

ligand (TRAIL) [169-170, 173, 254]. Previous studies demonstrated water movement during apoptosis occurs via AQPs [159-160, 162] , and inhibition of AQP-dependent water movement during the apoptotic volume decrease significantly slows apoptotic progression [160-161, 164]. In contrast to quiescent HSCs, activated cells were characterized by marked decreases in net AQP expression. Interestingly, while message was detected for 7 AQPs in quiescent HSCs, only 4 homologs were detected at the protein level. Future studies should examine the molecular mechanisms contributing to this discrepancy and determine the specific solute/s transported by each AQP within the HSC. Current literature has not indicated such a redundancy in AQP expression within other cell types; therefore, examination of specific cellular localization of each homolog would contribute to our overall understanding of which AQP/s may be critical for cellular functions. Using osmotic challenge, in the absence and presence of a non-specific AQP channel blocker ($HgCl_2$), rapid AQP-dependent water movement across the plasma membrane in quiescent HSCs was observed indicating the presence of functional AQP homologs within the plasma membrane. Conversely, activated HSCs failed to respond to osmotic challenge. Quiescent HSCs (4 hours), expressing multiple AQP homologs, were significantly more responsive to apoptotic stimulation versus activated HSCs. Finally, confirming in vitro studies, fluorescent immunohistochemistry showed strong colocalization between quiescent HSCs and AQPs 8 and 9, while α-SMA positive HSCs found in fibrotic liver tissue exhibited dramatically decreased AQP expression. These data demonstrate HSCs express AQPs and suggest regulation of AQP expression/function contributes to HSC susceptibility to apoptotic challenge. These data indicate it will be of considerable interest to study AQP expression and apoptosis in HSCs using animal

models of progressive liver injury in which the magnitude and duration of the hepatic insult can be manipulated. In doing so, direct or indirect modulation of AQP expression in HSCs may lead to the development of novel therapeutics for the treatment of hepatic fibrosis.

HSC transdifferentiation is highly complex with breadth and depth existing in pro-fibrotic signaling networks conferring phenotype-specific genetic reprogramming. This dissertation examined multiple points of the HSC transdifferentiation process to uncover novel molecular mechanisms regulating the pro-fibrotic condition that may be manipulated to create novel therapeutic strategies. Cumulatively these data show JAK/STAT signaling stimulates early HSC transdifferentiation, miR 19b regulates pro-fibrotic TGFβ signaling which both establishes and perpetuates the activated phenotype, and finally, decreased AQP expression contributes to increased resistance to apoptotic stimuli observed in activated cells. All of the aforementioned discoveries represent novel avenues to be explored.

Pharmaceutical intervention and gene therapy while previously unsuccessful for the treatment of fibrosis remain under constant revision with a flux of new information and technology driven advances. Specifically, new miR-targeted drug Miravirsen (SPC3649), developed by Santaris Pharma, is in Phase II clinical trials for treatment of HCV via inhibition of miR 122 (ClinicalTrials.gov). Additionally, new adeno-associated virus (AAV) constructs are being used in rodent models and hold deeper clinical promise than previous clinical trials using adenovirus based gene therapy. AAV is currently in use for several clinical trials including Duchennes' muscular dystrophy [270], Pompe Disease, and Parkinson's disease (ClinicalTrials.gov). Site-specific integration in the

absence of deleterious immunogenic response makes AAV therapy an attractive option. Delivery of miR 19b via AAV may prove to be a powerful therapeutic strategy as delivery of miRs for treatment of hepatocellular carcinoma has been extremely effective and devoid of deleterious side-effects in rodent models [241, 271]. Additionally, AAV vectors delivering JAK2 genetic/chemical inhibitors, or constructs designed to overexpress AQPs also hold promise. However, these treatments to be successful, an HSC-specific marker should be identified to avoid damaging neighboring cells and possible systemic effects. Deep sequencing of each HSC genetic program may provide novel mRNAs/non-coding RNAs that could be used for direct targeting.

In addition to therapies, it is important we improve our ability to predict disease progression and outcome. miR expression profiles have proven indicative of disease states in animal models of chronic liver disease and in patients with various underlying etiologies [175-176, 272-273]. miR 19b may prove to be a novel biomarker of hepatic fibrosis, and with new technological advances allowing measurement of miRs in serum, simple clinical testing and standard of care blood draws may facilitate non-invasive measurements of patient health status [274-275].

REFERENCES

1. Jiao J, Friedman SL, Aloman C: Hepatic fibrosis. *Curr Opin Gastroenterol* 2009, 25(3):223-229.

2. Brenner DA: Molecular pathogenesis of liver fibrosis. *Trans Am Clin Climatol Assoc* 2009, 120:361-368.

3. Friedman SL: Evolving challenges in hepatic fibrosis. *Nat Rev Gastroenterol Hepatol* 2010, 7(8):425-436.

4. Friedman SL: Mechanisms of disease: Mechanisms of hepatic fibrosis and therapeutic implications. *Nat Clin Pract Gastroenterol Hepatol* 2004, 1(2):98-105.

5. Zhao W, Zhang L, Yin Z, Su W, Ren G, Zhou C, You J, Fan J, Wang X: Activated hepatic stellate cells promote hepatocellular carcinoma development in immunocompetent mice. *Int J Cancer* 2011.

6. Diehl AM: Obesity and alcoholic liver disease. *Alcohol* 2004, 34(1):81-87.

7. Jou J, Choi SS, Diehl AM: Mechanisms of disease progression in nonalcoholic fatty liver disease. *Semin Liver Dis* 2008, 28(4):370-379.

8. Breitkopf K, Nagy LE, Beier JI, Mueller S, Weng H, Dooley S: Current experimental perspectives on the clinical progression of alcoholic liver disease. *Alcohol Clin Exp Res* 2009, 33(10):1647-1655.

9. Iredale JP: Hepatic stellate cell behavior during resolution of liver injury. *Semin Liver Dis* 2001, 21(3):427-436.

10. Iredale JP, Benyon RC, Pickering J, McCullen M, Northrop M, Pawley S, Hovell C, Arthur MJ: Mechanisms of spontaneous resolution of rat liver fibrosis. Hepatic stellate cell apoptosis and reduced hepatic expression of metalloproteinase inhibitors. *The Journal of clinical investigation* 1998, 102(3):538-549.

11. Aimes RT, Quigley JP: Matrix metalloproteinase-2 is an interstitial collagenase. Inhibitor-free enzyme catalyzes the cleavage of collagen fibrils and soluble native type I collagen generating the specific 3/4- and 1/4-length fragments. *J Biol Chem* 1995, 270(11):5872-5876.

12. Itoh Y, Seiki M: MT1-MMP: a potent modifier of pericellular microenvironment. *J Cell Physiol* 2006, 206(1):1-8.

13. Visse R, Nagase H: Matrix metalloproteinases and tissue inhibitors of metalloproteinases: structure, function, and biochemistry. *Circ Res* 2003, 92(8):827-839.

14. Schuppan D, Ruehl M, Somasundaram R, Hahn EG: Matrix as a modulator of hepatic fibrogenesis. *Semin Liver Dis* 2001, 21(3):351-372.

15. Friedman SL: Hepatic fibrosis -- overview. *Toxicology* 2008, 254(3):120-129.

16. Friedman SL: Hepatic stellate cells: protean, multifunctional, and enigmatic cells of the liver. *Physiol Rev* 2008, 88(1):125-172.

17. Lim YS, Lee HC, Lee HS: Switch of cadherin expression from E- to N-type during the activation of rat hepatic stellate cells. *Histochemistry and cell biology* 2007, 127(2):149-160.

18. Lim YS, Lee HS: [The expression of E-cadherin in human and rat hepatic stellate cells: evidence of epithelial-mesenchymal transition]. *Taehan Kan Hakhoe Chi* 2002, 8(1):90-99.

19. Carotti S, Morini S, Corradini SG, Burza MA, Molinaro A, Carpino G, Merli M, De Santis A, Muda AO, Rossi M *et al*: Glial fibrillary acidic protein as an early marker of hepatic stellate cell activation in chronic and posttransplant recurrent hepatitis C. *Liver Transpl* 2008, 14(6):806-814.

20. Asahina K, Zhou B, Pu WT, Tsukamoto H: Septum transversum-derived mesothelium gives rise to hepatic stellate cells and perivascular mesenchymal cells in developing mouse liver. *Hepatology* 2011, 53(3):983-995.

21. Asahina K, Tsai SY, Li P, Ishii M, Maxson RE, Jr., Sucov HM, Tsukamoto H: Mesenchymal origin of hepatic stellate cells, submesothelial cells, and perivascular mesenchymal cells during mouse liver development. *Hepatology* 2009, 49(3):998-1011.

22. Saga Y, Hata N, Kobayashi S, Magnuson T, Seldin MF, Taketo MM: MesP1: a novel basic helix-loop-helix protein expressed in the nascent mesodermal cells during mouse gastrulation. *Development* 1996, 122(9):2769-2778.

23. Friedman SL: Mechanisms of hepatic fibrogenesis. *Gastroenterology* 2008, 134(6):1655-1669.

24. Lang A, Brenner DA: Gene regulation in hepatic stellate cell. *Ital J Gastroenterol Hepatol* 1999, 31(2):173-179.

25. Gressner AM: The up-and-down of hepatic stellate cells in tissue injury: apoptosis restores cellular homeostasis. *Gastroenterology* 2001, 120(5):1285-1288.

26. Gong W, Pecci A, Roth S, Lahme B, Beato M, Gressner AM: Transformation-dependent susceptibility of rat hepatic stellate cells to apoptosis induced by soluble Fas ligand. *Hepatology* 1998, 28(2):492-502.

27. Xia Y, Chen R, Song Z, Ye S, Sun R, Xue Q, Zhang Z: Gene expression profiles during activation of cultured rat hepatic stellate cells by tumoral hepatocytes and fetal bovine serum. *J Cancer Res Clin Oncol* 2010, 136(2):309-321.

28. Roskams T: Relationships among stellate cell activation, progenitor cells, and hepatic regeneration. *Clin Liver Dis* 2008, 12(4):853-860, ix.

29. Kordes C, Sawitza I, Haussinger D: Hepatic and pancreatic stellate cells in focus. *Biol Chem* 2009, 390(10):1003-1012.

30. Novo E, Marra F, Zamara E, Valfre di Bonzo L, Caligiuri A, Cannito S, Antonaci C, Colombatto S, Pinzani M, Parola M: Dose dependent and divergent effects of superoxide anion on cell death, proliferation, and migration of activated human hepatic stellate cells. *Gut* 2006, 55(1):90-97.

31. Dooley S, Delvoux B, Lahme B, Mangasser-Stephan K, Gressner AM: Modulation of transforming growth factor beta response and signaling during transdifferentiation of rat hepatic stellate cells to myofibroblasts. *Hepatology* 2000, 31(5):1094-1106.

32. Dooley S, Delvoux B, Streckert M, Bonzel L, Stopa M, ten Dijke P, Gressner AM: Transforming growth factor beta signal transduction in hepatic stellate cells via Smad2/3 phosphorylation, a pathway that is abrogated during in vitro progression to myofibroblasts. TGFbeta signal transduction during transdifferentiation of hepatic stellate cells. *FEBS Lett* 2001, 502(1-2):4-10.

33. Aoyama T, Paik YH, Seki E: Toll-like receptor signaling and liver fibrosis. *Gastroenterol Res Pract* 2010, 2010.

34. Seki E, Tsutsui H, Nakano H, Tsuji N, Hoshino K, Adachi O, Adachi K, Futatsugi S, Kuida K, Takeuchi O *et al*: Lipopolysaccharide-induced IL-18 secretion from murine Kupffer cells independently of myeloid differentiation factor 88 that is critically involved in induction of production of IL-12 and IL-1beta. *J Immunol* 2001, 166(4):2651-2657.

35. Szabo G, Dolganiuc A, Mandrekar P: Pattern recognition receptors: a contemporary view on liver diseases. *Hepatology* 2006, 44(2):287-298.

36. Schwabe RF, Seki E, Brenner DA: Toll-like receptor signaling in the liver. *Gastroenterology* 2006, 130(6):1886-1900.

37. Paik YH, Schwabe RF, Bataller R, Russo MP, Jobin C, Brenner DA: Toll-like receptor 4 mediates inflammatory signaling by bacterial lipopolysaccharide in human hepatic stellate cells. *Hepatology* 2003, 37(5):1043-1055.

38. Seki E, De Minicis S, Osterreicher CH, Kluwe J, Osawa Y, Brenner DA, Schwabe RF: TLR4 enhances TGF-beta signaling and hepatic fibrosis. *Nat Med* 2007, 13(11):1324-1332.

39. Huang H, Shiffman ML, Friedman S, Venkatesh R, Bzowej N, Abar OT, Rowland CM, Catanese JJ, Leong DU, Sninsky JJ *et al*: A 7 gene signature identifies the risk of developing cirrhosis in patients with chronic hepatitis C. *Hepatology* 2007, 46(2):297-306.

40. Lee Y, Friedman SL: Fibrosis in the liver acute protection and chronic disease. *Prog Mol Biol Transl Sci* 2010, 97:151-200.

41. Li G, Li D, Xie Q, Shi Y, Jiang S, Jin Y: RNA interfering connective tissue growth factor prevents rat hepatic stellate cell activation and extracellular matrix production. *J Gene Med* 2008, 10(9):1039-1047.

42. Lee UE, Friedman SL: Mechanisms of hepatic fibrogenesis. *Best Pract Res Clin Gastroenterol* 2011, 25(2):195-206.

43. Bonner JC: Regulation of PDGF and its receptors in fibrotic diseases. *Cytokine Growth Factor Rev* 2004, 15(4):255-273.

44. Bonner JC: Regulation of platelet-derived growth factor (PDGF) and alveolar macrophage-derived PDGF by alpha 2-macroglobulin. *Ann N Y Acad Sci* 1994, 737:324-338.

45. Tsuneyama K, Kouda W, Nakanuma Y: Portal and parenchymal alterations of the liver in idiopathic portal hypertension: a histological and immunochemical study. *Pathol Res Pract* 2002, 198(9):597-603.

46. Rosmorduc O: Antiangiogenic therapies in portal hypertension: a breakthrough in hepatology. *Gastroenterol Clin Biol* 2010, 34(8-9):446-449.

47. Constandinou C, Henderson N, Iredale JP: Modeling liver fibrosis in rodents. *Methods Mol Med* 2005, 117:237-250.

48. Elsharkawy AM, Oakley F, Mann DA: The role and regulation of hepatic stellate cell apoptosis in reversal of liver fibrosis. *Apoptosis* 2005, 10(5):927-939.

49. Cales P: Apoptosis and liver fibrosis: antifibrotic strategies. *Biomed Pharmacother* 1998, 52(6):259-263.

50. Canbay A, Gieseler RK, Gores GJ, Gerken G: The relationship between apoptosis and non-alcoholic fatty liver disease: an evolutionary cornerstone turned pathogenic. *Z Gastroenterol* 2005, 43(2):211-217.

51. Priya S, Sudhakaran PR: Cell survival, activation and apoptosis of hepatic stellate cells: modulation by extracellular matrix proteins. *Hepatol Res* 2008, 38(12):1221-1232.

52. Novo E, Marra F, Zamara E, Valfre di Bonzo L, Monitillo L, Cannito S, Petrai I, Mazzocca A, Bonacchi A, De Franco RS *et al*: Overexpression of Bcl-2 by activated human hepatic stellate cells: resistance to apoptosis as a mechanism of progressive hepatic fibrogenesis in humans. *Gut* 2006, 55(8):1174-1182.

53. Ding X, Saxena NK, Lin S, Xu A, Srinivasan S, Anania FA: The roles of leptin and adiponectin: a novel paradigm in adipocytokine regulation of liver fibrosis and stellate cell biology. *Am J Pathol* 2005, 166(6):1655-1669.

54. Elinav E, Ali M, Bruck R, Brazowski E, Phillips A, Shapira Y, Katz M, Solomon G, Halpern Z, Gertler A: Competitive inhibition of leptin signaling results in amelioration of liver fibrosis through modulation of stellate cell function. *Hepatology* 2009, 49(1):278-286.

55. Zhou Y, Jia X, Wang G, Wang X, Liu J: PI-3 K/AKT and ERK signaling pathways mediate leptin-induced inhibition of PPARgamma gene expression in primary rat hepatic stellate cells. *Mol Cell Biochem* 2009, 325(1-2):131-139.

56. Choi SS, Syn WK, Karaca GF, Omenetti A, Moylan CA, Witek RP, Agboola KM, Jung Y, Michelotti GA, Diehl AM: Leptin promotes the myofibroblastic phenotype in hepatic stellate cells by activating the hedgehog pathway. *J Biol Chem* 2010, 285(47):36551-36560.

57. Handy JA, Saxena NK, Fu P, Lin S, Mells JE, Gupta NA, Anania FA: Adiponectin activation of AMPK disrupts leptin-mediated hepatic fibrosis via suppressors of cytokine signaling (SOCS-3). *J Cell Biochem* 2010, 110(5):1195-1207.

58. Yin M, Ikejima K, Wheeler MD, Bradford BU, Seabra V, Forman DT, Sato N, Thurman RG: Estrogen is involved in early alcohol-induced liver injury in a rat enteral feeding model. *Hepatology* 2000, 31(1):117-123.

59. Colantoni A, La Paglia N, De Maria N, Emanuele MA, Emanuele NV, Idilman R, Harig J, Van Thiel DH: Influence of sex hormonal status on alcohol-induced oxidative injury in male and female rat liver. *Alcohol Clin Exp Res* 2000, 24(9):1467-1473.

60. Yin W, Zhang P, Huang JH, Zhang QY, Fan R, Li J, Zhou JJ, Hu YZ, Guo HT, Zhang SM *et al*: Stimulation of kappa-opioid receptor reduces isoprenaline-induced cardiac hypertrophy and fibrosis. *Eur J Pharmacol* 2009, 607(1-3):135-142.

61. Ebrahimkhani MR, Kiani S, Oakley F, Kendall T, Shariftabrizi A, Tavangar SM, Moezi L, Payabvash S, Karoon A, Hoseininik H *et al*: Naltrexone, an opioid receptor antagonist, attenuates liver fibrosis in bile duct ligated rats. *Gut* 2006, 55(11):1606-1616.

62. Day SA, Lakner AM, Moore CC, Yen MH, Clemens MG, Wu ES, Schrum LW: Opioid-like compound exerts anti-fibrotic activity via decreased hepatic stellate cell activation and inflammation. *Biochem Pharmacol* 2011, 81(8):996-1003.

63. Jeong WI, Osei-Hyiaman D, Park O, Liu J, Batkai S, Mukhopadhyay P, Horiguchi N, Harvey-White J, Marsicano G, Lutz B *et al*: Paracrine activation of hepatic CB1 receptors by stellate cell-derived endocannabinoids mediates alcoholic fatty liver. *Cell Metab* 2008, 7(3):227-235.

64. Julien B, Grenard P, Teixeira-Clerc F, Van Nhieu JT, Li L, Karsak M, Zimmer A, Mallat A, Lotersztajn S: Antifibrogenic role of the cannabinoid receptor CB2 in the liver. *Gastroenterology* 2005, 128(3):742-755.

65. Munoz-Luque J, Ros J, Fernandez-Varo G, Tugues S, Morales-Ruiz M, Alvarez CE, Friedman SL, Arroyo V, Jimenez W: Regression of fibrosis after chronic stimulation of cannabinoid CB2 receptor in cirrhotic rats. *J Pharmacol Exp Ther* 2008, 324(2):475-483.

66. Teixeira-Clerc F, Belot MP, Manin S, Deveaux V, Cadoudal T, Chobert MN, Louvet A, Zimmer A, Tordjmann T, Mallat A *et al*: Beneficial paracrine effects of cannabinoid receptor 2 on liver injury and regeneration. *Hepatology* 2010, 52(3):1046-1059.

67. Cheng JH, She H, Han YP, Wang J, Xiong S, Asahina K, Tsukamoto H: Wnt antagonism inhibits hepatic stellate cell activation and liver fibrosis. *Am J Physiol Gastrointest Liver Physiol* 2008, 294(1):G39-49.

68. Shin HW, Park SY, Lee KB, Jang JJ: Down-regulation of Wnt signaling during apoptosis of human hepatic stellate cells. *Hepatogastroenterology* 2009, 56(89):208-212.

69. Myung SJ, Yoon JH, Gwak GY, Kim W, Lee JH, Kim KM, Shin CS, Jang JJ, Lee SH, Lee SM *et al*: Wnt signaling enhances the activation and survival of human hepatic stellate cells. *FEBS Lett* 2007, 581(16):2954-2958.

70. Zhu NL, Wang J, Tsukamoto H: The Necdin-Wnt pathway causes epigenetic peroxisome proliferator-activated receptor gamma repression in hepatic stellate cells. *J Biol Chem* 2010, 285(40):30463-30471.

71. Yoshiji H, Kuriyama S, Noguchi R, Ikenaka Y, Yoshii J, Yanase K, Namisaki T, Kitade M, Yamazaki M, Asada K *et al*: Amelioration of liver fibrogenesis by dual inhibition of PDGF and TGF-beta with a combination of imatinib mesylate and ACE inhibitor in rats. *Int J Mol Med* 2006, 17(5):899-904.

72. Zhou Y, Zheng S, Lin J, Zhang QJ, Chen A: The interruption of the PDGF and EGF signaling pathways by curcumin stimulates gene expression of PPARgamma in rat activated hepatic stellate cell in vitro. *Lab Invest* 2007, 87(5):488-498.

73. Wang Y, Gao J, Zhang D, Zhang J, Ma J, Jiang H: New insights into the antifibrotic effects of sorafenib on hepatic stellate cells and liver fibrosis. *J Hepatol* 2010, 53(1):132-144.

74. Paik YH, Kim JK, Lee JI, Kang SH, Kim DY, An SH, Lee SJ, Lee DK, Han KH, Chon CY *et al*: Celecoxib induces hepatic stellate cell apoptosis through inhibition of Akt activation and suppresses hepatic fibrosis in rats. *Gut* 2009, 58(11):1517-1527.

75. Wang Y, Jiang XY, Liu L, Jiang HQ: Phosphatidylinositol 3-kinase/Akt pathway regulates hepatic stellate cell apoptosis. *World J Gastroenterol* 2008, 14(33):5186-5191.

76. Yoshimura A, Naka T, Kubo M: SOCS proteins, cytokine signalling and immune regulation. *Nat Rev Immunol* 2007, 7(6):454-465.

77. Sahin H, Trautwein C, Wasmuth HE: Functional role of chemokines in liver disease models. *Nat Rev Gastroenterol Hepatol* 2010, 7(12):682-690.

78. Seki E, De Minicis S, Gwak GY, Kluwe J, Inokuchi S, Bursill CA, Llovet JM, Brenner DA, Schwabe RF: CCR1 and CCR5 promote hepatic fibrosis in mice. *The Journal of clinical investigation* 2009, 119(7):1858-1870.

79. Wasmuth HE, Lammert F, Zaldivar MM, Weiskirchen R, Hellerbrand C, Scholten D, Berres ML, Zimmermann H, Streetz KL, Tacke F *et al*: Antifibrotic effects of CXCL9 and its receptor CXCR3 in livers of mice and humans. *Gastroenterology* 2009, 137(1):309-319, 319 e301-303.

80. Hellerbrand, Wang SC, Tsukamoto H, Brenner DA, Rippe RA: Expression of intracellular adhesion molecule 1 by activated hepatic stellate cells. *Hepatology* 1996, 24(3):670-676.

81. Maher JJ, Friedman SL: Parenchymal and nonparenchymal cell interactions in the liver. *Semin Liver Dis* 1993, 13(1):13-20.

82. Notas G, Kisseleva T, Brenner D: NK and NKT cells in liver injury and fibrosis. *Clin Immunol* 2009, 130(1):16-26.

83. Saile B, Ramadori G: Inflammation, damage repair and liver fibrosis--role of cytokines and different cell types. *Z Gastroenterol* 2007, 45(1):77-86.

84. Breitkopf K, Godoy P, Ciuclan L, Singer MV, Dooley S: TGF-beta/Smad signaling in the injured liver. *Z Gastroenterol* 2006, 44(1):57-66.

85. Gressner AM, Weiskirchen R, Breitkopf K, Dooley S: Roles of TGF-beta in hepatic fibrosis. *Front Biosci* 2002, 7:d793-807.

86. Meyer C, Meindl-Beinker NM, Dooley S: TGF-beta signaling in alcohol induced hepatic injury. *Front Biosci* 2010, 15:740-749.

87. Friedman SL, Bansal MB: Reversal of hepatic fibrosis -- fact or fantasy? *Hepatology* 2006, 43(2 Suppl 1):S82-88.

88. Karaa A, Thompson KJ, McKillop IH, Clemens MG, Schrum LW: S-adenosyl-L-methionine attenuates oxidative stress and hepatic stellate cell activation in an ethanol-LPS-induced fibrotic rat model. *Shock* 2008, 30(2):197-205.

89. Thompson KJ, Lakner AM, Cross BW, Tsukada S, Rippe RA, McKillop IH, Schrum LW: S-adenosyl-l-methionine inhibits collagen secretion in hepatic stellate cells via increased ubiquitination. *Liver Int* 2011, 31(6):893-903.

90. Dooley S, Hamzavi J, Ciuclan L, Godoy P, Ilkavets I, Ehnert S, Ueberham E, Gebhardt R, Kanzler S, Geier A *et al*: Hepatocyte-specific Smad7 expression attenuates TGF-beta-mediated fibrogenesis and protects against liver damage. *Gastroenterology* 2008, 135(2):642-659.

91. Kanzler S, Meyer E, Lohse AW, Schirmacher P, Henninger J, Galle PR, Blessing M: Hepatocellular expression of a dominant-negative mutant TGF-beta type II receptor accelerates chemically induced hepatocarcinogenesis. *Oncogene* 2001, 20(36):5015-5024.

92. Nakamura T, Sakata R, Ueno T, Sata M, Ueno H: Inhibition of transforming growth factor beta prevents progression of liver fibrosis and enhances hepatocyte regeneration in dimethylnitrosamine-treated rats. *Hepatology* 2000, 32(2):247-255.

93. Ueno H, Sakamoto T, Nakamura T, Qi Z, Astuchi N, Takeshita A, Shimizu K, Ohashi H: A soluble transforming growth factor beta receptor expressed in

muscle prevents liver fibrogenesis and dysfunction in rats. *Hum Gene Ther* 2000, 11(1):33-42.

94. Lakner AM, Moore CC, Gulledge AA, Schrum LW: Daily genetic profiling indicates JAK/STAT signaling promotes early hepatic stellate cell transdifferentiation. *World J Gastroenterol* 2010, 16(40):5047-5056.

95. Mann J, Mann DA: Transcriptional regulation of hepatic stellate cells. *Adv Drug Deliv Rev* 2009, 61(7-8):497-512.

96. Buck M, Kim DJ, Houglum K, Hassanein T, Chojkier M: c-Myb modulates transcription of the alpha-smooth muscle actin gene in activated hepatic stellate cells. *Am J Physiol Gastrointest Liver Physiol* 2000, 278(2):G321-328.

97. Huang GC, Zhang JS, Tang QQ: Involvement of C/EBP-alpha gene in in vitro activation of rat hepatic stellate cells. *Biochem Biophys Res Commun* 2004, 324(4):1309-1318.

98. Wang X, Huang G, Mei S, Qian J, Ji J, Zhang J: Over-expression of C/EBP-alpha induces apoptosis in cultured rat hepatic stellate cells depending on p53 and peroxisome proliferator-activated receptor-gamma. *Biochem Biophys Res Commun* 2009, 380(2):286-291.

99. Garcia-Ruiz I, de la Torre P, Diaz T, Esteban E, Fernandez I, Munoz-Yague T, Solis-Herruzo JA: Sp1 and Sp3 transcription factors mediate malondialdehyde-induced collagen alpha 1(I) gene expression in cultured hepatic stellate cells. *J Biol Chem* 2002, 277(34):30551-30558.

100. Inagaki Y, Nemoto T, Nakao A, Dijke P, Kobayashi K, Takehara K, Greenwel P: Interaction between GC box binding factors and Smad proteins modulates cell lineage-specific alpha 2(I) collagen gene transcription. *J Biol Chem* 2001, 276(19):16573-16579.

101. Inagaki Y, Mamura M, Kanamaru Y, Greenwel P, Nemoto T, Takehara K, Ten Dijke P, Nakao A: Constitutive phosphorylation and nuclear localization of Smad3 are correlated with increased collagen gene transcription in activated hepatic stellate cells. *J Cell Physiol* 2001, 187(1):117-123.

102. Rippe RA, Almounajed G, Brenner DA: Sp1 binding activity increases in activated Ito cells. *Hepatology* 1995, 22(1):241-251.

103. Kim Y, Ratziu V, Choi SG, Lalazar A, Theiss G, Dang Q, Kim SJ, Friedman SL: Transcriptional activation of transforming growth factor beta1 and its receptors by the Kruppel-like factor Zf9/core promoter-binding protein and Sp1. Potential mechanisms for autocrine fibrogenesis in response to injury. *J Biol Chem* 1998, 273(50):33750-33758.

104. Ratziu V, Lalazar A, Wong L, Dang Q, Collins C, Shaulian E, Jensen S, Friedman SL: Zf9, a Kruppel-like transcription factor up-regulated in vivo during early hepatic fibrosis. *Proc Natl Acad Sci U S A* 1998, 95(16):9500-9505.

105. Liu C, Gaca MD, Swenson ES, Vellucci VF, Reiss M, Wells RG: Smads 2 and 3 are differentially activated by transforming growth factor-beta (TGF-beta) in quiescent and activated hepatic stellate cells. Constitutive nuclear localization of Smads in activated cells is TGF-beta-independent. *J Biol Chem* 2003, 278(13):11721-11728.

106. Schnabl B, Kweon YO, Frederick JP, Wang XF, Rippe RA, Brenner DA: The role of Smad3 in mediating mouse hepatic stellate cell activation. *Hepatology* 2001, 34(1):89-100.

107. Dooley S, Hamzavi J, Breitkopf K, Wiercinska E, Said HM, Lorenzen J, Ten Dijke P, Gressner AM: Smad7 prevents activation of hepatic stellate cells and liver fibrosis in rats. *Gastroenterology* 2003, 125(1):178-191.

108. Haughton EL, Tucker SJ, Marek CJ, Durward E, Leel V, Bascal Z, Monaghan T, Koruth M, Collie-Duguid E, Mann DA *et al*: Pregnane X receptor activators inhibit human hepatic stellate cell transdifferentiation in vitro. *Gastroenterology* 2006, 131(1):194-209.

109. Guo GL, Lambert G, Negishi M, Ward JM, Brewer HB, Jr., Kliewer SA, Gonzalez FJ, Sinal CJ: Complementary roles of farnesoid X receptor, pregnane X receptor, and constitutive androstane receptor in protection against bile acid toxicity. *J Biol Chem* 2003, 278(46):45062-45071.

110. Marek CJ, Tucker SJ, Konstantinou DK, Elrick LJ, Haefner D, Sigalas C, Murray GI, Goodwin B, Wright MC: Pregnenolone-16alpha-carbonitrile inhibits rodent liver fibrogenesis via PXR (pregnane X receptor)-dependent and PXR-independent mechanisms. *Biochem J* 2005, 387(Pt 3):601-608.

111. Milliano MT, Luxon BA: Rat hepatic stellate cells become retinoid unresponsive during activation. *Hepatol Res* 2005, 33(3):225-233.

112. Mezaki Y, Yoshikawa K, Yamaguchi N, Miura M, Imai K, Kato S, Senoo H: Rat hepatic stellate cells acquire retinoid responsiveness after activation in vitro by post-transcriptional regulation of retinoic acid receptor alpha gene expression. *Arch Biochem Biophys* 2007, 465(2):370-379.

113. Hellemans K, Verbuyst P, Quartier E, Schuit F, Rombouts K, Chandraratna RA, Schuppan D, Geerts A: Differential modulation of rat hepatic stellate phenotype by natural and synthetic retinoids. *Hepatology* 2004, 39(1):97-108.

114. Chen C, Zhang J, Li J, Huang J, Yang C, Huang G, Shi J: Hydrodynamic-based in vivo transfection of retinoic X receptor-alpha gene can enhance vitamin A-induced attenuation of liver fibrosis in mice. *Liver Int* 2004, 24(6):679-686.

115. Tsukamoto H: Adipogenic phenotype of hepatic stellate cells. *Alcohol Clin Exp Res* 2005, 29(11 Suppl):132S-133S.

116. Hazra S, Miyahara T, Rippe RA, Tsukamoto H: PPAR Gamma and Hepatic Stellate Cells. *Comp Hepatol* 2004, 3 Suppl 1:S7.

117. Hellemans K, Rombouts K, Quartier E, Dittie AS, Knorr A, Michalik L, Rogiers V, Schuit F, Wahli W, Geerts A: PPARbeta regulates vitamin A metabolism-related gene expression in hepatic stellate cells undergoing activation. *J Lipid Res* 2003, 44(2):280-295.

118. Ziouzenkova O, Plutzky J: Retinoid metabolism and nuclear receptor responses: New insights into coordinated regulation of the PPAR-RXR complex. *FEBS Lett* 2008, 582(1):32-38.

119. Sun K, Wang Q, Huang XH: PPAR gamma inhibits growth of rat hepatic stellate cells and TGF beta-induced connective tissue growth factor expression. *Acta Pharmacol Sin* 2006, 27(6):715-723.

120. Cheng Y, Ping J, Xu LM: Effects of curcumin on peroxisome proliferator-activated receptor gamma expression and nuclear translocation/redistribution in culture-activated rat hepatic stellate cells. *Chin Med J (Engl)* 2007, 120(9):794-801.

121. Zheng S, Chen A: Activation of PPARgamma is required for curcumin to induce apoptosis and to inhibit the expression of extracellular matrix genes in hepatic stellate cells in vitro. *Biochem J* 2004, 384(Pt 1):149-157.

122. Zheng S, Chen A: Disruption of transforming growth factor-beta signaling by curcumin induces gene expression of peroxisome proliferator-activated receptor-gamma in rat hepatic stellate cells. *Am J Physiol Gastrointest Liver Physiol* 2007, 292(1):G113-123.

123. Mann J, Oakley F, Akiboye F, Elsharkawy A, Thorne AW, Mann DA: Regulation of myofibroblast transdifferentiation by DNA methylation and MeCP2: implications for wound healing and fibrogenesis. *Cell Death Differ* 2007, 14(2):275-285.

124. Oakley F, Mann J, Nailard S, Smart DE, Mungalsingh N, Constandinou C, Ali S, Wilson SJ, Millward-Sadler H, Iredale JP *et al*: Nuclear factor-kappaB1 (p50) limits the inflammatory and fibrogenic responses to chronic injury. *Am J Pathol* 2005, 166(3):695-708.

125. Vasiliou V, Lee J, Pappa A, Petersen DR: Involvement of p65 in the regulation of NF-kappaB in rat hepatic stellate cells during cirrhosis. *Biochem Biophys Res Commun* 2000, 273(2):546-550.

126. Hellerbrand C, Jobin C, Licato LL, Sartor RB, Brenner DA: Cytokines induce NF-kappaB in activated but not in quiescent rat hepatic stellate cells. *Am J Physiol* 1998, 275(2 Pt 1):G269-278.

127. Mann DA, Mann J: Epigenetic regulation of hepatic stellate cell activation. *J Gastroenterol Hepatol* 2008, 23 Suppl 1:S108-111.

128. Mann J, Chu DC, Maxwell A, Oakley F, Zhu NL, Tsukamoto H, Mann DA: MeCP2 controls an epigenetic pathway that promotes myofibroblast transdifferentiation and fibrosis. *Gastroenterology* 2010, 138(2):705-714, 714 e701-704.

129. Tsukamoto H, Zhu NL, Asahina K, Mann DA, Mann J: Epigenetic cell fate regulation of hepatic stellate cells. *Hepatol Res* 2011.

130. Habu Y, Mathieu O, Tariq M, Probst AV, Smathajitt C, Zhu T, Paszkowski J: Epigenetic regulation of transcription in intermediate heterochromatin. *EMBO Rep* 2006, 7(12):1279-1284.

131. Imhof A: Epigenetic regulators and histone modification. *Brief Funct Genomic Proteomic* 2006, 5(3):222-227.

132. Ng RK, Gurdon JB: Epigenetic inheritance of cell differentiation status. *Cell Cycle* 2008, 7(9):1173-1177.

133. Lennartsson A, Ekwall K: Histone modification patterns and epigenetic codes. *Biochim Biophys Acta* 2009, 1790(9):863-868.

134. Mann JR, Szabo PE, Reed MR, Singer-Sam J: Methylated DNA sequences in genomic imprinting. *Crit Rev Eukaryot Gene Expr* 2000, 10(3-4):241-257.

135. Salvaing J, Mouchel-Vielh E, Bloyer S, Preiss A, Peronnet F: Regulation of Abd-B expression by Cyclin G and Corto in the abdominal epithelium of Drosophila. *Hereditas* 2008, 145(3):138-146.

136. Matarazzo MR, Boyle S, D'Esposito M, Bickmore WA: Chromosome territory reorganization in a human disease with altered DNA methylation. *Proc Natl Acad Sci U S A* 2007, 104(42):16546-16551.

137. Tiwari VK, McGarvey KM, Licchesi JD, Ohm JE, Herman JG, Schubeler D, Baylin SB: PcG proteins, DNA methylation, and gene repression by chromatin looping. *PLoS Biol* 2008, 6(12):2911-2927.

138. Schwartz YB, Pirrotta V: Polycomb silencing mechanisms and the management of genomic programmes. *Nat Rev Genet* 2007, 8(1):9-22.

139. Schwartz YB, Kahn TG, Nix DA, Li XY, Bourgon R, Biggin M, Pirrotta V: Genome-wide analysis of Polycomb targets in Drosophila melanogaster. *Nat Genet* 2006, 38(6):700-705.

140. Kerr TA, Davidson NO: Therapeutic RNA manipulation in liver disease. *Hepatology* 2010, 51(3):1055-1061.

141. Grimson A, Farh KK, Johnston WK, Garrett-Engele P, Lim LP, Bartel DP: MicroRNA targeting specificity in mammals: determinants beyond seed pairing. *Mol Cell* 2007, 27(1):91-105.

142. Qiu L, Fan H, Jin W, Zhao B, Wang Y, Ju Y, Chen L, Chen Y, Duan Z, Meng S: miR-122-induced down-regulation of HO-1 negatively affects miR-122-mediated suppression of HBV. *Biochem Biophys Res Commun* 2010, 398(4):771-777.

143. Zhang B, Wang Q, Pan X: MicroRNAs and their regulatory roles in animals and plants. *J Cell Physiol* 2007, 210(2):279-289.

144. Jiang X, Tsitsiou E, Herrick SE, Lindsay MA: MicroRNAs and the regulation of fibrosis. *FEBS J* 2010, 277(9):2015-2021.

145. Roderburg C, Urban GW, Bettermann K, Vucur M, Zimmermann H, Schmidt S, Janssen J, Koppe C, Knolle P, Castoldi M *et al*: Micro-RNA profiling reveals a role for miR-29 in human and murine liver fibrosis. *Hepatology* 2010.

146. Kwiecinski M EN, Noetel A, Schievenbusch S, Strack I, Toex U, Drebber U, Steffen H, Dienes HP, Odenthal M.: miR-29, inhibiting synthesis of profibrogenic mediators, is released into the blood stream after chronic hepatitis C infection, indicating progression of fibrosis. *Hepatology* 2010, 52(4(Suppl)):119A.

147. Venugopal SK, Jiang J, Kim TH, Li Y, Wang SS, Torok NJ, Wu J, Zern MA: Liver fibrosis causes downregulation of miRNA-150 and miRNA-194 in hepatic stellate cells, and their overexpression causes decreased stellate cell activation. *Am J Physiol Gastrointest Liver Physiol* 2010, 298(1):G101-106.

148. Guo CJ, Pan Q, Cheng T, Jiang B, Chen GY, Li DG: Changes in microRNAs associated with hepatic stellate cell activation status identify signaling pathways. *FEBS J* 2009, 276(18):5163-5176.

149. Guo CJ, Pan Q, Jiang B, Chen GY, Li DG: Effects of upregulated expression of microRNA-16 on biological properties of culture-activated hepatic stellate cells. *Apoptosis* 2009, 14(11):1331-1340.

150. Ogawa T, Iizuka M, Sekiya Y, Yoshizato K, Ikeda K, Kawada N: Suppression of type I collagen production by microRNA-29b in cultured human stellate cells. *Biochem Biophys Res Commun* 2010, 391(1):316-321.

151. Davis BN, Hilyard AC, Nguyen PH, Lagna G, Hata A: Smad proteins bind a conserved RNA sequence to promote microRNA maturation by Drosha. *Mol Cell* 2010, 39(3):373-384.

152. Davis BN, Hilyard AC, Lagna G, Hata A: SMAD proteins control DROSHA-mediated microRNA maturation. *Nature* 2008, 454(7200):56-61.

153. Hata A, Davis BN: Control of microRNA biogenesis by TGFbeta signaling pathway-A novel role of Smads in the nucleus. *Cytokine Growth Factor Rev* 2009, 20(5-6):517-521.

154. Henderson NC, Iredale JP: Liver fibrosis: cellular mechanisms of progression and resolution. *Clin Sci (Lond)* 2007, 112(5):265-280.

155. Song G, Sharma AD, Roll GR, Ng R, Lee AY, Blelloch RH, Frandsen NM, Willenbring H: MicroRNAs control hepatocyte proliferation during liver regeneration. *Hepatology* 2010, 51(5):1735-1743.

156. Liu EH, Chen MF, Yeh TS, Ho YP, Wu RC, Chen TC, Jan YY, Pan TL: A useful model to audit liver resolution from cirrhosis in rats using functional proteomics. *J Surg Res* 2007, 138(2):214-223.

157. Issa R, Zhou X, Constandinou CM, Fallowfield J, Millward-Sadler H, Gaca MD, Sands E, Suliman I, Trim N, Knorr A *et al*: Spontaneous recovery from micronodular cirrhosis: evidence for incomplete resolution associated with matrix cross-linking. *Gastroenterology* 2004, 126(7):1795-1808.

158. Guicciardi ME, Gores GJ: Apoptosis as a mechanism for liver disease progression. *Semin Liver Dis* 2010, 30(4):402-410.

159. Bortner CD, Cidlowski JA: Cell shrinkage and monovalent cation fluxes: role in apoptosis. *Arch Biochem Biophys* 2007, 462(2):176-188.

160. Jablonski E, Webb A, Hughes FM, Jr.: Water movement during apoptosis: a role for aquaporins in the apoptotic volume decrease (AVD). *Advances in experimental medicine and biology* 2004, 559:179-188.

161. Jablonski EM, Webb AN, McConnell NA, Riley MC, Hughes FM, Jr.: Plasma membrane aquaporin activity can affect the rate of apoptosis but is inhibited after apoptotic volume decrease. *American journal of physiology* 2004, 286(4):C975-985.

162. Jablonski EM, Mattocks MA, Sokolov E, Koniaris LG, Hughes FM, Jr., Fausto N, Pierce RH, McKillop IH: Decreased aquaporin expression leads to increased resistance to apoptosis in hepatocellular carcinoma. *Cancer letters* 2007, 250(1):36-46.

163. Carbrey JM, Agre P: Discovery of the aquaporins and development of the field. *Handbook of experimental pharmacology* 2009(190):3-28.

164. Bortner CD, Cidlowski JA: Apoptotic volume decrease and the incredible shrinking cell. *Cell Death Differ* 2002, 9(12):1307-1310.

165. Agre P, Kozono D: Aquaporin water channels: molecular mechanisms for human diseases. *FEBS Lett* 2003, 555(1):72-78.

166. Verkman AS: Mammalian aquaporins: diverse physiological roles and potential clinical significance. *Expert reviews in molecular medicine* 2008, 10:e13.

167. Masyuk AI, LaRusso NF: Aquaporins in the hepatobiliary system. *Hepatology* 2006, 43(2 Suppl 1):S75-81.

168. Wyllie AH: "Where, O death, is thy sting?" A brief review of apoptosis biology. *Mol Neurobiol* 2010, 42(1):4-9.

169. Taimr P, Higuchi H, Kocova E, Rippe RA, Friedman S, Gores GJ: Activated stellate cells express the TRAIL receptor-2/death receptor-5 and undergo TRAIL-mediated apoptosis. *Hepatology* 2003, 37(1):87-95.

170. Hagens WI, Olinga P, Meijer DK, Groothuis GM, Beljaars L, Poelstra K: Gliotoxin non-selectively induces apoptosis in fibrotic and normal livers. *Liver Int* 2006, 26(2):232-239.

171. Kweon YO, Paik YH, Schnabl B, Qian T, Lemasters JJ, Brenner DA: Gliotoxin-mediated apoptosis of activated human hepatic stellate cells. *J Hepatol* 2003, 39(1):38-46.

172. Orr JG, Leel V, Cameron GA, Marek CJ, Haughton EL, Elrick LJ, Trim JE, Hawksworth GM, Halestrap AP, Wright MC: Mechanism of action of the antifibrogenic compound gliotoxin in rat liver cells. *Hepatology* 2004, 40(1):232-242.

173. Wright MC, Issa R, Smart DE, Trim N, Murray GI, Primrose JN, Arthur MJ, Iredale JP, Mann DA: Gliotoxin stimulates the apoptosis of human and rat hepatic stellate cells and enhances the resolution of liver fibrosis in rats. *Gastroenterology* 2001, 121(3):685-698.

174. Rockey DC: Current and future anti-fibrotic therapies for chronic liver disease. *Clin Liver Dis* 2008, 12(4):939-962, xi.

175. Adachi T, Nakanishi M, Otsuka Y, Nishimura K, Hirokawa G, Goto Y, Nonogi H, Iwai N: Plasma microRNA 499 as a biomarker of acute myocardial infarction. *Clin Chem* 2010, 56(7):1183-1185.

176. Habbe N, Koorstra JB, Mendell JT, Offerhaus GJ, Ryu JK, Feldmann G, Mullendore ME, Goggins MG, Hong SM, Maitra A: MicroRNA miR-155 is a biomarker of early pancreatic neoplasia. *Cancer Biol Ther* 2009, 8(4):340-346.

177. Wang GK, Zhu JQ, Zhang JT, Li Q, Li Y, He J, Qin YW, Jing Q: Circulating microRNA: a novel potential biomarker for early diagnosis of acute myocardial infarction in humans. *Eur Heart J* 2010, 31(6):659-666.

178. Zhang Y, Jia Y, Zheng R, Guo Y, Wang Y, Guo H, Fei M, Sun S: Plasma MicroRNA-122 as a Biomarker for Viral-, Alcohol-, and Chemical-Related Hepatic Diseases. *Clin Chem* 2010.

179. Kawada N: Evolution of hepatic fibrosis research. *Hepatol Res* 2011, 41(3):199-208.

180. Lewis AP, Jopling CL: Regulation and biological function of the liver-specific miR-122. *Biochem Soc Trans* 2010, 38(6):1553-1557.

181. Shan Y, Zheng J, Lambrecht RW, Bonkovsky HL: Reciprocal effects of micro-RNA-122 on expression of heme oxygenase-1 and hepatitis C virus genes in human hepatocytes. *Gastroenterology* 2007, 133(4):1166-1174.

182. Lanford RE, Hildebrandt-Eriksen ES, Petri A, Persson R, Lindow M, Munk ME, Kauppinen S, Orum H: Therapeutic silencing of microRNA-122 in primates with chronic hepatitis C virus infection. *Science* 2010, 327(5962):198-201.

183. Hou W, Tian Q, Zheng J, Bonkovsky HL: MicroRNA-196 represses Bach1 protein and hepatitis C virus gene expression in human hepatoma cells expressing hepatitis C viral proteins. *Hepatology* 2010, 51(5):1494-1504.

184. Lakner AM, Bonkovsky HL, Schrum LW: microRNAs: Fad or future of liver disease. *World J Gastroenterol* 2011, 17(20):2536-2542.

185. Rosano L, Cianfrocca R, Spinella F, Di Castro V, Natali PG, Bagnato A: Combination therapy of zibotentan with cisplatinum and paclitaxel is an effective regimen for epithelial ovarian cancer. *Can J Physiol Pharmacol* 2010, 88(6):676-681.

186. Umeda T, Abe H, Cho H, Shimizu T, Mori T, Kubota Y, Kawai Y, Tanaka M, Kurumi Y, Tani T: [An effective case of liver metastasis of breast cancer treated with capecitabine + docetaxel combination therapy using vitamin B6]. *Gan To Kagaku Ryoho* 2010, 37(4):687-689.

187. Sakurai T, Umemura T, Jinta E, Suzuma T, Yoshimura G, Shimizu S: [Doxifluridine, medroxyprogesterone acetate and cyclophosphamide (DMpC) combination therapy is effective against recurrent triple negative breast cancer--a case report]. *Gan To Kagaku Ryoho* 2008, 35(13):2433-2435.

188. Hagens WI, Beljaars L, Mann DA, Wright MC, Julien B, Lotersztajn S, Reker-Smit C, Poelstra K: Cellular targeting of the apoptosis-inducing compound gliotoxin to fibrotic rat livers. *J Pharmacol Exp Ther* 2008, 324(3):902-910.

189. Gonzalo T, Talman EG, van de Ven A, Temming K, Greupink R, Beljaars L, Reker-Smit C, Meijer DK, Molema G, Poelstra K *et al*: Selective targeting of pentoxifylline to hepatic stellate cells using a novel platinum-based linker technology. *J Control Release* 2006, 111(1-2):193-203.

190. Iredale J: Defining therapeutic targets for liver fibrosis: exploiting the biology of inflammation and repair. *Pharmacol Res* 2008, 58(2):129-136.

191. Friedman SL: A deer in the headlights: BAMBI meets liver fibrosis. *Nat Med* 2007, 13(11):1281-1282.

192. Xia X, Xie Z: AMADA: analysis of microarray data. *Bioinformatics* 2001, 17(6):569-570.

193. Bolstad BM, Irizarry RA, Astrand M, Speed TP: A comparison of normalization methods for high density oligonucleotide array data based on variance and bias. *Bioinformatics* 2003, 19(2):185-193.

194. Lewis BP, Burge CB, Bartel DP: Conserved seed pairing, often flanked by adenosines, indicates that thousands of human genes are microRNA targets. *Cell* 2005, 120(1):15-20.

195. Lakner AM, Walling TL, McKillop IH, Schrum LW: Altered aquaporin expression and role in apoptosis during hepatic stellate cell activation. *Liver Int* 2011, 31(1):42-51.

196. Livak KJ, Schmittgen TD: Analysis of relative gene expression data using real-time quantitative PCR and the 2(-Delta Delta C(T)) Method. *Methods* 2001, 25(4):402-408.

197. Savage DF, Stroud RM: Structural basis of aquaporin inhibition by mercury. *Journal of molecular biology* 2007, 368(3):607-617.

198. Zhang JX, Pegoli W, Jr., Clemens MG: Endothelin-1 induces direct constriction of hepatic sinusoids. *Am J Physiol* 1994, 266(4 Pt 1):G624-632.

199. De Minicis S, Seki E, Uchinami H, Kluwe J, Zhang Y, Brenner DA, Schwabe RF: Gene expression profiles during hepatic stellate cell activation in culture and in vivo. *Gastroenterology* 2007, 132(5):1937-1946.

200. Liu XJ, Yang L, Luo FM, Wu HB, Qiang Q: Association of differentially expressed genes with activation of mouse hepatic stellate cells by high-density cDNA microarray. *World J Gastroenterol* 2004, 10(11):1600-1607.

201. Rose-John S, Waetzig GH, Scheller J, Grotzinger J, Seegert D: The IL-6/sIL-6R complex as a novel target for therapeutic approaches. *Expert Opin Ther Targets* 2007, 11(5):613-624.

202. Hirano T, Ishihara K, Hibi M: Roles of STAT3 in mediating the cell growth, differentiation and survival signals relayed through the IL-6 family of cytokine receptors. *Oncogene* 2000, 19(21):2548-2556.

203. Lapolla A, Ragazzi E, Andretta B, Fedele D, Tubaro M, Seraglia R, Molin L, Traldi P: Multivariate analysis of matrix-assisted laser desorption/ionization mass spectrometric data related to glycoxidation products of human globins in nephropathic patients. *J Am Soc Mass Spectrom* 2007, 18(6):1018-1023.

204. Miyahara T, Schrum L, Rippe R, Xiong S, Yee HF, Jr., Motomura K, Anania FA, Willson TM, Tsukamoto H: Peroxisome proliferator-activated receptors and hepatic stellate cell activation. *J Biol Chem* 2000, 275(46):35715-35722.

205. Buniatian G, Gebhardt R, Schrenk D, Hamprecht B: Colocalization of three types of intermediate filament proteins in perisinusoidal stellate cells: glial fibrillary acidic protein as a new cellular marker. *Eur J Cell Biol* 1996, 70(1):23-32.

206. Niki T, De Bleser PJ, Xu G, Van Den Berg K, Wisse E, Geerts A: Comparison of glial fibrillary acidic protein and desmin staining in normal and CCl4-induced fibrotic rat livers. *Hepatology* 1996, 23(6):1538-1545.

207. Niki T, Pekny M, Hellemans K, Bleser PD, Berg KV, Vaeyens F, Quartier E, Schuit F, Geerts A: Class VI intermediate filament protein nestin is induced during activation of rat hepatic stellate cells. *Hepatology* 1999, 29(2):520-527.

208. Ramadori G, Veit T, Schwogler S, Dienes HP, Knittel T, Rieder H, Meyer zum Buschenfelde KH: Expression of the gene of the alpha-smooth muscle-actin isoform in rat liver and in rat fat-storing (ITO) cells. *Virchows Arch B Cell Pathol Incl Mol Pathol* 1990, 59(6):349-357.

209. Hazra S, Xiong S, Wang J, Rippe RA, Krishna V, Chatterjee K, Tsukamoto H: Peroxisome proliferator-activated receptor gamma induces a phenotypic switch from activated to quiescent hepatic stellate cells. *J Biol Chem* 2004, 279(12):11392-11401.

210. Han YP: Matrix metalloproteinases, the pros and cons, in liver fibrosis. *J Gastroenterol Hepatol* 2006, 21 Suppl 3:S88-91.

211. McCrudden R, Iredale JP: Liver fibrosis, the hepatic stellate cell and tissue inhibitors of metalloproteinases. *Histol Histopathol* 2000, 15(4):1159-1168.

212. Wang DR, Sato M, Sato T, Kojima N, Higashi N, Senoo H: Regulation of matrix metallo-proteinase expression by extracellular matrix components in cultured hepatic stellate cells. *Comp Hepatol* 2004, 3 Suppl 1:S20.

213. Tsukamoto H: Cytokine regulation of hepatic stellate cells in liver fibrosis. *Alcohol Clin Exp Res* 1999, 23(5):911-916.

214. Takahara Y, Takahashi M, Wagatsuma H, Yokoya F, Zhang QW, Yamaguchi M, Aburatani H, Kawada N: Gene expression profiles of hepatic cell-type specific marker genes in progression of liver fibrosis. *World J Gastroenterol* 2006, 12(40):6473-6499.

215. Boers W, Aarrass S, Linthorst C, Pinzani M, Elferink RO, Bosma P: Transcriptional profiling reveals novel markers of liver fibrogenesis: gremlin and insulin-like growth factor-binding proteins. *J Biol Chem* 2006, 281(24):16289-16295.

216. Kamimura D, Ishihara K, Hirano T: IL-6 signal transduction and its physiological roles: the signal orchestration model. *Reviews of physiology, biochemistry and pharmacology* 2003, 149:1-38.

217. Friedman SL: Molecular mechanisms of hepatic fibrosis and principles of therapy. *J Gastroenterol* 1997, 32(3):424-430.

218. Greenwel P, Rubin J, Schwartz M, Hertzberg EL, Rojkind M: Liver fat-storing cell clones obtained from a CCl4-cirrhotic rat are heterogeneous with regard to proliferation, expression of extracellular matrix components, interleukin-6, and connexin 43. *Lab Invest* 1993, 69(2):210-216.

219. Tiggelman AM, Boers W, Linthorst C, Brand HS, Sala M, Chamuleau RA: Interleukin-6 production by human liver (myo)fibroblasts in culture. Evidence for a regulatory role of LPS, IL-1 beta and TNF alpha. *J Hepatol* 1995, 23(3):295-306.

220. Toda K, Kumagai N, Tsuchimoto K, Inagaki H, Suzuki T, Oishi T, Atsukawa K, Saito H, Morizane T, Hibi T *et al*: Induction of hepatic stellate cell proliferation by LPS-stimulated peripheral blood mononuclear cells from patients with liver cirrhosis. *J Gastroenterol* 2000, 35(3):214-220.

221. Cavaillon JM: Cytokines and macrophages. *Biomed Pharmacother* 1994, 48(10):445-453.

222. Potter JJ, Womack L, Mezey E, Anania FA: Transdifferentiation of rat hepatic stellate cells results in leptin expression. *Biochem Biophys Res Commun* 1998, 244(1):178-182.

223. Saxena NK, Saliba G, Floyd JJ, Anania FA: Leptin induces increased alpha2(I) collagen gene expression in cultured rat hepatic stellate cells. *J Cell Biochem* 2003, 89(2):311-320.

224. Chen Z, Shin MH, Moon YJ, Lee SR, Kim YK, Seo JE, Kim JE, Kim KH, Chung JH: Modulation of elastin exon 26A mRNA and protein expression in human skin in vivo. *Exp Dermatol* 2009, 18(4):378-386.

225. Lin S, Saxena NK, Ding X, Stein LL, Anania FA: Leptin increases tissue inhibitor of metalloproteinase I (TIMP-1) gene expression by a specificity protein 1/signal transducer and activator of transcription 3 mechanism. *Mol Endocrinol* 2006, 20(12):3376-3388.

226. Breitkopf K, Haas S, Wiercinska E, Singer MV, Dooley S: Anti-TGF-beta strategies for the treatment of chronic liver disease. *Alcohol Clin Exp Res* 2005, 29(11 Suppl):121S-131S.

227. Purps O, Lahme B, Gressner AM, Meindl-Beinker NM, Dooley S: Loss of TGF-beta dependent growth control during HSC transdifferentiation. *Biochem Biophys Res Commun* 2007, 353(3):841-847.

228. Guo CJ, Pan Q, Li DG, Sun H, Liu BW: miR-15b and miR-16 are implicated in activation of the rat hepatic stellate cell: An essential role for apoptosis. *J Hepatol* 2009, 50(4):766-778.

229. Ji J, Zhang J, Huang G, Qian J, Wang X, Mei S: Over-expressed microRNA-27a and 27b influence fat accumulation and cell proliferation during rat hepatic stellate cell activation. *FEBS Lett* 2009, 583(4):759-766.

230. Kitamura Y, Ninomiya H: Smad expression of hepatic stellate cells in liver cirrhosis in vivo and hepatic stellate cell line in vitro. *Pathol Int* 2003, 53(1):18-26.

231. Parsons CJ, Takashima M, Rippe RA: Molecular mechanisms of hepatic fibrogenesis. *J Gastroenterol Hepatol* 2007, 22 Suppl 1:S79-84.

232. Chen XM: MicroRNA signatures in liver diseases. *World J Gastroenterol* 2009, 15(14):1665-1672.

233. Dolganiuc A, Petrasek J, Kodys K, Catalano D, Mandrekar P, Velayudham A, Szabo G: MicroRNA expression profile in Lieber-DeCarli diet-induced alcoholic and methionine choline deficient diet-induced nonalcoholic steatohepatitis models in mice. *Alcohol Clin Exp Res* 2009, 33(10):1704-1710.

234. Jin X, Ye YF, Chen SH, Yu CH, Liu J, Li YM: MicroRNA expression pattern in different stages of nonalcoholic fatty liver disease. *Dig Liver Dis* 2009, 41(4):289-297.

235. Roderburg C, Urban GW, Bettermann K, Vucur M, Zimmermann H, Schmidt S, Janssen J, Koppe C, Knolle P, Castoldi M *et al*: Micro-RNA profiling reveals a role for miR-29 in human and murine liver fibrosis. *Hepatology* 2011, 53(1):209-218.

236. Mestdagh P, Bostrom AK, Impens F, Fredlund E, Van Peer G, De Antonellis P, von Stedingk K, Ghesquiere B, Schulte S, Dews M *et al*: The miR-17-92 microRNA cluster regulates multiple components of the TGF-beta pathway in neuroblastoma. *Mol Cell* 2010, 40(5):762-773.

237. Dews M, Fox JL, Hultine S, Sundaram P, Wang W, Liu YY, Furth E, Enders GH, El-Deiry W, Schelter JM *et al*: The myc-miR-17~92 axis blunts TGF{beta} signaling and production of multiple TGF{beta}-dependent antiangiogenic factors. *Cancer Res* 2010, 70(20):8233-8246.

238. van Almen GC, Verhesen W, van Leeuwen RE, van de Vrie M, Eurlings C, Schellings MW, Swinnen M, Cleutjens JP, van Zandvoort MA, Heymans S *et al*: MicroRNA-18 and microRNA-19 regulate CTGF and TSP-1 expression in age-related heart failure. *Aging Cell* 2011.

239. Hardie WD, Glasser SW, Hagood JS: Emerging concepts in the pathogenesis of lung fibrosis. *Am J Pathol* 2009, 175(1):3-16.

240. Yang X, Haurigot V, Zhou S, Luo G, Couto LB: Inhibition of hepatitis C virus replication using adeno-associated virus vector delivery of an exogenous anti-hepatitis C virus microRNA cluster. *Hepatology* 2010, 52(6):1877-1887.

241. Kota J, Chivukula RR, O'Donnell KA, Wentzel EA, Montgomery CL, Hwang HW, Chang TC, Vivekanandan P, Torbenson M, Clark KR *et al*: Therapeutic microRNA delivery suppresses tumorigenesis in a murine liver cancer model. *Cell* 2009, 137(6):1005-1017.

242. Zhang Y, Jia Y, Zheng R, Guo Y, Wang Y, Guo H, Fei M, Sun S: Plasma microRNA-122 as a biomarker for viral-, alcohol-, and chemical-related hepatic diseases. *Clin Chem* 2010, 56(12):1830-1838.

243. Kosaka N, Iguchi H, Ochiya T: Circulating microRNA in body fluid: a new potential biomarker for cancer diagnosis and prognosis. *Cancer Sci* 2010, 101(10):2087-2092.

244. Gui J, Tian Y, Wen X, Zhang W, Zhang P, Gao J, Run W, Tian L, Jia X, Gao Y: Serum microRNA characterization identifies miR-885-5p as a potential marker for detecting liver pathologies. *Clin Sci (Lond)* 2011, 120(5):183-193.

245. De Martin E, Senzolo M, Gambato M, Germani G, Vitale A, Russo FR, Burra P: Fibrosis progression and the pros and cons of antiviral therapy for hepatitis C virus recurrence after liver transplantation: a review. *Transplant Proc* 2010, 42(6):2223-2225.

246. Szabo G, Katz E, Bonkovsky HL: Management of recurrent hepatitis C after liver transplantation: a concise review. *Am J Gastroenterol* 2000, 95(9):2164-2170.

247. Berenguer M: Natural history of recurrent hepatitis C. *Liver Transpl* 2002, 8(10 Suppl 1):S14-18.

248. Ben-Ari Z, Pappo O, Druzd T, Sulkes J, Klein T, Samra Z, Gadba R, Tambur AR, Tur-Kaspa R, Mor E: Role of cytokine gene polymorphism and hepatic transforming growth factor beta1 expression in recurrent hepatitis C after liver transplantation. *Cytokine* 2004, 27(1):7-14.

249. Russo MW, Firpi RJ, Nelson DR, Schoonhoven R, Shrestha R, Fried MW: Early hepatic stellate cell activation is associated with advanced fibrosis after liver transplantation in recipients with hepatitis C. *Liver Transpl* 2005, 11(10):1235-1241.

250. Murakami Y, Tanaka M, Toyoda H, Hayashi K, Kuroda M, Tajima A, Shimotohno K: Hepatic microRNA expression is associated with the response to interferon treatment of chronic hepatitis C. *BMC Med Genomics* 2010, 3:48.

251. Verkman AS: Dissecting the roles of aquaporins in renal pathophysiology using transgenic mice. *Seminars in nephrology* 2008, 28(3):217-226.

252. Verkman AS: Physiological importance of aquaporin water channels. *Annals of medicine* 2002, 34(3):192-200.

253. Verkman AS: Knock-out models reveal new aquaporin functions. *Handbook of experimental pharmacology* 2009(190):359-381.

254. Jameel NM, Thirunavukkarasu C, Wu T, Watkins SC, Friedman SL, Gandhi CR: p38-MAPK- and caspase-3-mediated superoxide-induced apoptosis of rat hepatic stellate cells: reversal by retinoic acid. *J Cell Physiol* 2009, 218(1):157-166.

255. Woo J, Lee J, Kim MS, Jang SJ, Sidransky D, Moon C: The effect of aquaporin 5 overexpression on the Ras signaling pathway. *Biochem Biophys Res Commun* 2008, 367(2):291-298.

256. Marinelli RA, Gradilone SA, Carreras FI, Calamita G, Lehmann GL: Liver aquaporins: significance in canalicular and ductal bile formation. *Ann Hepatol* 2004, 3(4):130-136.

257. Marinelli RA: Molecular mechanisms of water transport in bile formation: aquaporin water channels. *Trends Mol Med* 2004, 10(12):584.

258. Huebert RC, Splinter PL, Garcia F, Marinelli RA, LaRusso NF: Expression and localization of aquaporin water channels in rat hepatocytes. Evidence for a role in canalicular bile secretion. *J Biol Chem* 2002, 277(25):22710-22717.

259. Morishita Y, Sakube Y, Sasaki S, Ishibashi K: Molecular mechanisms and drug development in aquaporin water channel diseases: aquaporin superfamily (superaquaporins): expansion of aquaporins restricted to multicellular organisms. *J Pharmacol Sci* 2004, 96(3):276-279.

260. Gorelick DA, Praetorius J, Tsunenari T, Nielsen S, Agre P: Aquaporin-11: a channel protein lacking apparent transport function expressed in brain. *BMC Biochem* 2006, 7:14.

261. Yakata K, Hiroaki Y, Ishibashi K, Sohara E, Sasaki S, Mitsuoka K, Fujiyoshi Y: Aquaporin-11 containing a divergent NPA motif has normal water channel activity. *Biochim Biophys Acta* 2007, 1768(3):688-693.

262. Portincasa P, Palasciano G, Svelto M, Calamita G: Aquaporins in the hepatobiliary tract. Which, where and what they do in health and disease. *European journal of clinical investigation* 2008, 38(1):1-10.

263. De Minicis S, Brenner DA: NOX in liver fibrosis. *Arch Biochem Biophys* 2007, 462(2):266-272.

264. Sato M, Suzuki S, Senoo H: Hepatic stellate cells: unique characteristics in cell biology and phenotype. *Cell Struct Funct* 2003, 28(2):105-112.

265. Senoo H, Yoshikawa K, Morii M, Miura M, Imai K, Mezaki Y: Hepatic stellate cell (vitamin A-storing cell) and its relative--past, present and future. *Cell Biol Int* 2010, 34(12):1247-1272.

266. Sussman MA, Volkers M, Fischer K, Bailey B, Cottage CT, Din S, Gude N, Avitabile D, Alvarez R, Sundararaman B *et al*: Myocardial AKT: The Omnipresent Nexus. *Physiol Rev* 2011, 91(3):1023-1070.

267. Tsuchiya Y, Takahashi N, Yoshizaki T, Tanno S, Ohhira M, Motomura W, Takakusaki K, Kohgo Y, Okumura T: A Jak2 inhibitor, AG490, reverses lipin-1 suppression by TNF-alpha in 3T3-L1 adipocytes. *Biochem Biophys Res Commun* 2009, 382(2):348-352.

268. Vij N, Sharma A, Thakkar M, Sinha S, Mohan RR: PDGF-driven proliferation, migration, and IL8 chemokine secretion in human corneal fibroblasts involve JAK2-STAT3 signaling pathway. *Mol Vis* 2008, 14:1020-1027.

269. Anselmi K, Stolz DB, Nalesnik M, Watkins SC, Kamath R, Gandhi CR: Gliotoxin causes apoptosis and necrosis of rat Kupffer cells in vitro and in vivo in the absence of oxidative stress: exacerbation by caspase and serine protease inhibition. *J Hepatol* 2007, 47(1):103-113.

270. Mendell JR, Campbell K, Rodino-Klapac L, Sahenk Z, Shilling C, Lewis S, Bowles D, Gray S, Li C, Galloway G *et al*: Dystrophin immunity in Duchenne's muscular dystrophy. *N Engl J Med* 2010, 363(15):1429-1437.

271. Montgomery RL, van Rooij E: Therapeutic advances in MicroRNA targeting. *J Cardiovasc Pharmacol* 2011, 57(1):1-7.

272. Heneghan HM, Miller N, Kerin MJ: MiRNAs as biomarkers and therapeutic targets in cancer. *Curr Opin Pharmacol* 2010, 10(5):543-550.

273. Ranade AR, Cherba D, Sridhar S, Richardson P, Webb C, Paripati A, Bowles B, Weiss GJ: MicroRNA 92a-2*: a biomarker predictive for chemoresistance and prognostic for survival in patients with small cell lung cancer. *J Thorac Oncol* 2010, 5(8):1273-1278.

274. Gui J, Tian Y, Wen X, Zhang W, Zhang P, Gao J, Run W, Tian L, Jia X, Gao Y: Serum microRNA characterization identifies miR-885-5p as a potential marker for detecting liver pathologies. *Clin Sci (Lond)* 2010.

275. Li LM, Hu ZB, Zhou ZX, Chen X, Liu FY, Zhang JF, Shen HB, Zhang CY, Zen K: Serum microRNA profiles serve as novel biomarkers for HBV infection and diagnosis of HBV-positive hepatocarcinoma. *Cancer Res* 2010, 70(23):9798-9807.

APPENDIX: ABSTRACTS AND MANUSCRIPTS PUBLISHED

PUBLICATIONS

1. W.M. Ellefson, **A.M. Lakner**, A Hamilton, I.H. McKillop, H.L. Bonkovsky, N.M. Steuerwald, Y.M. Huett, L.W. Schrum. Androgenization Increases Alcohol-Induced Liver Injury, an Effect Abrogated by Estrogen, **manuscript submitted**, *Endo*. 2011 August.

2. **A.M. Lakner**, N.M. Steuerwald, T.L. Walling, I.H. McKillop, M.W. Russo, H.L. Bonkovksy, L.W. Schrum, miR 19b: Novel Biomarker and Inhibitor of Hepatic Stellate Cell-Mediated Fibrogenesis, **manuscript submitted**, *Gastro*. 2011 July.

3. C.C. Moore, **A.M. Lakner,** C.M. Yengo, LW. Schrum, Expression and Function of Nonmuscle Myosin II Isoforms in Hepatic Stellate Cells, **manuscript in press,** *World Journal of Hepatology*.

4. **A.M. Lakner**, H.L. Bonkovsky, L.W. Schrum, microRNAs: Fad or Future of Liver Disease, *World J Gastroenterol*. 2011 May 28;17(20):2536-42.

5. K.J. Thompson, **A.M. Lakner**, B.W. Cross, S. Tsukada, R.A. Rippee, I.H. McKillop, L.W. Schrum, S-Adenosyl-L-Methionine Inhibits Collagen Secretion in Hepatic Stellate Cells via Increased Ubiquitination, *Liver Int.* 2011. Jul;31(6):893-903.

6. S.A. Day*, **A.M. Lakner***, M.G. Clemens, E. Wu, L.W. Schrum, Novel Opiod Compounds Exert Anti-fibrotic Activity in Hepatic Stellate Cells, *Biochem Pharmacol*. 2011 April 15;81(8):996-1003. * *authors contributed equally*

7. **A.M. Lakner**, T.L .Walling, I.H. McKillop, L.W. Schrum, Altered Aquaporin Expression and Role in Apoptosis During Hepatic Stellate Cell Activation, *Liver Int.* 2011 Jan 31(1):42-51.

8. **A.M. Lakner**, C.C. Moore, A.A. Gulledge, L.W. Schrum, Daily genetic profiling indicates JAK/STAT signaling promotes early hepatic stellate cell transdifferentiation. *World J Gastroenterol*. 2010, Oct 28;(16):5047-5056**.**

ABSTRACTS

1. **Lakner AM**, Walling TL, Steuerwald NM, IH McKillop, MW Russo, HL Bonkovsky, LW Schrum. miR 19b: Novel Biomarker and Inhibitor of Hepatic Stellate Cell-Mediate Fibrogenesis, **abstract accepted**, Annual Meeting of AASLD, 2011.

2. Steuerwald N, Schrum L, Ellefson W, **Lakner A**, Parsons J, Hamilton A, McKillop I, Bonkovsky H, Huet Y. Testosterone imprinting influences alcohol-induced liver injury. Endocrine Society Annual Meeting. Boston, MA (2011).

3. Ellefson WM, **Lakner AM**, McKillop IH, Bonkovsky HL, Huet YM, Steuerwald N, Schrum LW. Hormonal imprinting influences early alcohol-induced liver injury. [Abstract 1655 presented at Annual Meeting of AASLD, 2010]. Hepatology 52 [4, Suppl]: 1110A-1111A, 2010.

4. **Ashley M. Lakner**, Tracy L. Walling, Iain H. McKillop, Laura W. Schrum. Hepatic Stellate Cell Apoptosis is Mediated through Differential Aquaporin Expression, IV Falk Gastro-Conference Liver and Pancreatic Diseases: Consequences of Chronic Alcohol Consumption. Freiburg, Germany (2010).

5. **A.M. Lakner**, T.L. Walling, I.H. McKillop, L.W. Schrum Hepatic Stellate Cell Apoptosis is Mediated through Differential Aquaporin Expression. Center for Biomedical Engineering Systems Graduate Poster Competition, Charlotte, NC (2010).

6. **A.M. Lakner**, I.H. McKillop, L.W. Schrum, Differential Aquaporin Expression in Hepatic Stellate Cells During Transdifferentiation, [Abstract Presented at Experimental Biology, New Orleans, LA, 2009]. FASEB J. 2009 23:981.6.

7. C.C. Moore, **A.M. Lakner**, A.A. Gulledge, L.W. Schrum, Interleukin-6 as a Key Regulator for Early Hepatic Stellate Cell Transdifferentiation, [Abstract Presented at Experimental Biology, New Orleans, LA, 2009]. FASEB J. 2009 23:981.5.

8. **A.M. Lakner,** J.D. Oliver, Survival of Two Genotypes of *Vibrio vulnificus* Exposed to Oyster (*Crassostrea virginica*) Hemolymph, American Society for Microbiology, Boston, Massachusetts (2008).